Technoeconomic Analysis of Photoelectrochemical (PEC) Hydrogen Production

Final Report
December 2009

Prepared by:
Brian D. James
George N. Baum
Julie Perez
Kevin N. Baum

One Virginia Square
3601 Wilson Boulevard, Suite 650
Arlington, Virginia 22201
(703) 243-3383

DOE Contract Number: GS-10F-009J
DOE Technical Monitor: David Peterson
Deliverable Task 5.1: Draft Project Final Report

Acknowledgements

The authors of this report would like to acknowledge the contributions of the US Department of Energy (DOE) Photoelectrochemical (PEC) Hydrogen Working Group, whose members provided invaluable technical and programmatic guidance throughout the analysis project.

While the working group consists of approximately 31 members from academia, industry, and the DOE, a core group of six individuals worked closely with DTI to assist in the technical direction of the analysis. These members merit particular recognition:

Dr. Eric Miller, University of Hawaii, PEC H_2 Working Group Leader
Ms. Roxanne Garland, Technology Development Manager, US DOE, EER&E
Dr. Eric McFarland, University of California, Santa Barbara
Dr. Thomas Jaramillo, Stanford University
Dr. John Turner, National Renewable Energy Laboratory (NREL)
Mr. Robert Perret, Nevada Technical Services, LLC.

The work described in this report was performed under contract to the US Department of Energy, Office of Fuel Cell Technologies, DOE Office of Energy Efficiency and Renewable Energy.

Table of Contents

Table of Figures

1. Executive Summary

Photoelectrochemical (PEC) production of hydrogen is a promising renewable energy technology for generation of hydrogen for use in the future hydrogen economy. PEC systems use solar photons to generate a voltage in an electrolysis cell sufficient to electrolyze water, producing H_2 and O_2 gases. A major advantage of PEC systems is that they involve relatively simple processes steps as compared to many other H_2 production systems. Additionally, they possess a wide operating temperature ranges, with no intrinsic upper temperature limit and a lower temperature of slightly below 0^oC without a warm-up period, and well below 0^oC with a warm-up period dependent on outside temperature. The primary challenges for PEC are to develop materials with sufficient photovoltage to electrolyze water, to minimize internal resistance losses, to have long lifetime (particularly corrosion life), to maximize photon utilization efficiencies, and to reduce plant capital cost.

Under contract to the US Department of Energy, Directed Technologies Inc. (DTI) has conducted a techno-economic evaluation of conceptual PEC hydrogen production systems. Four basic system configurations are chosen by DOE's PEC Working Group to encompass the technology spread of potential future PEC production systems. Overall system designs and parameters, costs of implementation, and costs of the output hydrogen were determined for each of the four conceptual systems. Each system consisted of a PEC reactor that generates H_2 and O_2, a gas processing system that compresses and purifies the output gas stream, and ancillary equipment.

The first two of the four system configurations examined utilize aqueous reactor beds containing colloidal suspensions of PV-active nanoparticles, each nanoparticle being composed of the appropriate layered PV materials to achieve sufficient bandgap voltage to carry out the electrolysis reaction. The third and fourth system configurations use multi-layer planar PV cells in electrical contact with a small electrolyte reservoir and produce oxygen gas on the anode face and hydrogen gas on the cathode face. They are positioned in fixed or steered arrays facing the sun.

The four specific system types conceptually designed and evaluated in the report are:
Type-1: A single electrolyte -filled reactor bed containing a colloidal suspension of PEC nanoparticles which produce a mixture of H_2 and O_2 product gases.
Type-2: Dual electrolyte-filled reactor beds containing colloidal suspensions of PEC nanoparticles, with one bed carrying out the $H_2O \Rightarrow \frac{1}{2} O_2 + 2 H^+$ half-reaction, the other bed carrying out the $2H^+ \Rightarrow H_2$ half-reaction, and including a mechanism for circulating the ions between beds.
Type-3: A fixed PEC planar array tilted toward the sun at local latitude angle, using multi-junction PV/PEC cells immersed in an electrolyte reservoir.
Type-4: A PEC solar concentrator system, using reflectors to focus the solar flux at a 10:1 intensity ratio onto multi-junction PV/PEC cell receivers immersed in an electrolyte reservoir and pressurized to 300 psi.

Solar Irradiation

The first step in determining hydrogen production was to evaluate the useable solar insolation levels for the four system types. For this report, we have assumed the location of the PEC reactors to be at Daggett, CA, at 35^o North latitude near Barstow, CA. This is a high insolation NREL solar measurement site and is near the solar-thermal power field at Kramer Junction, CA. For solar inputs we used the solar radiation tables for ground radiation compiled by NREL in the Solar Radiation Data Manual[1] and the SOLPOS[2] program to calculate hourly solar variation over a year.

For Type 1 and Type 2 reactor beds, the solar input consists of the component of direct radiation incident on the horizontal bed plus the diffuse radiation from the sky. For these, the yearly mean of the average daily radiation energy input (after window refraction loss) is 5.55 kW-hr/m^2 per 24 hour period. One issue for these horizontal bed PEC systems is that the H_2 output variation between summer and winter can vary by a factor of 3.2 for a clear environment and by a greater factor in the event of extensive winter cloud cover. Since this study didn't include a monthly hydrogen demand profile, the beds were sized for an average yearly production (averaging 1,000 kg H_2/day over a year) without regard for potential seasonal demand varations. The number of beds will need to be increased if the winter H_2 demand is greater than 31% of the summer demand.

The Type 3 system fixed planar PEC cell panels are inclined toward the equator at an angle equal to local latitude. This inclination allows the array, in general, to maximize overall capture of direct solar flux throughout the year and results in a much more leveled output between summer and winter. The system captures the solar direct component determined by panel tilt angle and the solar zenith and azimuth angles, and also captures much of the diffuse radiation component. The yearly mean of the average daily radiation energy input (after window refraction and inter-array shading losses) is 6.19 kW-hr/m^2 per 24 hour period.

The Type 4 system reactor consists of arrays that track solar direct radiation and focus the energy onto PEC receivers. While it captures the maximal direct solar radiation, it receives only a very small amount of diffuse radiation, since the concentrating mirrors have a narrow Field of View. The yearly mean of the average daily radiation energy input (after window refraction and inter-array shading losses) is 6.55 kW-hr/m^2 per 24 hour period.

Type 1 and Type 2 Particle Bed Systems

The Type 1 and 2 reactors are shallow horizontal pools or beds, filled with water, nanoparticles, and a KOH electrolyte, and having a flexible clear plastic thin-film envelope, or baggie, to contain the slurry and capture the gas produced while simultaneously allowing light to penetrate to the particles. With no gas production, the thin-film plastic cover will float on the water, however, as gas is produced, the cover will lift to accumulate output gas. The cover is sized to allow it to rise and fall over a 24 hour day and thus average out the gas flow to the gas handling

[1] Solar Radiation Data Manual for Flat Plate and Concentrating Collectors, 1961-1990, NREL Report, W. Merion, S. Wilcox.

[2] NREL MIDS SOLPOS (Solar Position and Intensity) model, Distributed by the NREL , Center for Renewable Energy Resources, Renewable Resource Data Center t http://rredc.nrel.gov/solar/codesandalgorithms/solpos/ .

subassembly. This gas handling subassembly is therefore sized for the average daily gas output rate over the highest production day (June 21) rather than the peak hourly output.

Type 1 System Reactor

The PEC nanoparticles are modeled as 40 nm conductive substrate particles onto which ~5nm thick anodic and cathodic photo-active coatings are deposited. This results in a multi-layer PV/PEC unit with a multi-photon response to achieve the requisite electrolysis voltage either from single above-threshold photons or from multiple below-threshold-energy photons. Details of the PEC nanoparticle material system are not yet well defined through experimental data, so reasonable extrapolations have been made from the current level of knowledge. Thus, in consultation with the PEC Working Group, we have modeled the nanoparticles as 40nm diameter Fe_2O_3 particles coated with an additional photoactive layer. For the Type 1 system particles, both hydrogen and oxygen are evolved from the surface of the nanoparticle. For current experimental particles, lab tests measuring conversion of absorbed photons to electrons have demonstrated an Incident-Photon-to electron Conversion Efficiency (IPCE) peak value of 2.5% for 360nm (3.4 eV) photons, and values to 10% have been predicted.

An end view of three baggie/bed structures is shown in Figure 1-1. A single baggie/bed is 1060 ft long x 40 ft wide. The assumed baseline Solar-to-Hydrogen (STH) conversion efficiency[3] is 10%. The system for 1 tonne per day (TPD) H_2 yearly average production consists of 18 baggies. This Type 1 reactor is the simplest PEC embodiment and has the lowest capital cost.

Figure 1-1: Type 1 End View

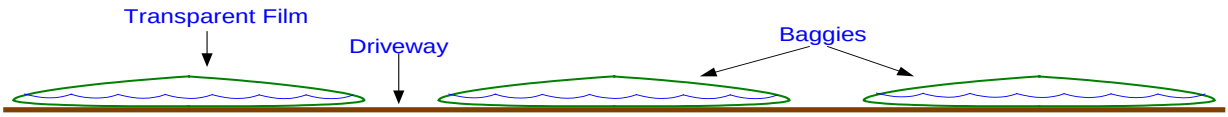

Type 2 System Reactor

Type 2 is the second type of colloidal suspension reactor and employs separate beds for the O_2 gas production reaction and the H_2 gas production reaction. The O_2 and H_2 beds are linked together with diffusion bridges to allow the transport of ions but prevent gas and particle mixing. A 0.1M KOH electrolyte is common to both beds and facilitates transport of ionic species. These beds also contain an intermediary reactant denoted "A", which participates in the reactions, but is not consumed. "A" can be iodine, bromine, iron or other elements. A typical set of equations describing the nanoparticle photoreactions is:

Bed I (O_2 evolution bed): 4 photons + 4 A + 2 H_2O => 1 O_2 + 4H^+ + 4 A^-
Bed II (H_2 evolution bed): 4 photons + 4H^+ + 4 A^- => 2 H_2 + 4 A

The nanoparticles are similar in structure to nanoparticles in the Type 1 system; however, the anodic particles would differ somewhat from the cathodic particles. We have modeled the Type 2 nanoparticles as Fe_2O_3 substrate particles onto which an additional photoactive layer is deposited.

[3] Solar-to-hydrogen (STH) conversion efficiency is the energy ratio of the H_2 produced (lower heating value) by a reactor divided by the total solar energy incident on the reactor.

As with the Type 1 single bed system, a baggie system is utilized, but with the addition of a continuous feed-through bridge passage between bed pairs (for ion diffusion between beds) and a slurry mixing system. The slurry mixer, to facilitate mixing within the bags and diffusion across the bridges, consists of perforated pipes through which the slurry is continuously pumped and circulated from the bed center to the bed edges

The multi-baggie/bed assembly, shown in Figure 1-2, consists of one half-baggie (H_2), one full size baggie (O_2), a second full size baggie (H_2), and a second half-baggie (O_2). Dimensions of the baggie/bed assembly shown in the figure are 200 ft long x 20 ft wide. The width of the bed is reduced compared to Type 1 baggies to reduce the diffusion distances.

Figure 1-2: Type 2 Multi-Baggie Assembly End View

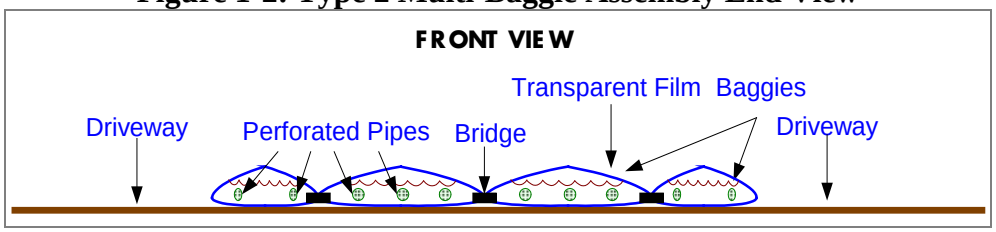

The Type 2 system requires approximately twice the solar absorption area as Type 1 because of the separation of the complete reaction into dual beds. Thus the STH efficiency is 5% and the system for 1 TPD H_2 average production consists of 347 such assemblies. The costs for the Type 2 reactor are 4.2 times higher than the Type 1 because of the near- doubling of reactor area and amount of nanoparticles, the added porous membranes, the added slurry circulation system, the additional number of ports, and the added manufacturing complexity

The Type 1 and 2 systems are innovative and promising approaches to PEC hydrogen generation, but are relatively immature compared with the standard PEC planar cell approach. Consequently they have greater uncertainty in prediction of performance and costs, such as:

- Detailed definition of Nanoparticle PV materials and fabrication
- Production costing of particle fabrication
- Effective photo-reactive area (photon capture area) on a given nanoparticle
- For the Type 2 reactor: uncertainty in diffusion times across diffusion bridge
- For the Type 2 reactor: uncertainty in whether there is 100% exclusive generation of O_2 in Bed I and H_2 in Bed II.

Type 3 and Type 4 Photocell Systems

The Type 3 and Type 4 Systems are extrapolated from current experimental PEC systems, using planar PV cells. Most PEC research to date has dealt with this type of cell. The photocell PEC system utilizes a PV cell generating sufficient voltage to electrolyze water, with modifications to allow it to survive in an electrolyte. The cell generates electrons from incident photons and has either integral electrodes immersed in the electrolyte as shown in Figure 1-3, or electrically connected spaced apart electrodes immersed in the electrolyte. For the PEC cell, the PV materials absorb photons to generate electrons for electrolysis at a total voltage on the order of 1.6-2.0 volts and conduct the electrons between the oxygen gas generating anode and the

hydrogen gas generating cathode. In experimental systems, the required voltage is higher due to losses in ion and electron transport and other losses. The electrolysis gases are separated by their physically separate reaction sites to create separate outlets for pure H_2 and pure O_2. In a common embodiment, the cell front face illuminated by solar radiation is a conductive window that functions as the electrolysis anode. Multi-junction PV active layers are used to use multiple sub-threshold photons to reach desired overall voltage and increase solar spectrum utilization.

Figure 1-3: Schematic of a Generic PEC Photocell

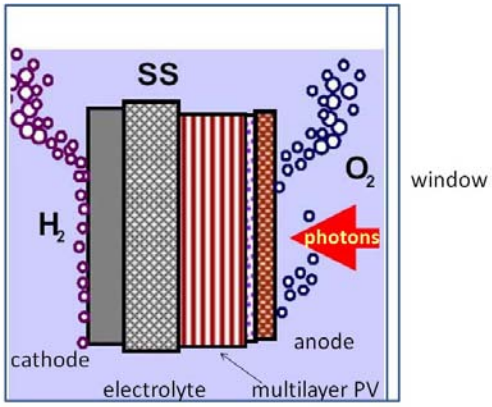

There are multiple PEC cell configurations which can be used, some using membrane separation of the gases and others relying solely on buoyancy separation. For this costing study, we have based our cell design on the simplest generic design assuming an open electrolyte compartment and buoyant separation of gases.

Costing of the PV/PEC active components relies heavily on the cost estimates, projections, and achievements in the solar cell industry. To estimate cell cost, we have assumed the PV cell advances of:

- Minimized thickness of individual PV layers
- Use of low cost printing techniques for material deposition
- Use of lower cost PV materials, when possible
- Low cost conductive coatings to protect against corrosion

To predict PEC cell costs, a cell component cost analysis was carried out, consistent with an NREL solar cell costing study[4] and consistent with recent solar cell predictions of $1/W for thin film solar cells.

Type 3 PEC Panel

Planar PEC arrays are similar to planar solar cell PV arrays, except that the cell electrodes are in direct contact with the PEC electrolyte and output is H_2 and O_2 gas rather than an external electric current. Each panel is made up of multiple cells, with the cell area being as large as can be readily manufactured. The arrays are fixed in place and inclined toward the sun at a tilt angle from horizontal equal to the local latitude.

[4] "Thin film PV manufacturing: materials costs and their optimization", Zweibel, K., Solar Energy Materials & Solar Cells, 2000, Elsevier.

Figure 1-4: Type 3 PEC Panel Layout

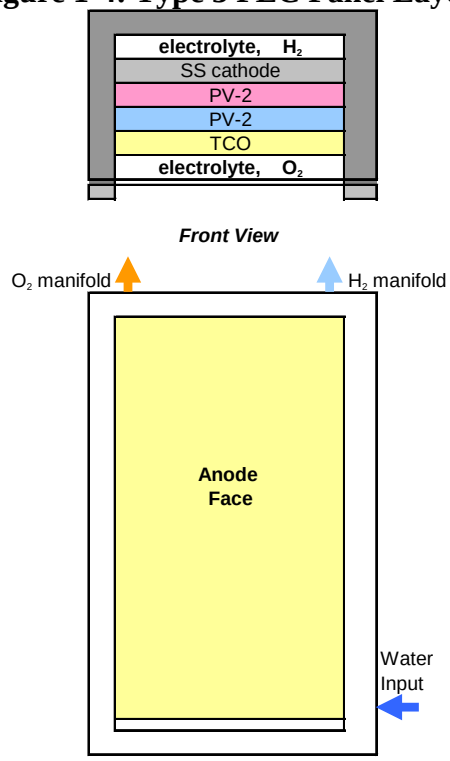

Each individual panel is 1 m wide and 2 m in length, and has a baseline STH efficiency of 10%. The system for 1 TPD H_2 average production consists of 26,923 such panels.

Type 4 Solar Concentrator PEC

The Type 4 system uses a solar concentrator reflector to focus solar direct radiation onto the PEC cell. A solar tracking system is used to maximize direct radiation capture. Solar concentrators, which can use reflectors or lenses to focus the solar energy, substantially reduce the cost impact of the PV component of the system, but add the costs of the concentrators and steering systems. Therefore, the PV components comprise a smaller fraction of the Type 4 total system cost, and more costly cell materials (i.e., GaAs/GaInAs) with higher efficiencies, are cost effective. A PEC concentrator system can potentially use a concentration ratio of 10-50 suns; however, we limited our system to 10:1, which has been demonstrated in lab tests.

For the concentrator PEC system, the water reservoir and the H_2 and O_2 collected are pressurized by the inlet water pump at relatively low added cost. Pressurization to 300 psi obviates the need for a separate compressor, minimizes water vapor loss by the reactor, and reduces O_2 gas bubble size, which minimizes potential bubble scattering of incident photons at the anode face.

The concentrator PEC design for this analysis uses an offset parabolic cylinder array to focus radiation on a linear PEC receiver, as shown in Figure 1-5. The offset parabolic array has advantages of reduced structural weight, no aperture blockage, and location of the active receiver components, water feed, and hydrogen collection piping in the reflector base assembly. The

PEC receiver component is a linear array of PEC cells at the parabolic reflector focal point. The array has 2-axis steering to track the solar direct radiation.

Figure 1-5: Type 4 Concentrator PEC Design

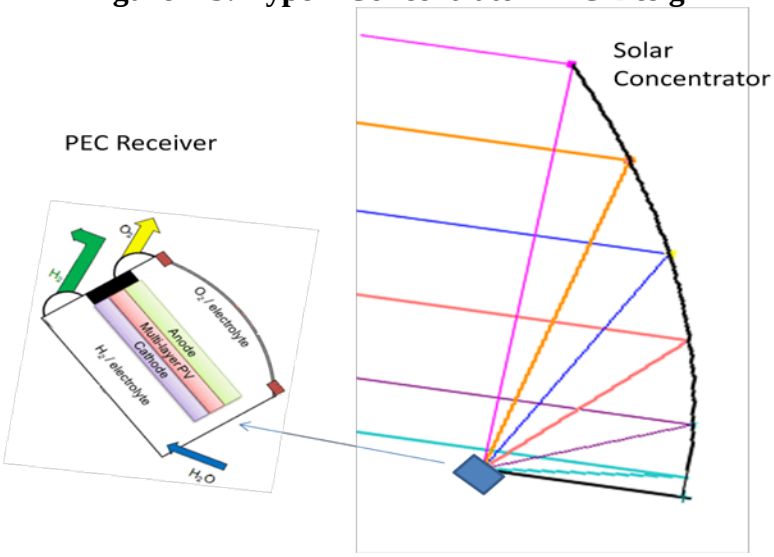

Each individual concentrator array is 6 m wide and 3 m in height with a baseline STH efficiency of 15%. The system for 1 TPD H_2 average production consists of 1,885 such reactors. In estimating reflector/collector costs for the Type 4 system, we based our costs on an NREL study of parabolic trough solar thermal power systems.

The Baseline Receiver uses a concentration ratio of 10:1. Increasing concentration ratio to 20:1 with the same PEC cell reduces the Plexiglas window span, with a thinner/lower cost window, and also reduces the PV surface area/cost and cell encapsulation area/cost. It is estimated that a doubling of concentration ratio to 20:1 could reduce the basic reactor cost by 17%.

Gas Processing

The gas processing subassembly collects, compresses, purifies and delivers the product hydrogen to the production facility limits. The outlet pressure of hydrogen at the plant gate is 300 psi (20.4 atm., 20.7 bar) to provide a system comparable to other DOE H2A-modeled production plants.

In all of the PEC systems, oxygen and hydrogen are produced, which raises combustibility issues. In the Type 2, 3, and 4 systems, the H_2 and O_2 are inherently separated in the PEC reactor so combustibility problems don't arise. However, in the Type 1 system, the product gas within the headspace of the reactor bed (and subsequently fed to the gas processing systems) is a stoichiometric mixture of oxygen and hydrogen with a small amount of water vapor. As these gases are a combustible mixture, special precautions must be taken to ensure safety. However, in numerous industrial processes, compression of flammable mixtures is routinely accomplished. Consequently, hydrogen/oxygen mixtures are deemed a design concern rather than a problem.

For compressing the gas mixture, a compressor with intercooling is used in Type 1, 2, and 3 systems. For Type 1 systems, the compressor compresses an H_2/O_2 mix to 305psi prior to input into the H_2 separation unit to allow for a 5 psi pressure loss in the separation. For Type 2 and Type 3 systems, the compressor compresses nominally pure H_2 to 300psi for delivery to the

plant gate. For Type 4 systems, no compressor is needed as the pure H_2 gas is already at 300psi coming out of the reactor.

A pressure swing adsorption (PSA) system is selected as the best H_2 separation system for this application. PSA operates by flowing a pressurized stream of gases (e.g., at 305 psi) across a multi-component adsorbent bed (commonly layers of activated carbon, zeolite, silica gel, etc.) to preferentially capture an undesired gaseous species on the surface of the adsorbent. In the process, there is loss of hydrogen that is contained in the absorption bed at the beginning of the vent cycle. As the bed is depressurized, this hydrogen is expelled and lost out the vent. A second H_2 loss occurs during the purge cycle, as pure hydrogen that is used to actively vent the system of impurities. Because of these PSA losses, the Type 1 system must produce about 11% more hydrogen from its reactor than the other systems.

Plant Control System

Plant control systems serve many functions including local and remote monitoring, alarming and controlling of plant equipment and functions. We have assumed a level of control sophistication consistent with full functionality and safe operation.

General Cost Assumptions

Several baseline assumptions were made to obtain the estimated yearly capital costs and operating costs for each of the four systems. On assessing yearly costs for each system's capital equipment investment, an appropriate return on investment (ROI) was used. In order to evaluate the ROI, a discounted cash flow (DCF) analysis was performed using the H2A Production Model, Version 2.0. The H2A Costing Model provides a structured format to enter parameters which impact cash inflows and outflows associated with the construction and operation of a Hydrogen Production Plant. There are numerous plant-specific parameters which must be entered. Additionally, there are H2A Default values for many of the parameters which can be modified to meet specific circumstances. Once all parameters have been entered, the H2A model computes the levelized cost of hydrogen in $\$/kgH_2$. For this study, we have not taken a cost credit for the byproduct O_2 generated by the reactors.

Specific Capital Costs for baseline systems

PEC reactor sizes and system costs are summarized and compared in Figure 1-6.

Figure 1-6: PEC System Capital Cost Summary

	Type 1 Single Bed Colloidal Suspension	Type 2 Dual Bed Colloidal Suspension	Type 3 Fixed Flat Panel	Type 4 Tracking Concentrator
Gross Production (kgH_2/day)	1,111	1,000	1,000	1,000
Net Production (kgH_2/day)	1,000	1,000	1,000	1,000
Mean Solar Input (kWh/m2/day)	5.25	5.25	6.19	6.55
Baseline Efficiency (STH)	10%	5%	10%	15%
Dimensions of reactor	1060'x40'x0.3' bed	200'x20'x1.2' bed	2m x 1m panel	6m x 3m reflector
Number of Reactors	18	347	26,923	1,885
Photon Capture Area (m^2)	70,540	126,969	53,845	33,924
Reactor total cost	$212,257	$892,934	$8,343,345	$3,135,209
Gas Processing Cost	$684,283	$356,654	$917,338	$33,771
Controls Cost	$173,944	$440,826	$319,862	$279,774
Hardware total cost	$1,070,484	$1,690,414	$9,580,545	$3,448,754
Land Cost	$11,330	$20,393	$27,076	$27,537
Total capital cost	$1,081,814	$1,710,807	$9,607,621	$3,476,291

The control system makes up a substantial part of total capital cost. Much of this cost comes from the hydrogen/oxygen sensors which monitor the gas stream for any leaks or contamination.

Overall Hydrogen Production Costs of Baseline Systems

The total cost of produced hydrogen assumed a 10 tonne per day (TPD) plant consisting of ten of the baseline 1TPD modules described above. The hydrogen production cost results calculated from the baseline system designs and the H2A model are:

- Type 1: $ 1.63/kg H_2
- Type 2: $ 3.19/kg H_2
- Type 3: $10.36/kg H_2
- Type 4: $ 4.05/kg H_2

Figure 1-7 shows a breakdown of these costs into: capital costs, decommissioning costs, fixed O&M, and variable costs. Note that these are the H_2 production costs for producing 300 psi hydrogen at the plant gate, and do not include delivery or dispensing costs.

Figure 1-7: Comparison of PEC System Levelized H_2 Cost

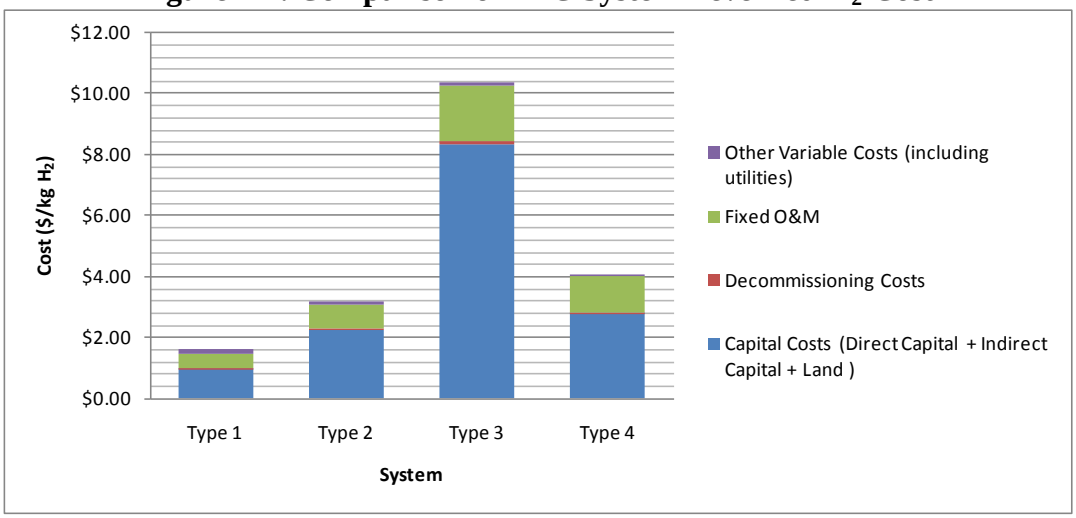

For the Type 1 and Type 2 systems, the levelized cost is quite low, but there is a large amount of development work and uncertainty in producing an operating system having these baseline performance parameters. The Type 3 system is the most mature of the concepts, with multiple small scale examples fabricated, but the substantial capital costs dominate H_2 production cost. The Type 4 system has been implemented at lab scale with good efficiency. For the Type 4 production system, costs are moderately low and are dominated by the solar collector structure.

Hydrogen Cost Sensitivity

An H_2 production cost sensitivity analysis assessed the variation in H_2 cost as a function of STH efficiency, PEC cell component cost, and PEC cell lifetime. The range of evaluation parameters for the sensitivity analyses and the results for the four systems are shown in Figure 1-8.

Figure 1-8: Hydrogen Cost Sensitivity Analysis Results

Type 1 Sensitivity Analysis Parameters			Type 2 Sensitivity Analysis Parameters		
Efficiency	**Particle Cost**	**Particle Lifetime**	**Efficiency**	**Particle Cost**	**Particle Lifetime**
5%	0.1x	1 Year	2.5%	0.1x	1 Year
10%	1x	5 Year	5%	1x	5 Year
15%	20x	10 Year	7.5%	20x	10 Year
Type 3 Sensitivity Analysis Parameters			**Type 4 Sensitivity Analysis Parameters**		
Efficiency	**PEC Cell Cost**	**PEC Cell Lifetime**	**Efficiency**	**PEC Cell Cost**	**PEC Cell Lifetime**
5%	$\$80/m^2$	5 year	10%	$\$200/m^2$	5 year
10%	$\$153/m^2$	10 year	15%	$\$316/m^2$	10 year
20%	$\$200/m^2$	20 year	25%	$\$450/m^2$	20 year

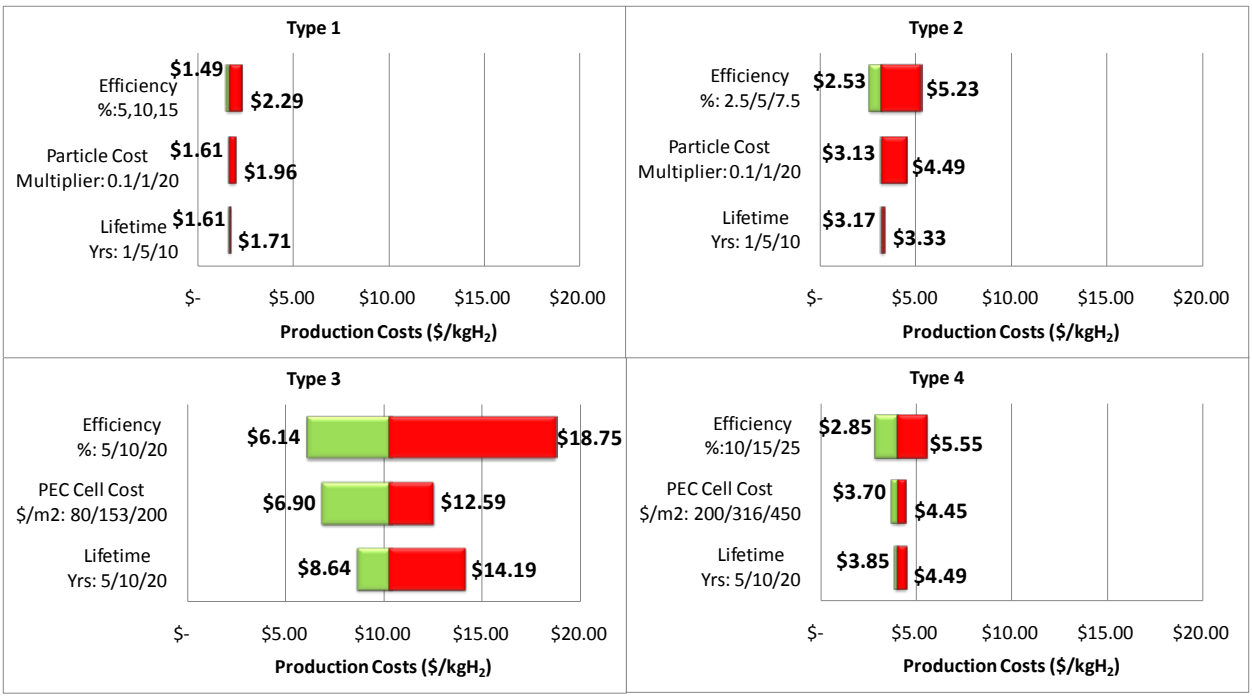

Discussion of Results

This study has shown that, within the cost assumptions used, production of H_2 by PEC systems can be economically viable in several configurations, upon successful resolution of the research challenges. Each system is discussed below.

Type 1 and 2 particle bed systems are innovative and cost effective PEC approaches, but they are immature and unproven compared with the standard PEC cell approach. Given the study assumptions as to efficiency and nanoparticle effectiveness, the Type 1 and 2 systems yield the lowest cost hydrogen. A unique advantage of these systems vs. the Type 3 panel array is that the gas collection bags are capable of storing the product gas output over a day's production to average out the demands on the gas processing system rather than requiring the processors to handle the peak gas output (as is the case for the Type 3 system).

Key Unique Type 1 characteristics include:

1. Lowest predicted H_2 costs, given study efficiency assumptions
2. Product gas in this system is a stoichiometric mixture of H_2 and O_2 raising safety concern
3. December output is 31% of June output, so the system would need to be enlarged if December output were a driving requirement rather than just the yearly average.

Key Unique Type 2 characteristics include:

1. Low predicted H_2 costs, given study efficiency assumptions
2. Performance results hinge on minimal losses due to ion transport
3. Nanoparticles separately tailored for O_2 production and H_2 production
4. December output is 31% of June output, so the system would need to be enlarged if December output were a driving requirement rather than just the yearly average.

The greater uncertainties in the Type 1 and 2 systems include:

- Incomplete definition and demonstration of the optimal nanoparticle PEC materials, including effective photon voltages, resistance losses, corrosion effects, lifetime
- Incomplete definition of fabrication techniques and production costing of the particles
- Fraction of effective photo-reactive area (photon capture area) on a given base nanoparticle
- Annual production quantity of the photoactive nanoparticles. (This study assumed an annual production quantity sufficient for supplying a 500 tonne H_2 capacity each year, yielding a particle cost of $304/kg. Nanoparticle cost would increase significantly if annual production corresponded to that required to produce only 10 tonnes H_2 each year.)

Type 3 and 4 Photocell Systems have benefited extensively from the current high development activity in the solar cell area, particularly in efforts to drive down the costs of thin film solar cells. Solar cells can be used to generate solar electricity to separately electrolyze water. However, with sufficient development, the PEC cell concept has the potential to be more efficient than separate solar cell/electrolyzer systems, since it eliminates the materials and fabrication costs of the solar cell current carrier conductor grid. The PEC cell can also be used under pressure to eliminate the need for a separate compression stage. Relative to the particle bed systems, variation in output between summer and winter for the photocell systems is significantly less.

Key unique Type 3 characteristics include:

1. Highest H_2 production costs, due to large areas of PEC cell component
2. Benefits from and relies on development of low cost thin film PV materials
3. For PEC cells, the cell packaging costs are significantly higher than the PV material costs
4. Highest gas compression cost, because compressor is sized for peak hourly production
5. Tilt angle, nominally the latitude angle, can be optimized to achieve the most level H_2 gas output over the year of all the options over the full year including environmental variations.

Key unique Type 4 characteristics include:

1. Moderately low H_2 costs, near the Type 2 estimate
2. In-cell compression of gas eliminates need for separate compressor
3. Increased efficiency possible with PEC development, and high temperature operation
4. Decreased H_2 cost with higher concentration ratio – to potentially below $3/kg
5. Offset reflector array for the concentrator reduces structural and piping costs.
6. December output is 53% of June output, so the system would need to be enlarged if December output were the driving requirement rather than just the yearly average.

Organization of Report

The body of the main report is divided into several sections for ease of use. Initially, the basic science aspects are discussed. Next, the engineering designs for hydrogen production,

purification, and compression are laid out. Finally, the resulting system capital costs and corresponding hydrogen production costs are determined.

2. Introduction

Directed Technologies Inc. (DTI) has conducted a techno-economic evaluation of several postulated configurations of photoelectrochemical (PEC) hydrogen production systems. This report documents the engineering and cost characteristics of four PEC hydrogen production systems selected by DOE to represent canonical embodiments of future systems. The report is divided into several sections for ease of use. Initially, the basic science aspects are discussed. Next, the engineering designs for hydrogen production, purification, and compression are laid out. Finally, the resulting system capital costs and corresponding hydrogen production costs are determined.

3. PEC Operating Principles

3.1 *PEC Electrolysis*

PEC systems, as defined in this analysis, use solar photon energy to generate sufficient energy to electrolyze water to produce hydrogen and oxygen. The advantage of PEC direct conversion over separate photovoltaic (PV) generation plus conventional electrolysis is the elimination of the electrical current collection network and concomitant current transmission losses. However, the PEC technology must overcome the increased electrochemical issues in order to be viable. The photoactive element within a PEC device is a photovoltaic component that converts photon energy to a current as long as the photon energy level exceeds the bandgap of the PV junction materials. The electrolysis reaction (i.e., water splitting reaction) is represented by the equation

$$H_2O + 1.23V \Rightarrow H_2 + \tfrac{1}{2} O_2$$

Thus the minimum electrochemical voltage to carry out the reaction is 1.23 Volts. However, with the normal losses in carrying out direct electrolysis of water, in practice >1.6 Volts is generally required to initiate the reaction. Only a portion of the solar spectrum includes photons with energies sufficient to generate voltages above this level (see Figure 3-1). Since these low energy photons would otherwise be "lost" to the reaction, multilayer PV components are used to allow multiple photons to produce a total combined voltage which is above the electrolysis threshold. In this manner solar flux utilization is maximized for hydrogen production and has been demonstrated in the 12.4% efficient PEC cells developed by NREL. Both dual layer and triple layer solar cells have been developed and are commonly produced by the PV industry with new low cost manufacturing embodiments being commercialized. We postulate that analogous multi-layer devices can be used to generate the requisite PEC electrolysis voltages.

For direct PEC decomposition of water to occur, several requirements must be simultaneously met by the PEC components:

- PV total bandgap significantly larger than the H_2/O_2 redox potential of 1.23V: generally with a goal of 1.5-2.0 V, and, in practice, as high as 3.0V when there are significant resistive losses
- PV bandgap matching with the H_2/O_2 redox potential
- Fast charge transfer across the electrode/electrolyte interface to prevent corrosion and reduce energy losses
- Electrode surfaces stable against corrosion

For photon energies greater than the bandgap voltage, the photoelectrons transfer more energy than needed for electrolysis and the extra energy is absorbed as heat. After satisfying these four threshold requirements for basic functionality, the subsequent measures of PEC cell economic viability for H_2 production are photon utilization efficiency and cost.

3.2 *PEC Efficiency*

Overall photoelectrolysis performance is measured by solar-to-hydrogen (STH) conversion efficiency, η.

The hydrogen production rate is based on the following formula:

$$H_2 \text{ generation rate/area} = \frac{I_s \ \eta}{LHV_{H2}} \quad kg\ H_2/hr/m^2$$

where:

I_s = solar intensity (1000 kW/m^2 at 1 sun)
η = photon conversion efficiency
LHV H_2 = lower heating value of hydrogen (LHV) = 33.3 kWh/kg

Figure 3-1 plots bandgap energy and solar spectrum vs. photon wavelength. From this figure, it can be seen that a single layer PEC cell with sufficient bandgap energy for electrolysis, ~1.8 eV, would be unable to electrolyze water over a significant part of the solar spectrum. Therefore, for best efficiency, a PEC cell would utilize a multi-layer PV component to generate the requisite electrolysis voltage from two low energy photons.

Figure 3-1: Bandgap Energy for PV Materials

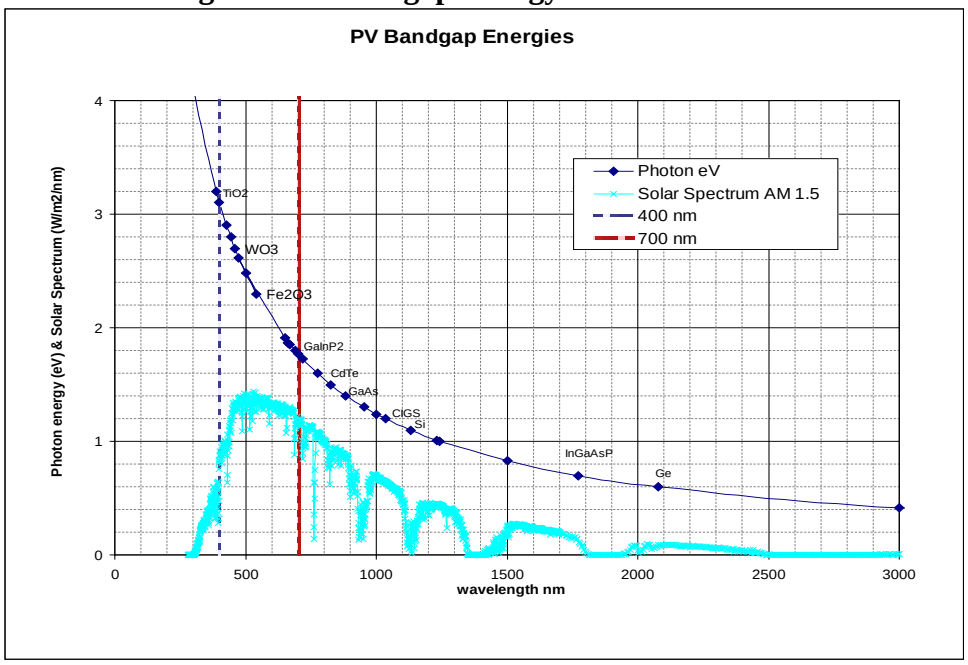

3.3 *PEC Reactor Types*

The PEC reactor is the system component that receives solar photons, converts them to electrons of sufficient voltage to electrolyze water, and carries out water electrolysis. This study investigates the operation and economics of four basic PEC system configurations. The first two utilize aqueous reactor beds containing colloidal suspensions of PV-active nanoparticles, each nanoparticle being composed of the appropriate layered PV materials to achieve sufficient bandgap voltage to carry out the electrolysis reaction. The next two configurations use planar PV cells which are positioned in arrays facing the sun and are immersed in a small water reservoir such that oxygen gas is produced on the anode face of the PV material and hydrogen gas on the cathode face. The specific systems types evaluated in the report are:

1. Type-1: Single water bed colloidal suspension of PV nanoparticles producing mixture of H_2 and O_2 product gases.
2. Type -2: Dual water bed colloidal suspension of PV nanoparticles, with one bed carrying out the $H_2O \Rightarrow \frac{1}{2} O_2 + 2 H^+$ half-reaction, the other bed carrying out the $2H^+ \Rightarrow H_2$ half-reaction , and including a mechanism for circulating the ions between beds.
3. Type -3: PEC fixed planar array tilted toward the sun at local latitude , using multi-junction PV cells immersed in a water reservoir.
4. Type -4: PEC solar concentrator system, using reflectors to concentrate solar flux at greater than 10:1 intensity ratio onto multi-junction PEC element receivers immersed in a water reservoir and pressurized to approximately 300 psi.

3.4 *PEC Optical Windows*

All four systems utilize a solar transmitting window to contain reactant water and gases. For Types 1 and 2, the window is a thin high density polyethylene (HDPE) film, and for Types 3 and 4, it is rigid Plexiglas sheet.

3.4.1 PEC Reactor Window Refraction/Reflection Effects

Ideally the reactor window would transmit 100% of incident photons through the window to the PEC nanoparticles or planar array below. However, the widows are not completely transparent and the percentage transmittance of incident solar flux depends both on window material and the solar angle of incidence. The incidence geometry is diagramed in Figure 3-2. For Types 3 and 4, there is refraction at the air/window interface followed by a second refraction at the window/water interface. Types 1 and 2 have similar properties when the plastic cover is in contact with the water, however, as gases are produced, a gas layer develops under the plastic and the radiation goes through 3 refractions: air/window, window/air and air/water. This gas layer is not continuous across the bed, so averaged conditions were assumed. Indices of refraction used were 1.5 for the window and 1.33 for the water.

Figure 3-2: PEC Window Refraction

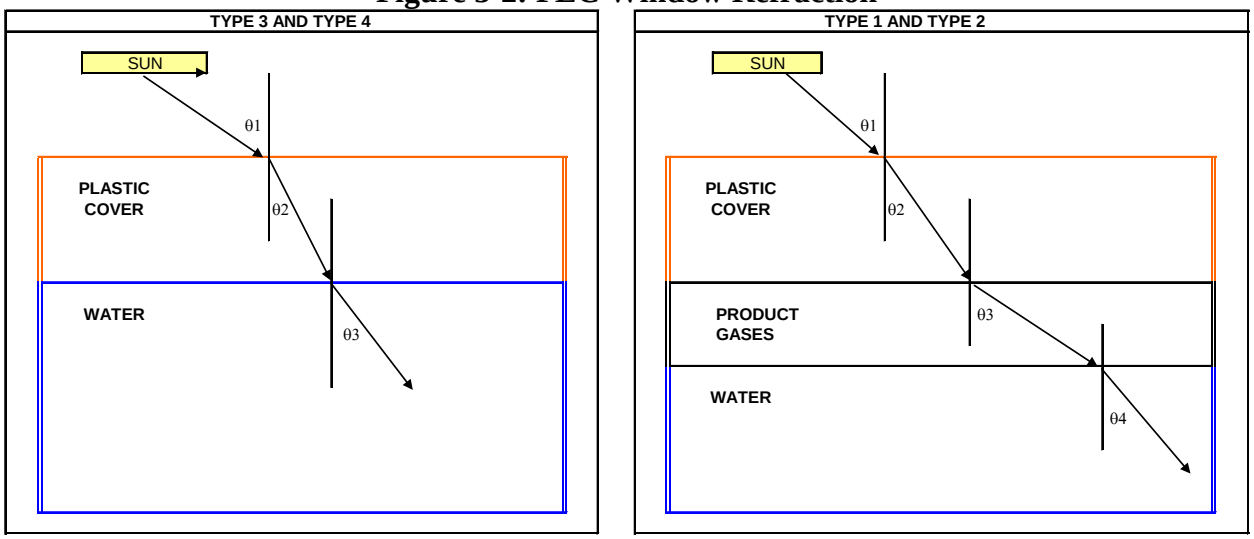

Figure 3-3 shows the solar angles of refraction into the water reservoir as a function of the angle of incidence θ_1 measured normal to the window. In the case of a horizontal bed, the angle of incidence is the zenith angle. In addition, the horizontal bed will often have a gas gap between the window and the water slurry, resulting in an additional refraction. For zero degree angle of incidence there is no refraction (100% reflection). In addition to the reflection, there are also absorption losses in the plastic window, assumed to vary between 90 and 95%.

Figure 3-3: PEC Window Refraction

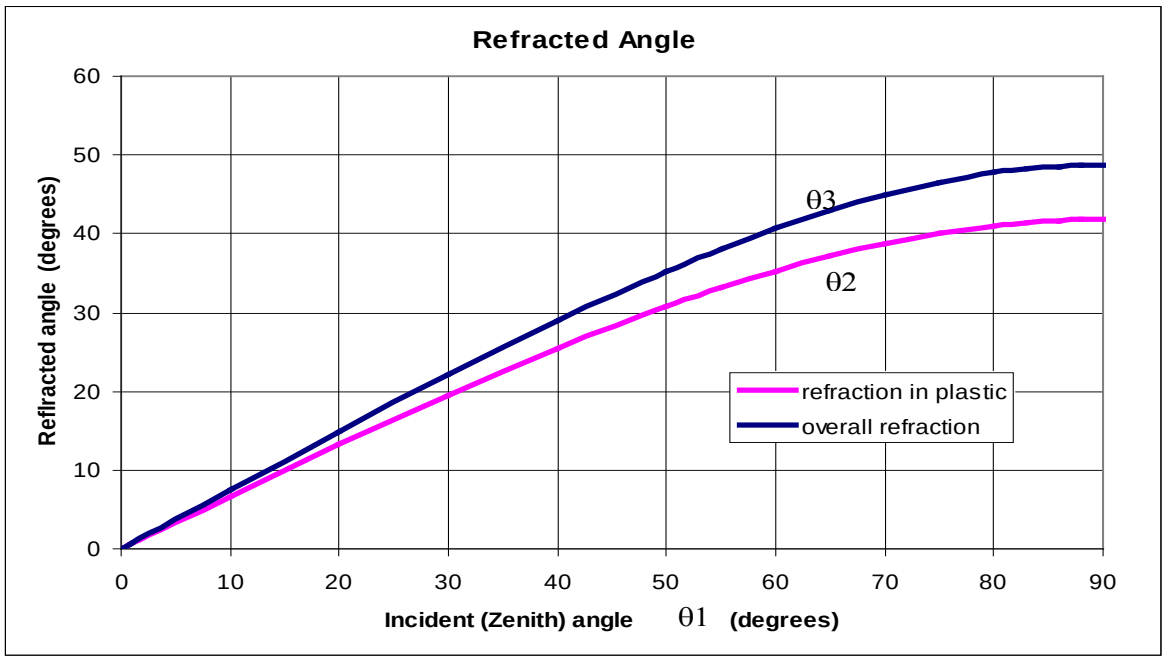

Figure 3-4 shows reflectance as a function of incidence angle, calculated from the Fresnel reflection equations. At normal incidence (0^o), there is 5% absorption/re-radiation by the plastic.

Figure 3-4: PEC Window Reflectance using Fresnel Reflection Equations

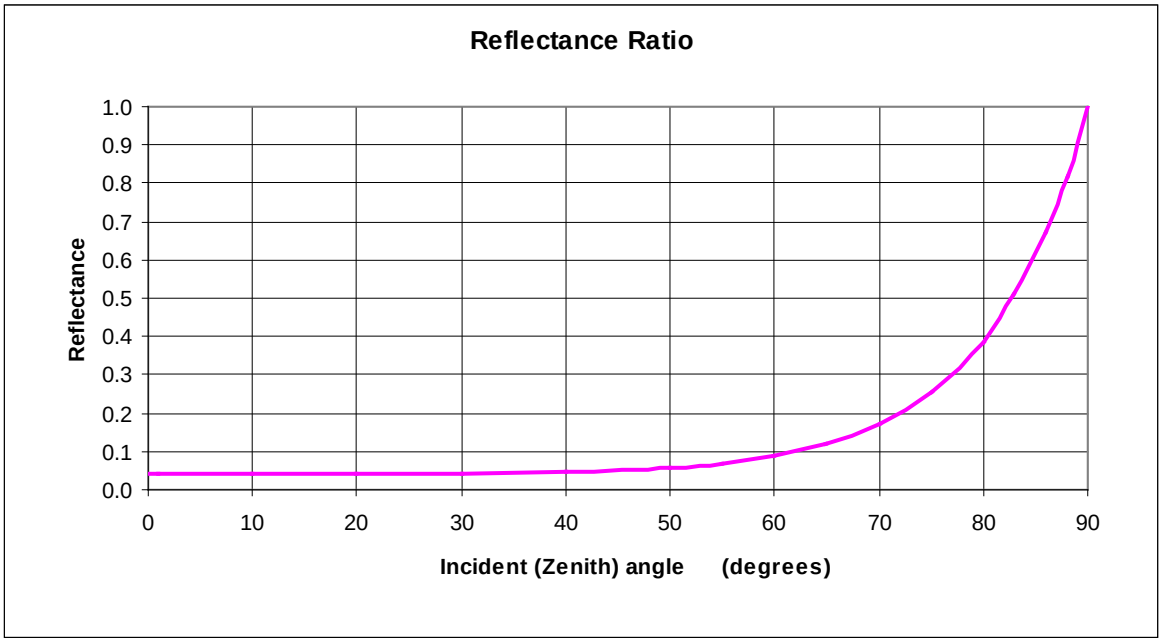

This calculated curve is similar to the published properties for Plexiglas[5] as shown in Figure 3-5.

Figure 3-5: Plexiglas Specification Window Reflectance

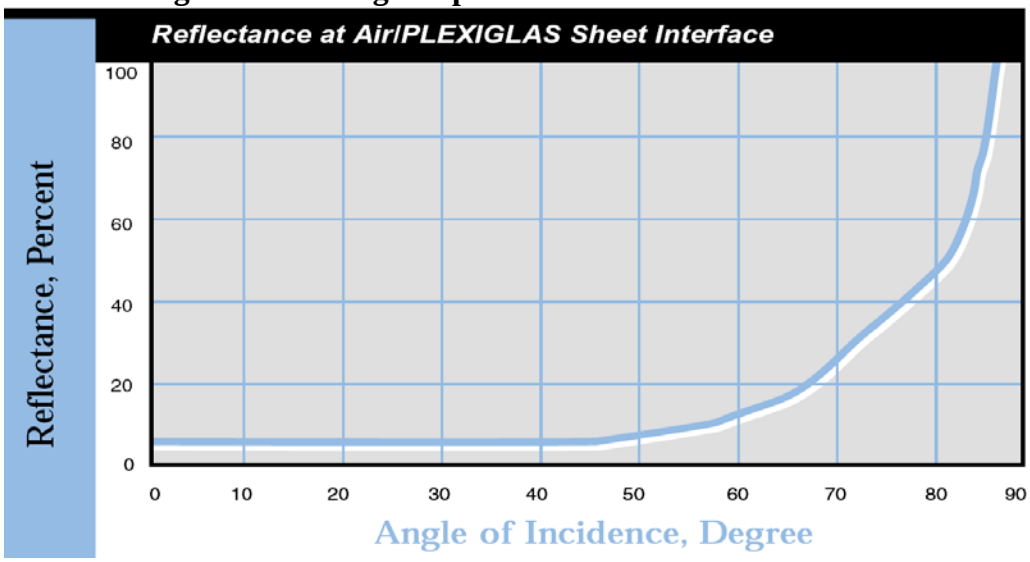

3.4.2 Type 1 and 2 PEC Cell Window Transmittance

The reactor beds use a plastic film to contain the H_2 produced in the PEC reaction. A 2005 NREL report[6] on H_2 reactor windows assessed tests of 17 thin films and 11 polycarbonate sheets for H_2 permeability and weather resistance. The tests showed low H_2 permeability and showed

[5] "Plexiglas Acrylic Sheet", Atoglas Division, ATOFINA Chemicals, Inc., Philadelphia, PA

[6] "Hydrogen Reactor Development & Design for Photofermentative and Photolytic Processes," Blake, D., Kennedy, C., Sept 2005, NREL Milestone Report-AOP 3.1.5, subtask 3.1.5.1

that high transmittance properties could be retained by most films for 4-5 years. The fluoropolymers, in accelerated testing, maintained a 90-95% transmittance for greater than 26 years. The report indicates that there are a number of products that can meet the film requirements for Type 1 and 2 reactors.

3.4.3 Type 3 and 4 PEC Window Transmittance

A high transmittance PEC cell window is necessary to transmit photons and contain the electrolyte on the anode side. Two options for plastic cell windows are acrylic (e.g. Plexiglas) and polycarbonate (e.g. Lexan). Basic characteristics of these two materials are listed below:

	Plexiglas Acrylic	Lexan Polycarbonate
Types	G sheet: Cell-cast process MC sheet: Melt calendering process	UV stabilized and non-UV stabilized
Transmission	high to 290nm with G-UVT high to 380nm with MC. See Figure 3-6.	high to 380 nm with non-UV stabilized. See Figure 3-7.
UV transmittance:	Some drop in first 2 yrs No change in next 10+ years	UV stabilized - 5% drop in 5 yrs
Chemical attack	Unaffected by dilute acids/bases	Unaffected by dilute acids/bases

Figure 3-6: Spectral Transmission - Plexiglas Acrylic[7]

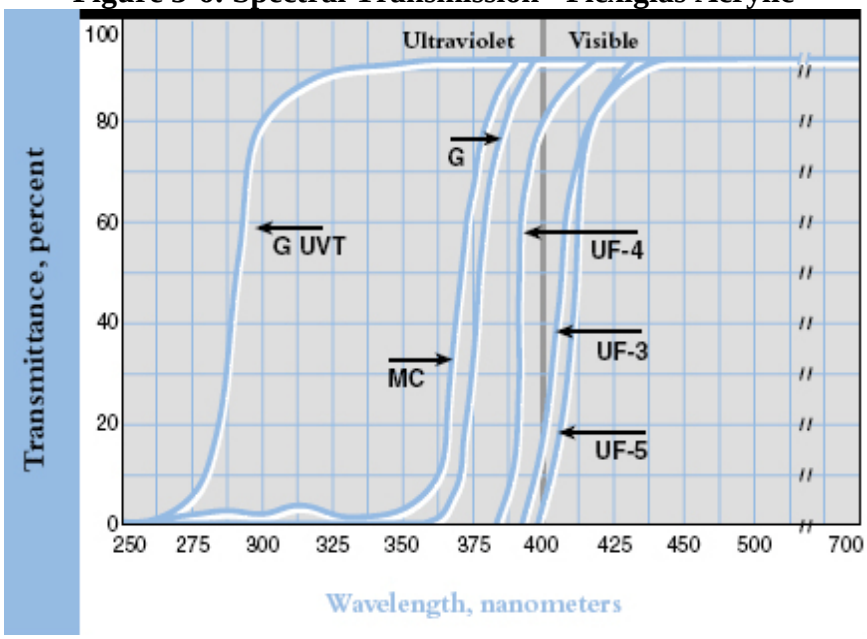

[7] "Plexiglas Acrylic Sheet", Atoglas Division, ATOFINA Chemicals, Inc., Philadelphia, PA.

Figure 3-7: Spectral Transmission - Lexan Polycarbonate[8]

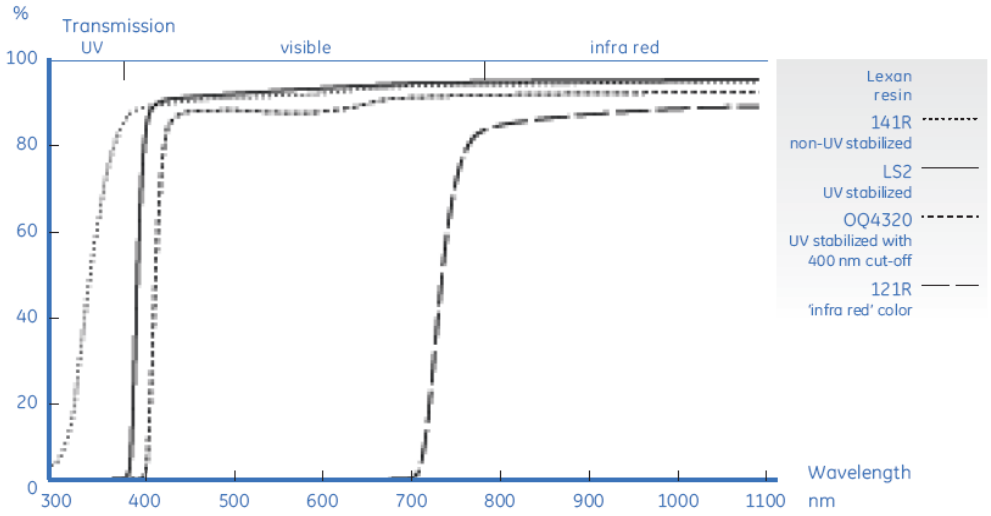

It is desirable to use window material that will allow some transmission of short wavelength UV (<400nm) energy to maximize PEC cell output, since these high energy photons readily release single reaction PEC electrons. In the solar spectrum, as shown in Figure 3-8, the UV energy below 400 nm contains a significant number of the high energy photons that can be used in the PEC reaction. For a Single-Layer PEC cell, and a 1.8 eV electrolysis threshold, only the photons with wavelength < 690 nm have enough energy to bring about electrolysis.

Figure 3-8: Solar Spectrum[9]

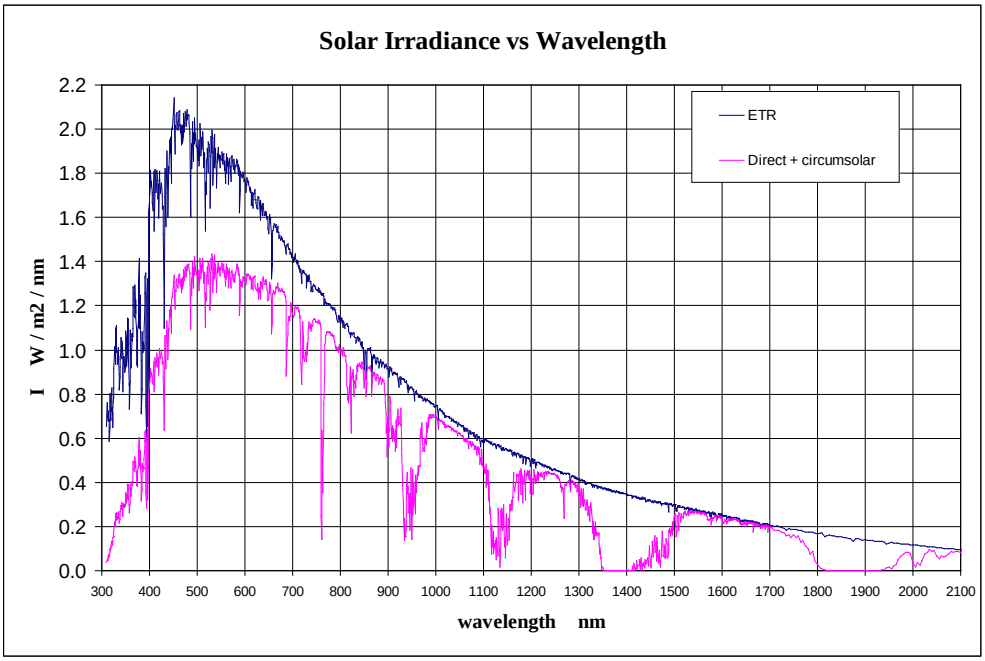

[8] "Lexan PC Resin Product Brochure", GE Plastics, Pittsfield, MA.
[9] ASTM G173-03 Reference Spectra Derived from SMARTS v. 2.9.2.

3.4.4 Window Chemical Properties

The windows must also resist deterioration by the PEC electrolyte, nominally 0.1 molar KOH. Chemical resistance characteristics for Plexiglas are shown in Figure 3-9, and indicate minimal adverse effects in mild bases and acids, with G-sheet performing better than MC sheet.

Figure 3-9: Plexiglas Chemical Resistance[10]

Compound Class	Name	Type (3)	Conc., %	PLEXIGLAS (% weight gain) G .236"	MC .236"
Acids	Acetic	glacial	100	R-S	DL
	Acetic		5	0.4	0.5
	Chromic		40	0.2	4-D
	Citric		10	0.3	0.4
	Hydrochloric	concentrated	38	0.2	A
	Hydrochloric		10	0.3	0.4
	Hydrofluoric		40	8.5E	—
	Nitric	concentrated	70	A-D	A
	Nitric		40	2.8	5-A
	Nitric		10	0.3	0.4
	Oleic		–	0.0	-0.1
	Sulfuric	concentrated	98	D-R-S	DL
	Sulfuric		30	0.2	0.3
	Sulfuric		3	0.4	0.5
Bases	Ammonium hydroxide	concentrated	28	0.2	0.3
	Ammonium hydroxide		10	0.4	0.5
	Sodium carbonate		20	0.2	0.3
	Sodium carbonate		2	0.4	0.5
	Sodium hydroxide		60	-0.2	-0.4
	Sodium hydroxide		10	0.3	0.4
	Sodium hydroxide		1	0.4	0.5

Chemical Resistance Code:
A = Attacked
C = Crazed
D = Discolored
DL = Dissolved
E = Edge Swelling
R = Rubbery
S = Swollen

Weight change is affected by the thickness of the material. Values given are for .236" thickness.
(1) Values given are averages and should not be used for specification purposes.
(2) Samples conditioned per ASTM D618, Procedure B, except where noted.
(3) Although exposure to carbon tetrachloride causes only negligible weight change in Plexiglas sheet, it does cause optical distortion of the surface. Carbon tetrachloride should NOT be used on Plexiglas sheet.

3.4.5 Type 1 and Type 2 Covered Pond Water Vaporization

The Type 1 and 2 PEC reactor ponds are covered with transparent HDPE plastic film to contain the evolved H_2 gas. The film has the secondary effect of capturing the water vapor generated by water heating by the sun. In an uncovered pond, water evaporates and, being much lighter than air, the buoyant vapor rises and is effectively removed from the system. This provides evaporative cooling to the pond. With the PEC pond, the HDPE film prevents this loss and the vapor under the film reaches a partial pressure equilibrium density, which is function of the water temperature. Analysis indicates that with constrained evaporative cooling (i.e., with a film cover), the water temperature can rise to temperatures exceeding 60^{o} C in the summer. This higher than ambient operation temperature has the beneficial effect of providing a small reduction in the energy required to electrolyze the water.

[10] "Plexiglas Acrylic Sheet", Atoglas Division, ATOFINA Chemicals, Inc., Philadelphia, PA.

3.5 *Solar Insolation*

As a first step in determining PEC system hydrogen production, the useable solar insolation levels for the four system types must be determined. The specific geographical location determines hours and angles of extraterrestrial (ETR) exposure, and the atmospheric conditions determine the amount of radiation absorbed and scattered by the atmosphere. Monthly solar radiation tables for ground radiation have been compiled by NREL and are available in the Solar Radiation Data Manual[11] using data from the 239 data sites in the 1961-1990 National Solar Radiation Data Base (NSRDB). For purposes of this report, we have assumed a PEC reactor location of Daggett, CA, at 35^{o} North latitude near Barstow, CA. This site was the best of the 239 NSRDC sites, having high terrestrial insolation levels and minimal cloud cover. This area is close to the large solar-thermal power generation field at Kramer Junction, CA (further validating the location as well suited to solar operations).

Net solar insolation is a function of three primary factors:

- Extra terrestrial radiation (ETR) intensity and sun position relative to the PEC reactor antenna face, which varies with geographical location, time of day, and day of the year,
- Clearness Index, Kt, the average atmospheric loss factor reducing the ETR due to atmospheric absorption and average cloud obscuration for a given geographical location,
- Diffuse and albedo radiation inputs due to diffuse sky-light inputs and ground albedo reflected by the atmosphere.

For calculation of the daily radiation variation, the NREL SOLPOS model[12] was used to determine ETR intensity values and solar position angles. This model calculates ETR and solar angles at 15 minute time intervals for a given day and geographical location. The Clearness Index, Kt, which was derived from the "Solar Radiation Data Manual", is multiplied by the ETR to obtain the net direct radiation at the ground.

3.5.1 Type 1 and Type 2 System Insolation

For a Type 1 or Type 2 horizontal reactor bed, the solar input consists of the component of the direct solar radiation incident on the bed plus the diffuse radiation. Direct solar varies over a day with the cosine of the sun zenith angle (measured from directly overhead of the bed). The direct and diffuse are combined to yield the total insolation on the bed as a function of time of day and month of the year. The map in Figure 3-10 shows average yearly insolation on a horizontal flat plate.

[11] Solar Radiation Data Manual for Flat Plate and Concentrating Collectors, 1961-1990, NREL Report, W. Merion, S. Wilcox.

[12] NREL MIDS SOLPOS (Solar Position and Intensity) model Distributed by the NREL , Center for Renewable Energy Resources, Renewable Resource Data Center t http://rredc.nrel.gov/solar/codesandalgorithms/solpos/ .

Figure 3-10: Yearly Average Solar Irradiance On Horizontal Surfaces

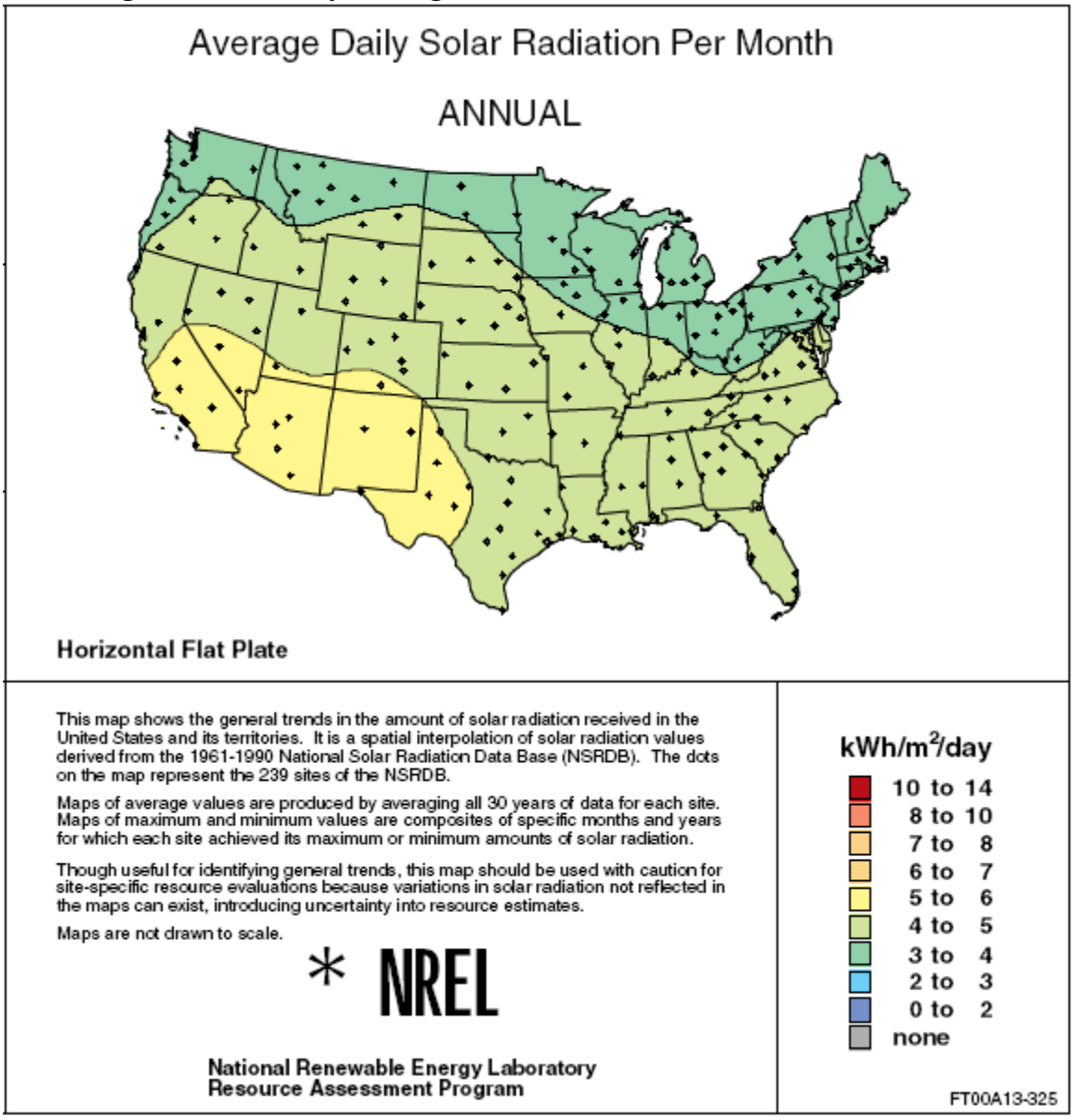

For the PEC reactor bed geographical location, Daggett, CA, (34.87^{o} N, 116.78 W) was used. For the horizontal PEC bed, the typical daily radiation energy for each month, along with yearly averages, is shown in Figure 3-11.

Figure 3-11: Monthly Variation of Daily Radiation on Horizontal Surface

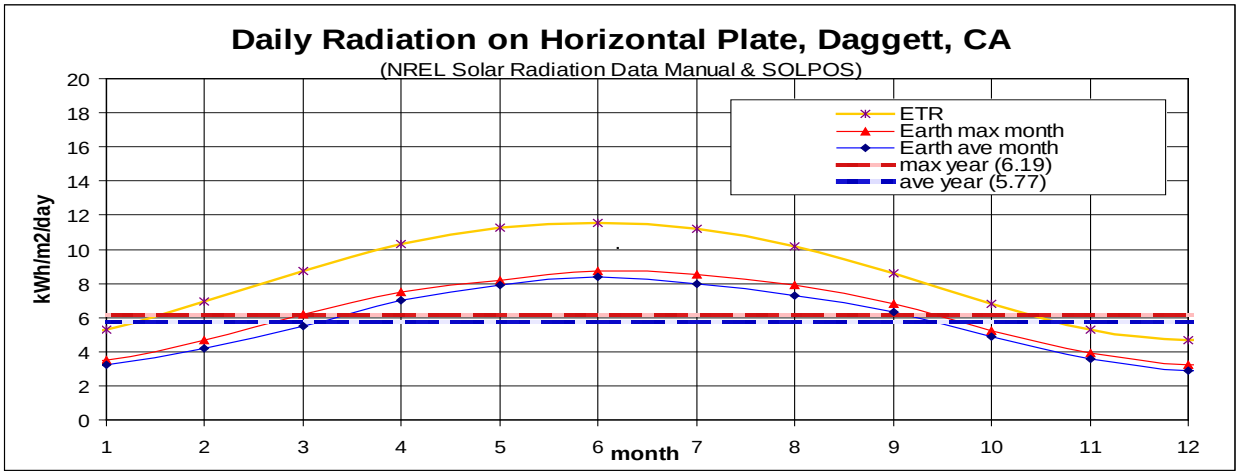

The five curves in Figure 3-11 represent: (1) Extraterrestrial radiation (ETR) incident on a horizontal plate, (2) maximum terrestrial daily radiation for each month, (3) average terrestrial daily radiation for each month, (4) yearly mean of maximum month radiations, 6.19 kW-hr/m^2/day, and (5) yearly mean of average month radiations, 5.77 kW-hr/m^2/day. The ETR curve is from SOLPOS and the other curves are derived from the ETR value and data from the "Solar Radiation Data Manual for Flat Plate and Concentrating Collectors". Due to the high variation in insolation between June and December, the daily incident radiation on the Type 1 and 2 systems will vary over a year by a factor of 2.9, resulting in a highly varying output of hydrogen (kg/day) over a year, which may not match the user requirements for hydrogen.

While the preceding graph shows substantial seasonal insolation variation, the PEC systems must also deal with substantial hourly variation. Hourly radiation variation over a day at this location, for a Type 1 or Type 2 horizontal reactor bed is shown in Figure 3-12 for average atmospheric conditions.

Figure 3-12: Hourly Irradiance on a Horizontal Surface

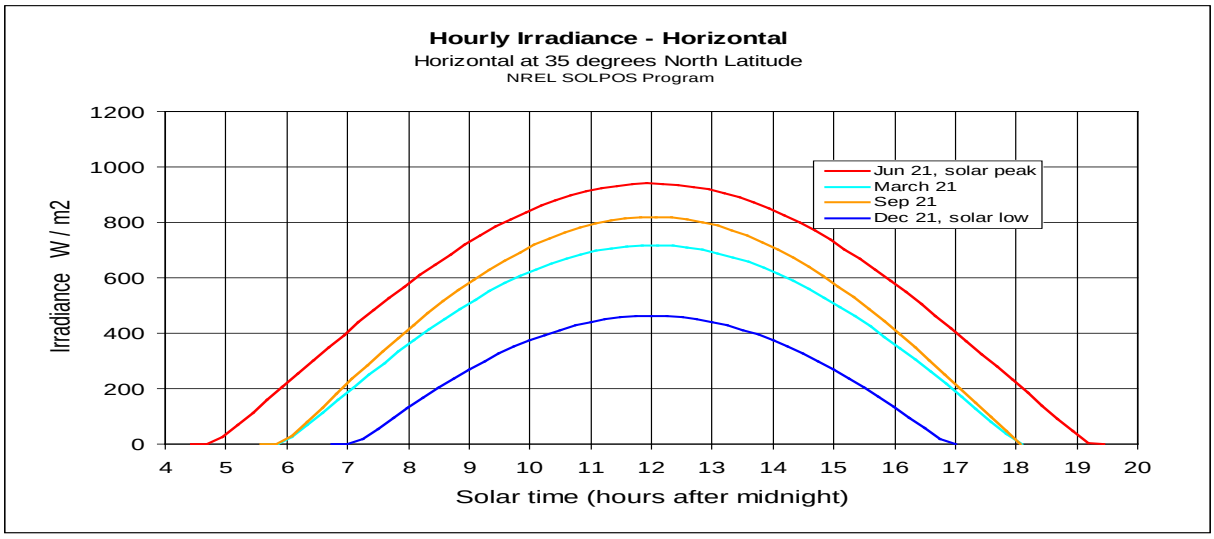

The four curves show the solar maximum on June 21, the spring equinox on March 21, the autumnal equinox on September 21, and the solar minimum on December 21. The higher radiation level in September relative to March is due to reduced atmospheric attenuation.

3.5.1.1 *Type 1 and Type 2 System Refracted Solar Input*

As discussed earlier, there are reflection losses and additionally, absorption losses in the transparent film cover, these losses depending on sun zenith angle. Figure 3-13 is a re-plot of Figure 3-11 which takes into account this angle-dependent loss. Due to the low zenith angle in December and consequent higher reflection, the transmitted energy ratio between June and December is 3.2, as opposed to the incident energy ratio of 2.9.

Figure 3-13: Variation of Daily Refracted Radiation on Horizontal Surface over a Year

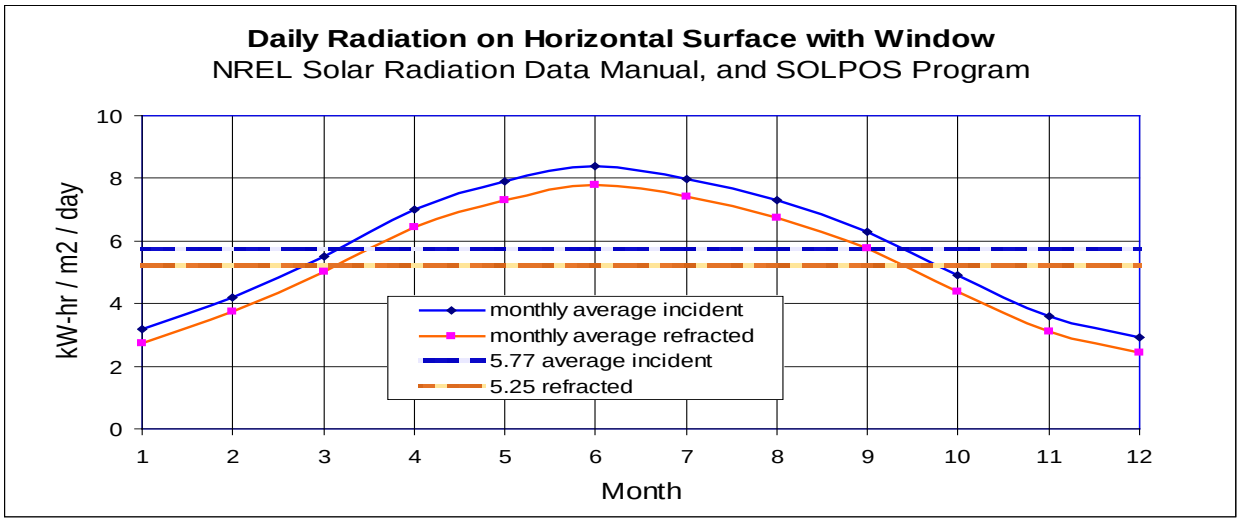

Variations in refracted energy over a day are shown in Figure 3-14.

Figure 3-14: Hourly Refracted Input Energy on a Horizontal Surface

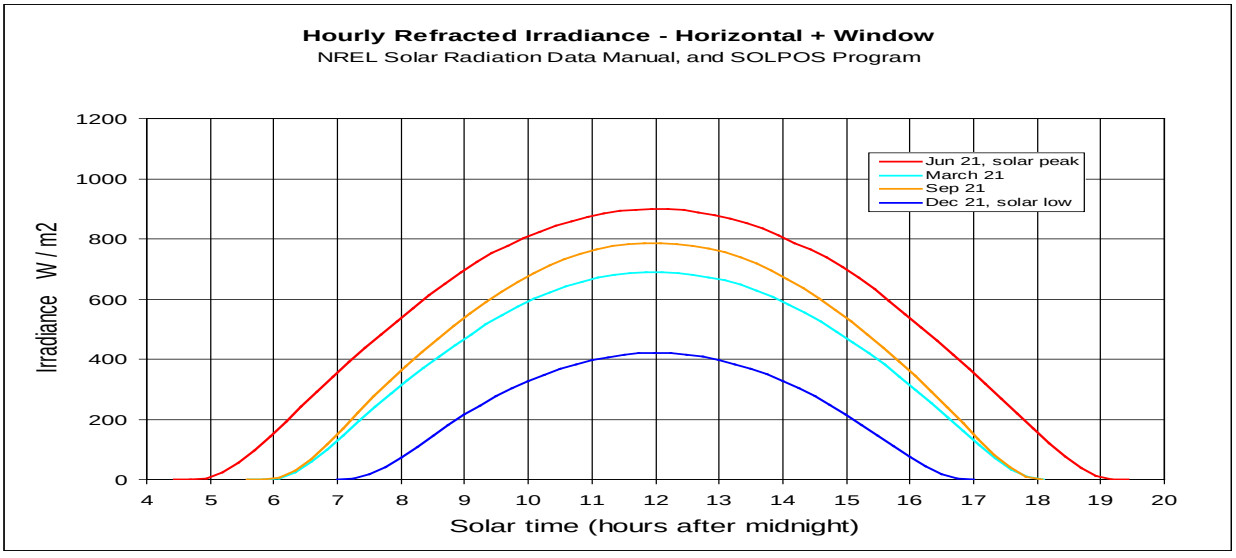

Reactor bed size and gas handling capacity are calculated from radiation transmitted to the bed:

- Module Size: An H_2 production module is sized to produce an average of 1,000 kg H_2/day over a year, at average transmitted radiation of 5.25 kW-hr/m^2/day (Figure 3-13).
- Gas handling subsystem size: For the gas handling system of the Type 1 and 2 systems, the reactor bed HDPE cover is allowed to rise to accumulate H_2, O_2 gas and H_2O vapor outputs over a day and average out the hourly variation in production and thus reduce the input to the compressor from the instantaneous gas output at noon to the average output over a day. Since daily solar transmitted radiation in maximized on June 21, the gas handling subsystem is designed to accommodate the daily gas production with this radiation schedule. For June 21, the average daily transmitted radiation is 7.78 kW-hr/m^2/day (Figure 3-13) and the maximum daily transmitted radiation is 1.04 times this, or 8.06 kW-hr/m^2/day.

3.5.2 Type 3 Tilted Planar Array System Insolation

The Type 3 system consists of a field of fixed planar PEC cell panels inclined toward the equator at an angle equal to the local latitude. This inclination allows the array, in general, to maximize overall capture of the direct solar flux throughout the year and also results in a much more leveled output between summer and winter. The system captures the solar direct component determined by panel tilt angle and the solar zenith and azimuth angles, and it also captures much of the diffuse radiation component. Depending on the inter-array spacing, there can be some shading of direct radiation between adjacent arrays when the sun is near the horizon, however, because the solar flux on the array is at a minimum at sunup and sundown, the shading affect is of minor impact. Figure 3-15 shows the yearly average irradiance incident on a surface that is inclined at an angle equal to the local latitude.

Figure 3-15: Yearly Average Solar Irradiance on Surface Inclined at Local Latitude

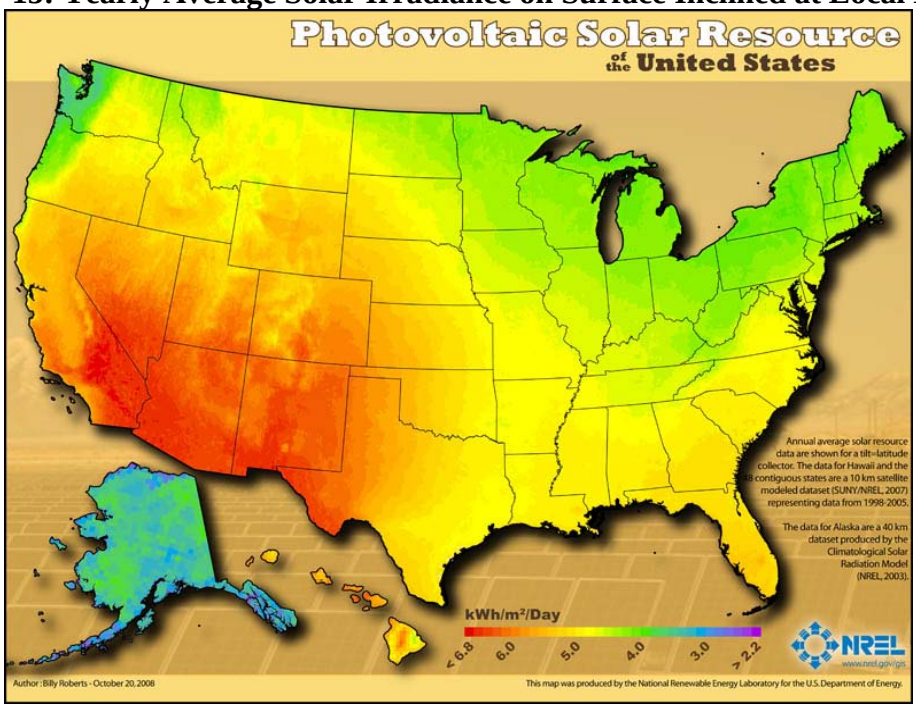

For an inclined surface at Daggett (at 35^{o} tilt angle), the typical daily incident radiation energy for each month, along with yearly averages is shown in Figure 3-16.

Figure 3-16: Monthly Variation of Daily Radiation on Surface Inclined at 35^{o} Latitude Angle

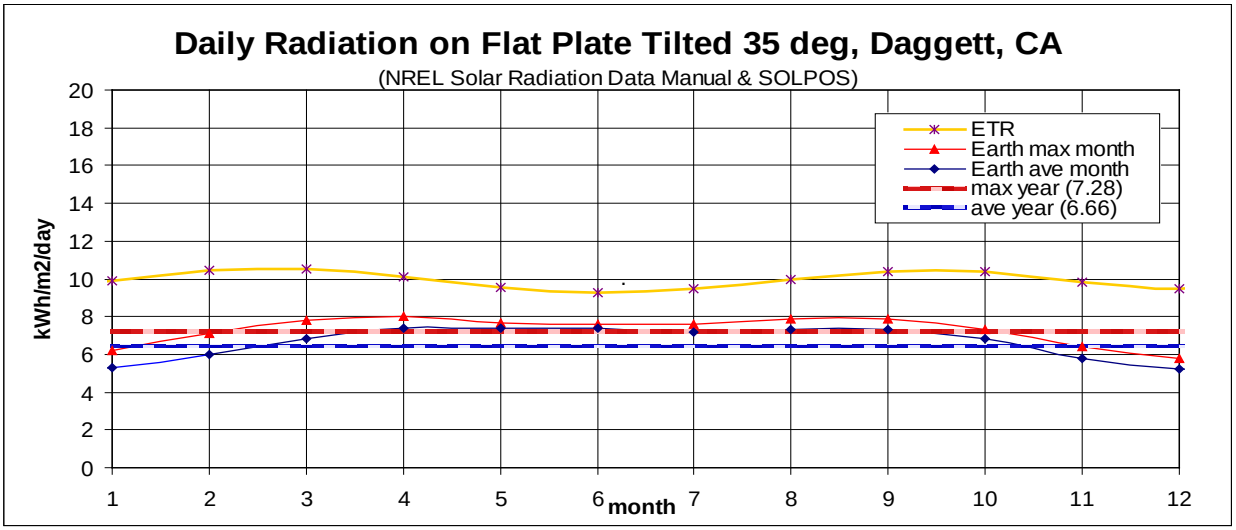

The five curves in Figure 3-16 represent: (1) Extraterrestrial radiation (ETR) incident on the inclined panel, (2) maximum level of monthly radiation, (2) average level of monthly radiation, (3) yearly mean of maximum radiation, 7.28 kW-hr/m^2/day, and (4) yearly mean of average radiation, 6.66 kW-hr/m^2/day. The ETR curve is from SOLPOS and the other curves are derived from "Solar Radiation Data Manual for Flat Plate and Concentrating Collectors".

For the radiation variation over a day at this location, the hourly solar terrestrial irradiance for a Type 3 PEC panel is shown in Figure 3-17 for the average atmospheric conditions. The four curves show the solar peak on June 21, the autumnal equinox on September 21, the spring equinox on March 21, and the solar low on December 21.

Figure 3-17: Hourly Irradiance on a 35° Inclined Surface

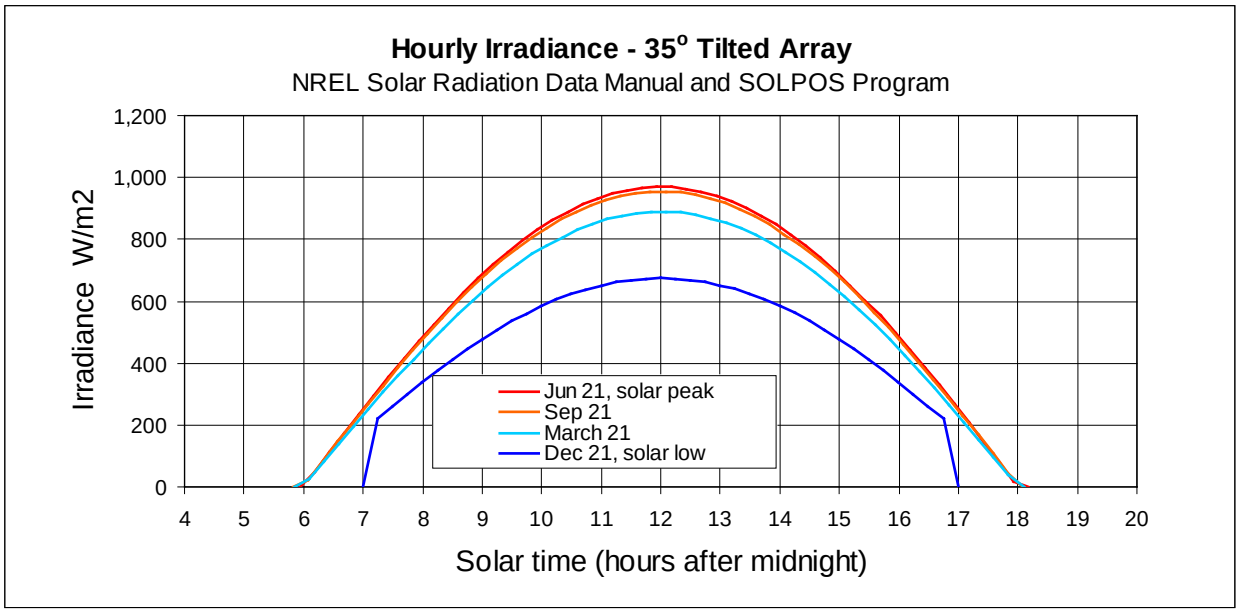

3.5.2.1 *Type 3 System Refracted Solar Input*

There are reflection and absorption losses due to the transparent Plexiglas cover on the PEC reactor cells which vary depending on sun angle relative to the cell face. Figure 3-18 is a re-plot of Figure 3-17 which takes this loss into account.

Figure 3-18: Variation of Daily Refracted Radiation on 35° Inclined Surface

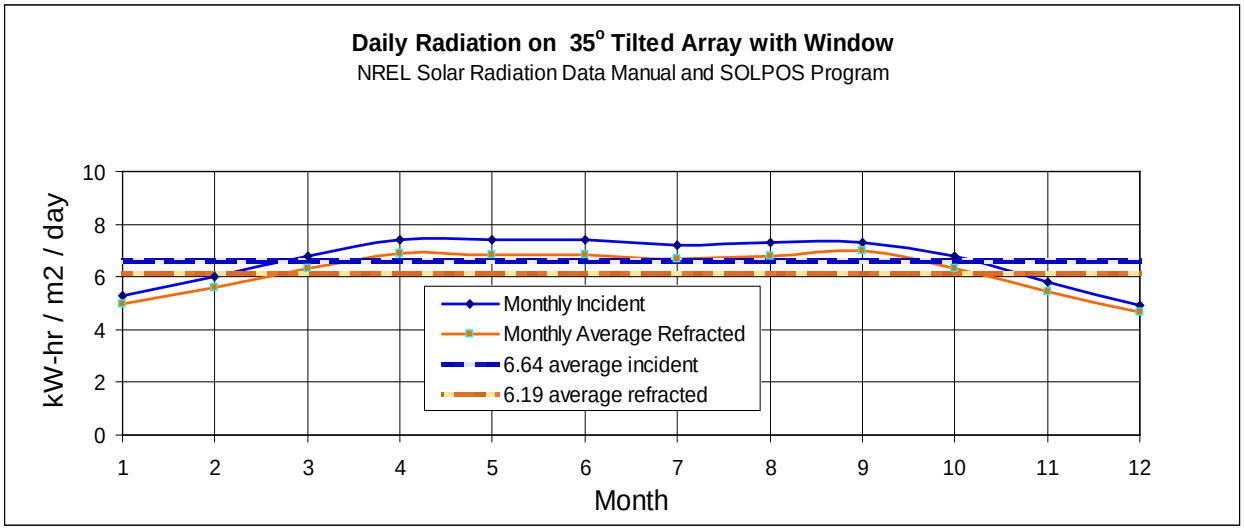

The variations in refracted energy over a day are shown in Figure 3-19.

Figure 3-19: Hourly Refracted Input Energy on 35° Tilted Panel

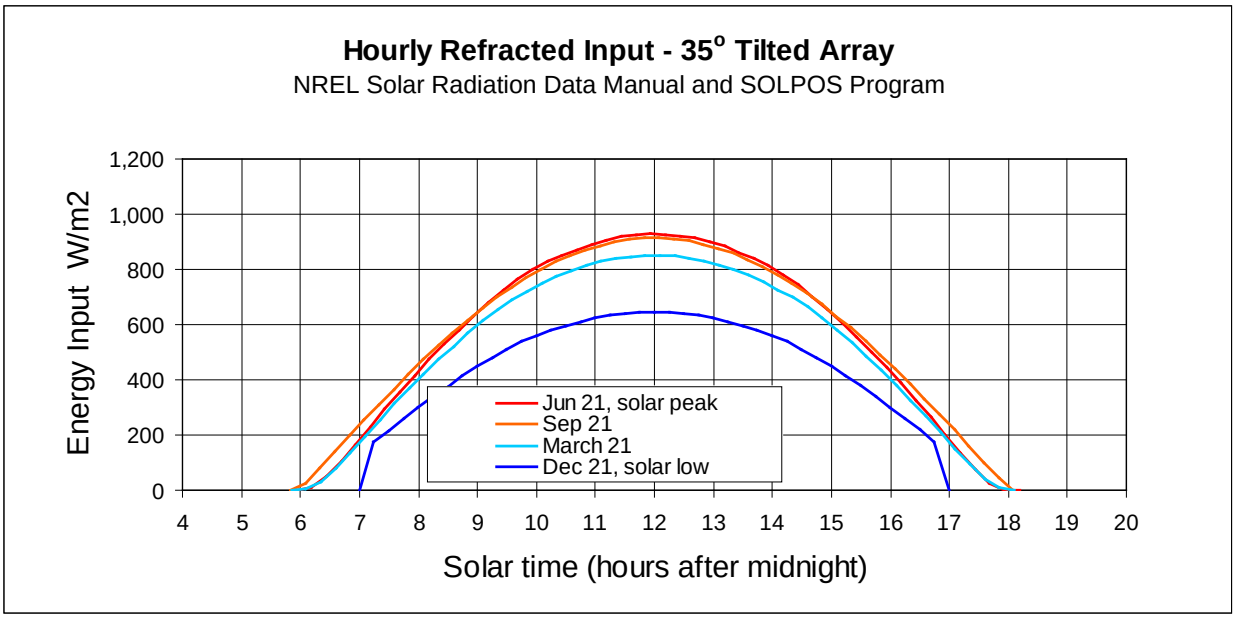

The Type 3 system is sized based on average and peak radiation. The average yearly refracted energy (Figure 3-18) determines the reactor size, and, since the system can't store output H_2 and water vapor, the instantaneous peak refracted radiation (Figure 3-19) determines the gas handling capacity:

- Module Size: Each system module is sized to produce an average of 1,000 kg H_2/day over a year, using the yearly average solar energy of 6.19 kW-hr/m^2/day (Figure 2-18).
- Gas handling subsystem size: This subsystem is sized to handle the peak hourly gas production rate reached over the year, which is based on the June 21 maximum refracted radiation of 952 W/m^2 and the resulting output constituents of H_2 and H_2O.

3.5.3 Type 4 Tracking Concentrator System Insolation

The Type 4 system reactor consists of arrays that track solar direct radiation and concentrate the energy onto the PEC receiver. While it captures the maximal solar direct, it receives only a small portion of the diffuse radiation. NREL measurements of solar direct normal irradiance over the U.S., shown in Figure 3-20, indicate substantial regions in the Southwest and Southern California where maximum average yearly irradiance is 8.10-8.31 W/m^2/day.

Figure 3-20: Yearly Average Solar Direct Normal Irradiance

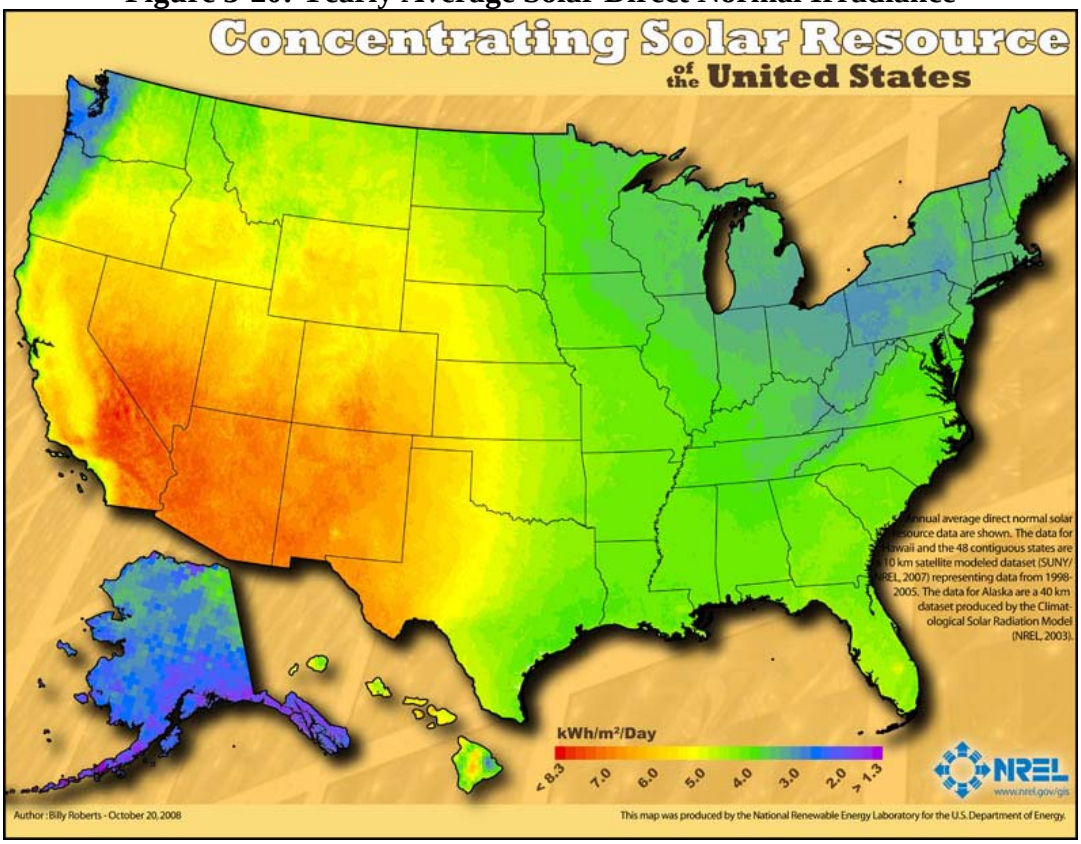

The Solar Radiation Data Manual tabulates average, minimum, and maximum radiation energy for a direct beam concentrating collector from the NSDB data. For a tracking concentrator at the 34.87^{o} North 116.78^{o} West locale, the typical daily incident radiation energy for each month, along with yearly averages, is shown in Figure 3-21.

Figure 3-21: Monthly Variation of Daily Radiation on Tracking Concentrator (No Shading)

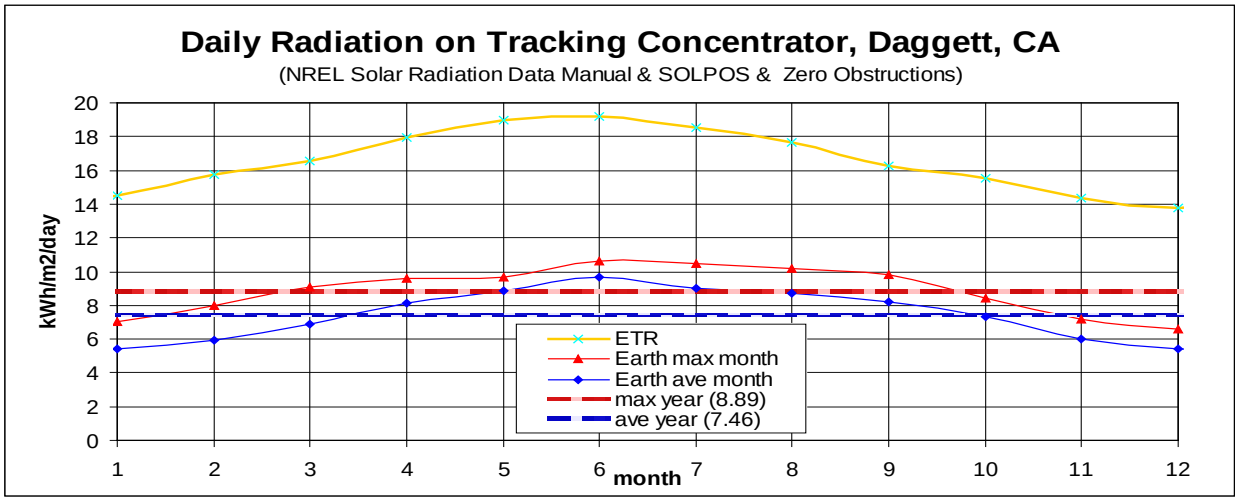

The five curves in Figure 3-21 represent: (1) Extraterrestrial radiation (ETR) incident on an unobstructed tracking concentrator, (2) maximum daily radiation for each month, (3) average daily radiation for each month, (4) yearly mean of maximum monthly radiation, 8.89 kW-hr/m^2/day, and (5) yearly mean of average monthly radiation, 7.46 kW-hr/m^2/day. The ETR curve is from SOLPOS and the other curves are derived from "Solar Radiation Data Manual for Flat Plate and Concentrating Collectors".

For the tracking concentrator, irradiance at 15 min time intervals throughout a day was calculated using SOLPOS and the NREL "Solar Radiation Manual for Flat Plate and Concentrating Collectors". Radiation is plotted in Figure 3-22 for the case with no shading.

Figure 3-22: Daily Variation of Radiation Incident on Tracking Concentrator (No Shading)

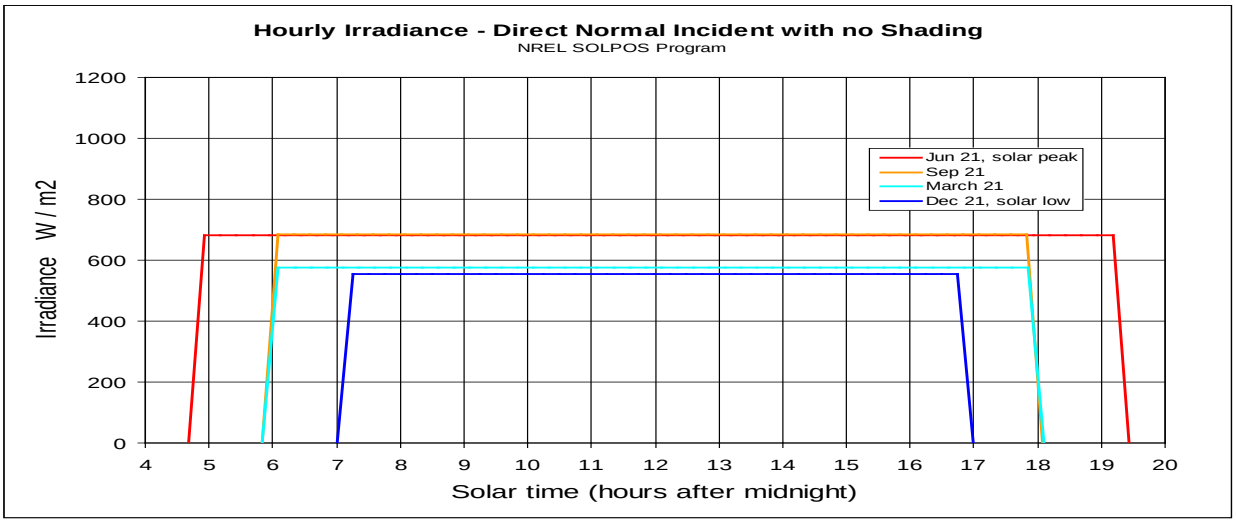

3.5.3.1 *Shading Effects*

Depending on the inter-array spacing, there is shading between adjacent arrays when the sun is near the horizon. For this design, the PEC trough reflector units are placed at intervals such that there is no shading of the reflectors at sun angles greater than 10^o above the horizon.

3.5.3.2 *Window Refraction*

Since the Concentrating Tracker is always aimed at the sun and the collector/parabolic reflector focuses the radiation approximately normal to the reactor cylindrical arc window, the window losses due to reflection are minimized, and 95% transmission is assumed. Figure 3-23 plots PV surface-received solar irradiance with this 10^o shadowing angle and window transmission loss under the following constraints:

- Concentrators aimed at sun
- No inter-trough reflector shading at sun angle > 10 degrees
- Window transmission loss of 5%

Figure 3-23: Average Day Hourly Irradiance with Inter-array Shading and Window Loss

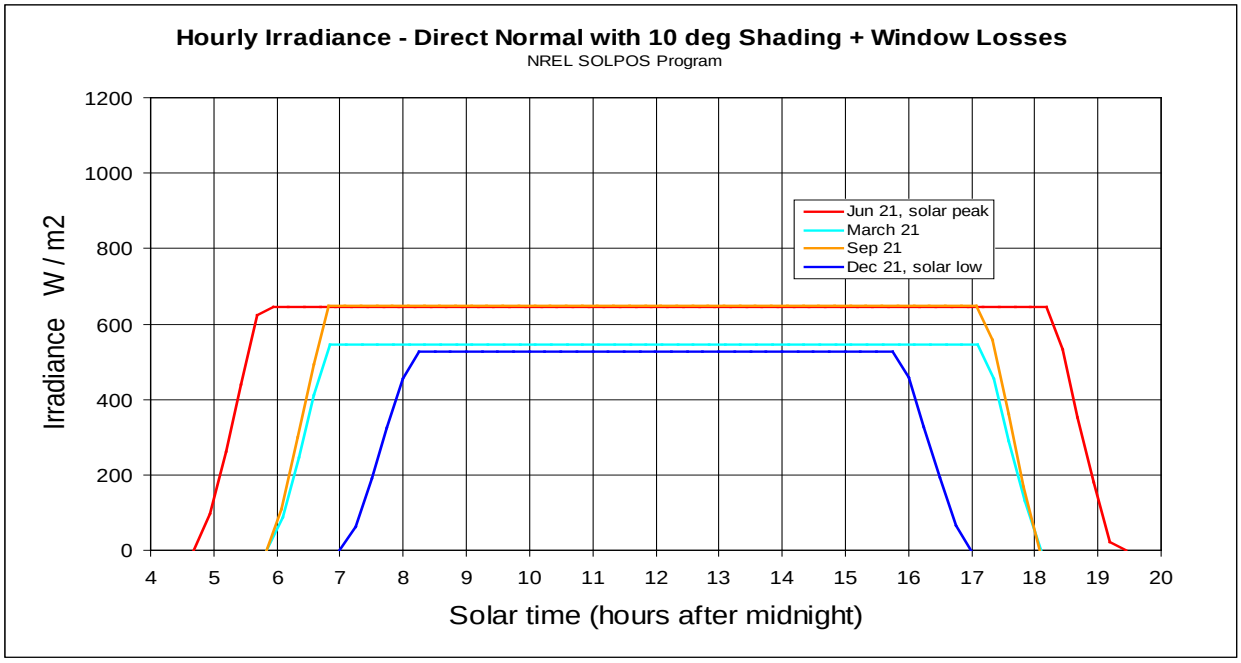

Since this system makes minimal use of the diffuse radiation component, the June 21 peak of average day transmitted radiation is 646 W/m^2 and the peak of the maximum day transmitted radiation is 1.09 times greater, or 706 W/m^2.

The daily total radiation incident on the PEC reactor with shading effects and also the radiation on the PV active surface is plotted in Figure 3-24 for an average day for each of 12 months.

Figure 3-24: Average Month's Daily Radiation on Tracking Concentrator (With Shading)

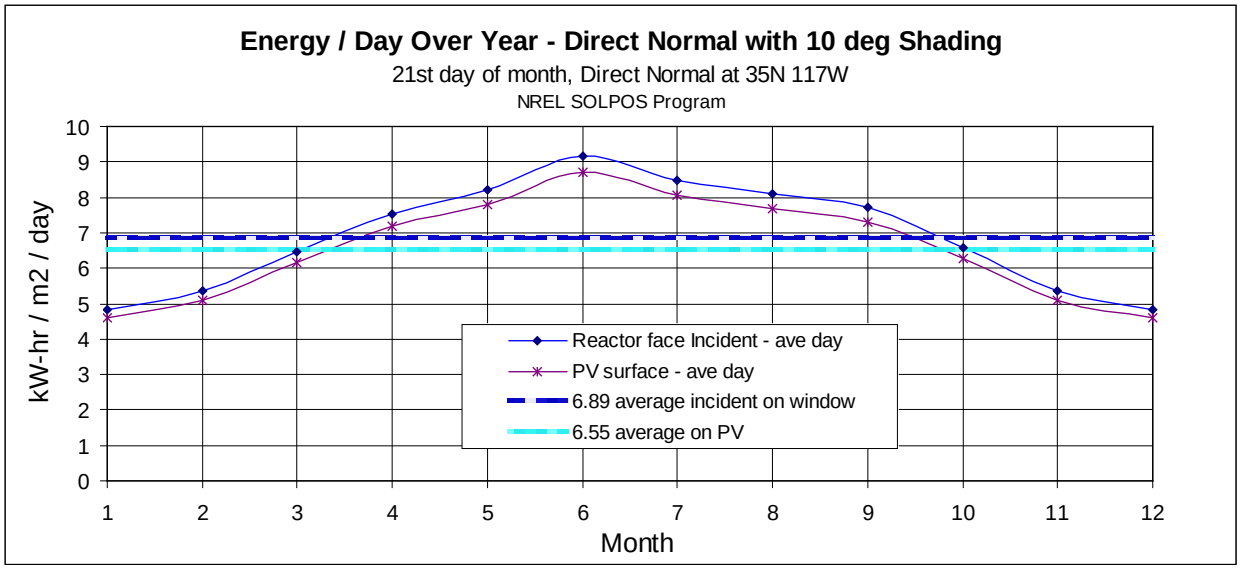

The Type 4 System is sized based on average and peak radiation. The average yearly refracted energy (Figure 3-24) determines the reactor size, and, since the system can't store output H_2 and water vapor, the instantaneous peak transmitted radiation determines gas handling capacity:

- Module Size: Each system module is sized to produce an average of 1,000 kg H_2/day over a year, using the yearly average solar energy of 6.55 kW-hr/m^2/day (Figure 3-24).
- Gas handling subsystem size: This subsystem is sized to handle the peak hourly gas production rate reached over the year, which is based on the June 21 maximum refracted radiation of 646 W/m^2 and the resulting output constituents of H_2 and H_2O.

3.6 *Solar Shadowing*

Since PEC Types 3 and 4 are not horizontally placed, when the multiple arrays or panels are deployed in the field, attention must be directed to reducing the potential shading on an array by adjacent arrays. For this reason, the arrays were placed with substantial area around them, as discussed below.

3.6.1 Type 3 Panel Separation Distance for Minimal Shadowing

Type 3 panels (1m width by 2m length) are fixed in place facing south at a 35° angle, and need only avoid undue shadowing from the southward direction. Figure 3-25 shows the geometry that allows partial obscuration at sun angles below 10°. This requires a separation distance of 8.1 meters and results in an emplacement area ratio of 4.07 m^2 of land per m^2 of panel.

Figure 3-25: Type 3 Shadowing North-South Separation Limit

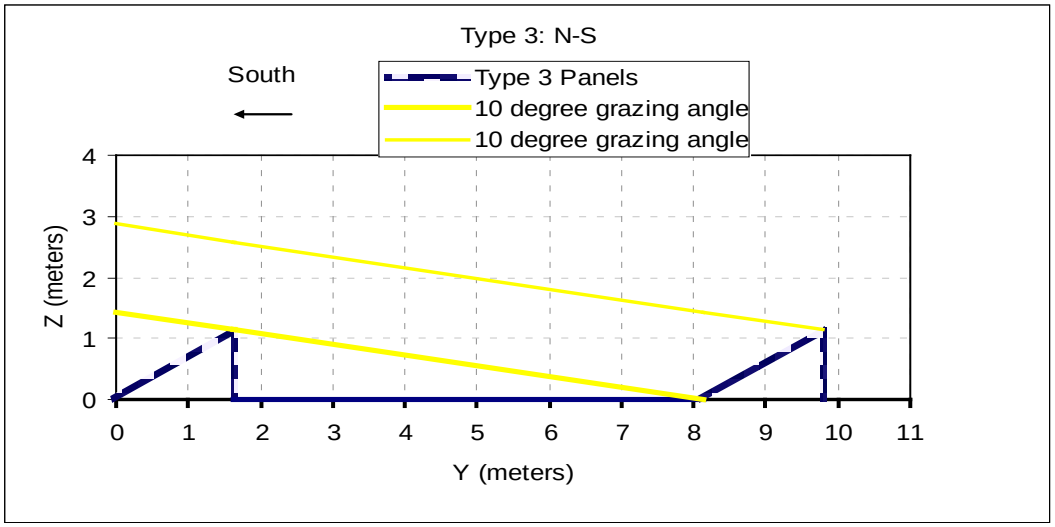

3.6.2 Type 4 Panel Separation Distance for Low Shadowing

Since Type 4 reflectors are steerable in azimuth and elevation, they must be placed to minimize shadowing in both east-west and north-south directions. The reflectors are aligned normal to the sun's rays and are 6m width by 3m height (smaller than SEGS LS-2 solar/thermal collectors that are 7.8 m wide by 5m high.) When facing directly east or west, they are placed to prevent shadowing for sun rays above 10°, requiring east-west separation of 17.3 meters (Figure 3-26).

Figure 3-26: Type 4 Shadowing East-West Separation Limit

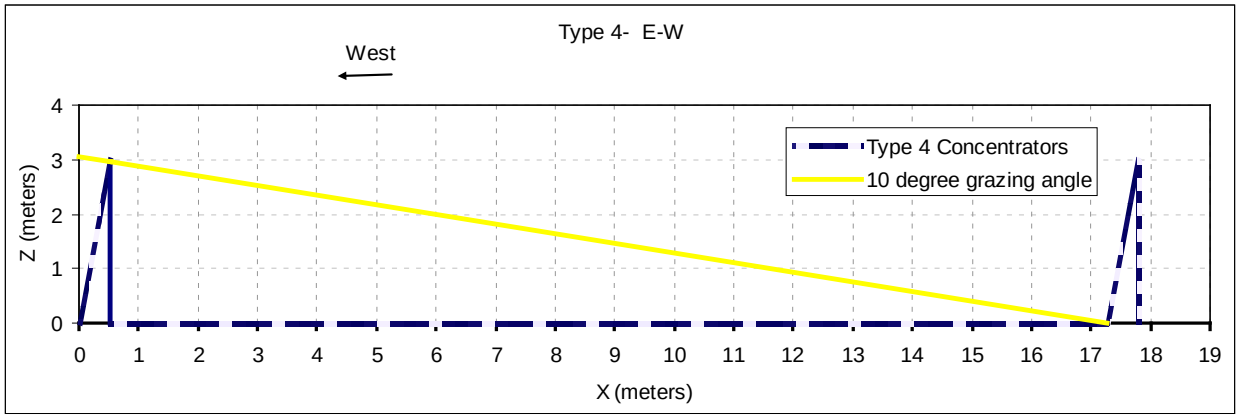

In the north-south direction, the reflectors are separated by a minimum of 6.71 m to allow clearance of the collectors when they rotate. This separation would result in shadowing only at angles below 26° at noon, an angle that prevents shadowing of the southward sun at its lowest angles, i.e., on Dec 21. (The sun is above 26° between 1000 and 1400 hours on that day and the shadowing is essentially zero.) This limit is shown in Figure 3-27.

With the East-West and North-South separations, the emplacement area ratio is 6.57 m^2 of land per m^2 of concentrator.

Figure 3-27: Type 4 Shadowing North-South Separation Limit

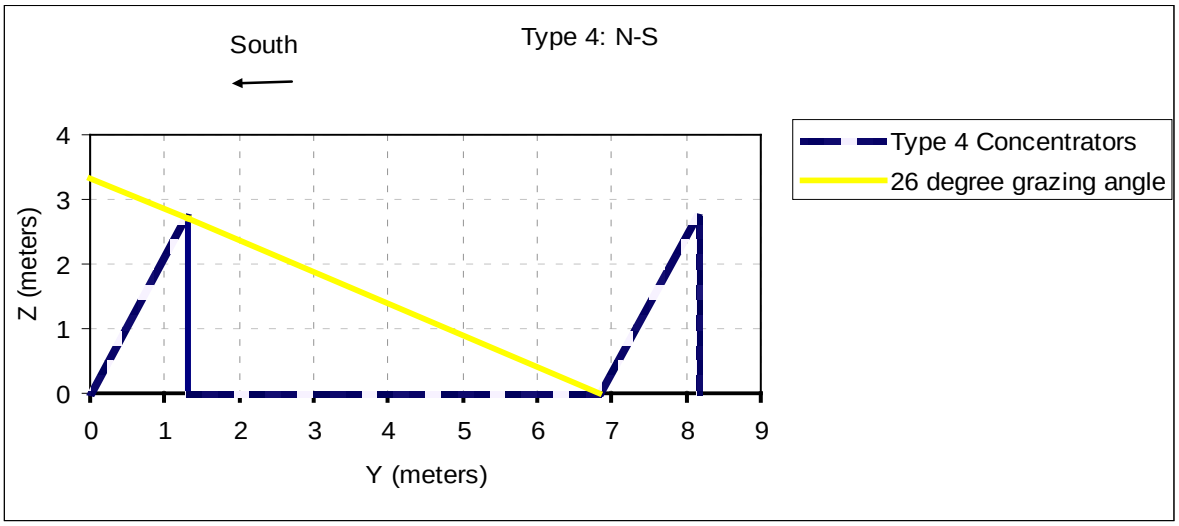

4. Photoelectrolysis Reactor Engineering Designs and Costs

The PEC production plant consists of four major components, each corresponding to a major system function:

1. PEC Reactor (for H_2 generation)
2. Gas Processing Subassembly (for centralized collection of the product gases)

3. Gas Compression Subassembly (for compression to ~300 psi to allow purification or pipeline transport)
4. Gas Separation Subassembly (for purification of the product gas to 99.999% hydrogen purity – not including water vapor fraction)

This section describes the PEC reactor types and affiliated sub-components, with the subsequent section describing the gas processing subassemblies.

Four types of PEC systems were analyzed:

Type 1: Single horizontal water bed with colloidal suspension of PEC nanoparticles

Type 2: Dual horizontal water beds with colloidal suspension of PEC nanoparticles, each bed carrying out a half-reaction

Type 3: Fixed planar array tilted toward the sun at the angle of the latitude

Type 4: Steered solar concentrator and tracker system, focusing solar flux on PEC planar element receivers pressurized to approximately 300 psi

The different system types all perform the four component functions listed above, but some systems are able to combine or shortcut specific functions by component integrations. The Type 2 and 3 systems use reactors that inherently separate O_2 from H_2 and thus their gas capture components and compressors are 2/3 the size of that for the Type 1 system and don't require a Gas Separator. The Type 4 reactor also inherently separates O_2 from H_2 and additionally performs the gas compression function within the PEC cells, using a pump to pressurize reactor inlet water, and thus the output H_2 and O_2, to 300 psi (20 atm). Therefore, the Type 4 system doesn't need a separate compressor or Gas Separator.

All systems use condensers and intercoolers to remove the water vapor to a small molar percent of the output gases without a separate water absorption unit (e.g., product gas outputs of 99.6% H_2 and 0.4% water vapor).

The basic H_2 production system modules are designed for 1 tonne H_2/day averaged over a year (i.e., 365 tonne H_2/year). For this study's calculation of H_2 production costs, it is assumed that ten of these modules are combined to reach a total goal production of 10 tonne/day. In the hydrogen production cost section of this report, the baseline cost estimates are derived for a 10 tonne/day plant.

Type 1 and Type 2 systems, use horizontal bed reactors, rather than being aimed toward the sun, and as a result have a much greater variation in hydrogen production between winter and summer (a ratio of 3.2) than the Type 3 and 4 systems. Therefore, they would have to be enlarged if the winter demand is greater than 31% of the summer demand.

The Type 1 and 2 reactors have flexible plastic film covers to capture the gas produced and are able to accumulate the gas produced over a day in the bed-cover headspace. This allows the gas handling subassembly to be sized for the average daily gas output rate over the highest production day (June 21). In contrast, the Type 3 and Type 4 systems have no inherent capacity to store gas and their gas handling is sized to accommodate the peak production occurring over the year. The Type 3 system has relatively level monthly output over the year, and the Type 4 system's December monthly output is 53% of the June output.

A unique characteristic of the PEC systems is that they don't have an upper temperature limit, as do some other solar/hydrogen production systems[13]. PEC performance is enhanced somewhat by the high water temperatures (60-70^{o}C) which can be reached in the summer. This temperature, or higher, can be reached because the enclosed water beds prevent evaporative cooling of the reactor. This study, however, assumes average, moderate temperature performance over the year and does not take an efficiency credit for any increased temperature in the summer. In the winter, the PEC reactor can operate at low temperatures, however, freezing would be a design issue on cold winter nights.

4.1 *Type 1 Single Bed Colloidal Suspension Reactor*

4.1.1 Photoelectrode Reactor Bed Particles

The Type 1 PEC system is a basic single bed colloidal suspension reactor and consists of a suspension of photo-active nanoparticles in a shallow pool, or bed, of electrolyte. The exact composition and fabrications techniques for the nanoparticles are not well-understood as the full functionality of the postulated nanoparticles has not been demonstrated in the lab, let alone in a complete system. Consequently, we have postulated a representative nanoparticle system on which to base our analysis. We model the PEC nanoparticles as 40 nm conductive substrate particles onto which ~5nm thick anodic and cathodic photo-active coatings are deposited, as shown in Figure 4-1, resulting in a multi-layer PV unit with multi-photon response to achieve the requisite electrolysis voltage from a combination of below-threshold-energy photons. The voltage and associated electrolysis reaction is generated by multiple photons absorbed by the photo-active particle. Total voltage generated by incident photons for electrolysis must exceed approximately 1.4V. (With particulates, due to low current density, overpotential requirements can be less than the 1.6V threshold of planar electrode PEC cells).

The PEC nanoparticle material system details have not been well defined through experimental data, so reasonable extrapolations were made from the current knowledge base. However, in consultation with the PEC Working Group, we model the nanoparticles as 40nm diameter Fe_2O_3 particles coated with an additional photoactive layer. These materials will likely change as development continues, but are meant to be cost surrogates for the future functional materials.

For the Type 1 system particles, both hydrogen and oxygen are evolved from the surface of the nanoparticle. Consequently, both the anodic and cathodic materials must be in contact with the electrolyte to facilitate the electron transfer to the hydrogen and oxygen ions in the electrolyte. Thus while we describe the layers as being 5nm thick, this is primarily for purposes of material

[13] Biological hydrogen production systems, which fundamentally are solar conversion systems, have strict temperature limits to maintain the life/productivity of the organisms.

usage calculation, as the 5nm layer may in actuality coalesce into very small diameter droplets on the surface of the 40nm substrate particle as shown in Figure 4-1.

Figure 4-1: Type 1 PEC Nanoparticle Structure

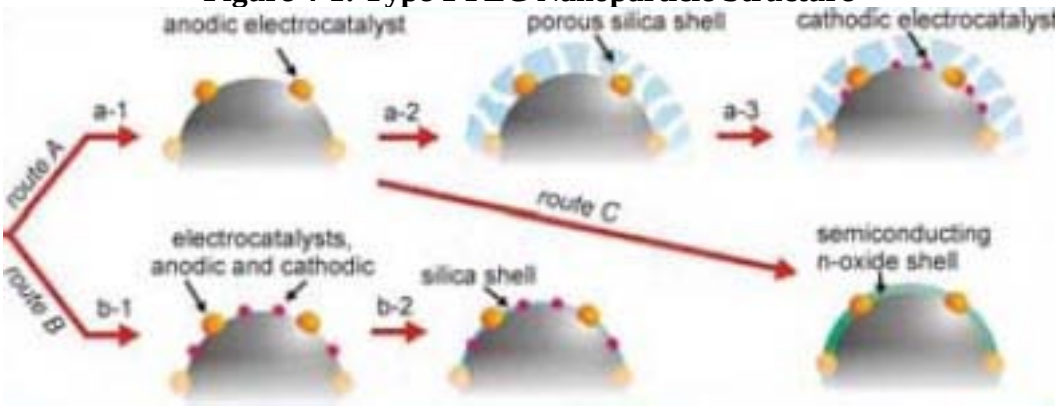

Basic research on fabrication and testing of these particles is ongoing at UCSB [14] and numerous other locations. Figure 4-2 shows electron micrographs of particles fabricated at UCSB.

Figure 4-2: PEC Nanoparticle Micrograph

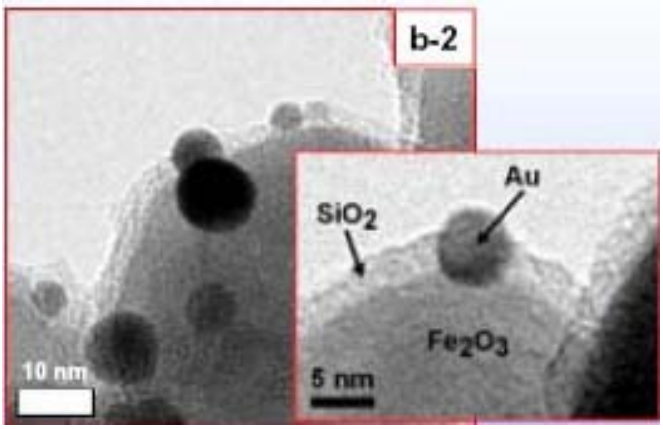

UCSB in lab tests has demonstrated an Incident-Photon-to electron Conversion Efficiency (IPCE) peak value of 2.5% at 360nm (3.4eV) with zero bias voltage, and values to 10% have been predicted. UCSB lab results[15] in 2007 on α-Fe_2O_3 nanorods with RuO_2 catalyst and with 0.1V applied bias achieved a PEC efficiency of 1.6%. The stated goal of this UCSB project is to achieve a Chemical conversion process Efficiency (CE) of 10% and an STH efficiency of 8%.

For the current study, we have assumed that a baseline STH of 10% can be achieved with more optimal nanoparticles For this performance, we assumed that the small photoactive particles are pervasive over the surface of the 40nm diameter substrate particle and thus, of the incident

[14] "Development and Optimization of Cost Effective Material Systems for Photoelectrochemical Hydrogen Production", Eric McFarland, University of California-Santa Barbara, Project ID # PD-38 presented at the 2008 DOE Hydrogen Program Review, Washington, DC., 12 June 2008.

[15] "Photoelectrochemical Hydrogen Production Using New Combinatorial Chemistry Derived Materials", DOE Hydrogen Program FY2007 Annual Progress Report, Program II.G.7, McFarland, E. , UCSB

photons that are captured, a significant percentage of them can generate a photoelectric voltage. It is additionally assumed that the slurry of these particles in the reactor bed is at a sufficiently high concentration that all incident photons will strike the substrate particles. Light extinction analysis conducted by Eric McFarland at UCSB indicates that a bed depth of 10 cm for a nanoparticle size of 40nm and a particle concentration of 200 nm equivalent thickness[16] of 40 nm particles is sufficient to capture all light entering the bed. An advantage to using more dilute particles and deeper beds is the mass transfer rate from the bulk to the particle becomes inconsequential. Consequently these parameters have been adopted for this analysis.

4.1.2 Nanoparticle Fabrication and Cost

Cost of the PEC nanoparticles is based on a slurry coating process of a substrate particle. As stated previously, the exact material composition has not yet been finalized. For purposes of cost estimation, the PEC nanoparticles are modeled as 40 nm particles of iron oxide (Fe_2O_3) upon which 5 nm layers of TiO_2 have been deposited[17]. The slurry deposition method is analogous to the Niro Precision Coater[18], a pharmaceutical coating technology used to precisely apply multiple layers to pills. Major coating assumptions are shown in Figure 4-3.

Figure 4-3: Particle Coating Major Assumptions

Parameter	**Value**
Iron Oxide[19] Material Cost (40nm diameter Fe_2O_3)	$188/kg
Titanium Oxide[20] Material Cost(<5nm particles)	$278/kg
Coating System Capital Cost	$2.5M
Number of Spray Nozzles	5
Coating Material Mass Flow Rate per Nozzle	7.84 kg/h
Slurry Solids Content	14%
Markup Rate[21]	35%

Coating of 30nm iron oxide particles (for medical purposes) has been demonstrated by Emory University and Georgia Tech for organic coatings using a liquid coating process in chloroform.[22].

A brief DFMA-style (Design for Manufacture and assembly) analysis of the PEC nanoparticle cost based on the above parameters suggests a cost of $304/kg in production quantities of 41,600 kg/year (based on production of a 500 TPD H_2/year capacity, with 74.6 kg of nanoparticles per 1 TPD module and 500 modules per year) and is shown in Figure 4-4: PEC Nanoparticle Production Cost Breakdown . Variation in nanoparticle cost with annual production rate is displayed in Figure 4-5: Nanoparticle Cost vs. Annual Production Rate .

[16] Equivalent thickness is defined as the depth of the particle layer if all particles settled to the bottom

[17] The material usage for the outer layer is calculated as if it was a continuous 5nm thick layer. However, in actuality the outer layer would most likely be a discontinuous layer of small diameter particles

[18] http://www.niroinc.com/pharma_systems/fluid_bed_coating.asp

[19] Cost of the Fe_2O_3 is obtained from a price quote from Reade Advanced Materials in purchases quantities of 10kg.

[20] Cost of the TiO_2 is obtained from a price quote from Reade Advanced Materials in purchases quantities of 10kg.

[21] A percentage markup is applied to the base material plus manufacturing cost to account for scrap, G&A, R&D, and profit.

[22] J. Phys. Chem. C, Duan, H., Kuang, M., Wang,. X., Mao, H., Nie, S., future 2009 publication

Figure 4-4: PEC Nanoparticle Production Cost Breakdown

	$/kg
Materials	$209
Coating	$17
Markup	$79
Total	$304

Figure 4-5: Nanoparticle Cost vs. Annual Production Rate

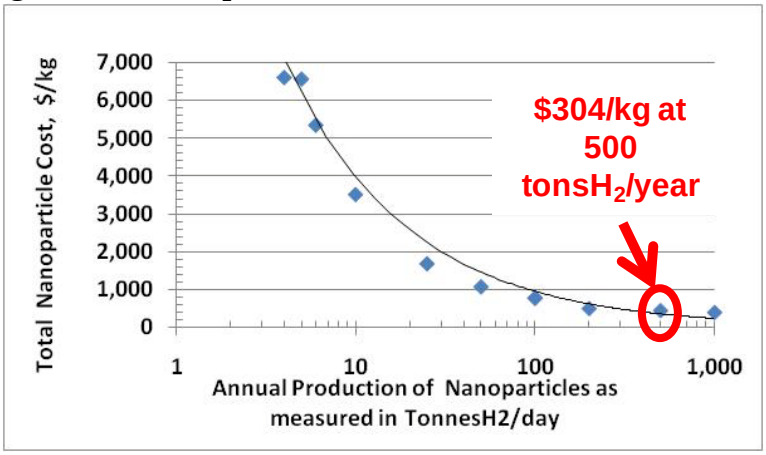

A precipitation method of nanoparticle production is currently used by researchers at UC Santa Barbara to produce Fe_2O_3 particles. The procedure[23] consists of adding an aqueous solution of Iron (III) chloride dropwise in a stirred solution of aqueous base pH>10 (e.g., sodium bicarbonate, sodium hydroxide, etc.). Iron oxide nanoparticles are the precipitate product with particle size controlled by temperature or the rate of iron chloride addition. Particles are separated by filtration or centrifuge and washed with water. This pathway offers a low cost pathway to iron oxide nanoparticle production, perhaps a lower price than the $188/kg used in the analysis based on an actual industrial price quote. However, as shall be discussed in the cost summary, even at $304/kg, the coated nanoparticles only add a small amount to the total capital cost of the 1TPD module (74.6 kg x $304/kg = $22,679 out of $1,070,485 of total uninstalled system capital cost for the Type 1 System). As a result, the final cost of PEC H_2 in $/kg is quite insensitive to PEC nanoparticle cost.

4.1.3 Type 1 Solar-to-Hydrogen Conversion Efficiency

The effective solar-to-hydrogen (STH) conversion efficiency of the nanoparticle system is of obvious importance to the economic evaluation. Single particle PEC for water splitting has been demonstrated with both UV and visible light[24], however, the efficiencies are far below the target value of 10%. A means of protecting the hydrogen evolution sites on the particle from the energy-losing back-reaction has also been demonstrated. In light of the lack of a fully

[23] Private communication with Arnold Forman, University of California at Santa Barbara.
[24] Photocatalyst releasing hydrogen from water, Maeda, K., Teramura, K., Lu, D., Takata, T., Saito, N., Inoue, Y and Domen, K., Nature 440, 295 (16 March 2006)

demonstrated PEC nanoparticle water-splitting H_2 production system, and in consultation with the PEC Working Group, we assume future PEC Type 1 reactors will achieve an STH of between 5% and 15%, with the nominal value of 10%. This range is not obtained by rigorous first principle computation but rather was felt by the Working Group to be a credible estimate of future system performance. Consequently, we have used that range in our system analysis.

Figure 4-6 displays the reactor STH bounds used in the cost analysis. Note that these STH conversion efficiencies reflect only reactions within the reactor bed: they do not include hydrogen losses through the HDPE film, hydrogen losses due to gas separation, or lost hydrogen associated with maintenance or plant down-time.

Figure 4-6: Type 1 System STH Bounds

Lower Bound STH	Nominal STH	Upper Bound STH
5%	10%	15%

4.1.4 Type 1 Reactor Bed

The reactor bed, diagrammed in Figure 4-7, is filled with water, nanoparticles, and an electrolyte (e.g., 0.1M KOH), and covered by a transparent plastic film which captures H_2 and O_2 products of the reaction along with water vapor (water vapor quantity depends on vapor pressure at bed temperature). The plastic film further prevents large scale evaporation of the water from the bed.

Figure 4-7: Type 1 Colloidal Suspension Reactor

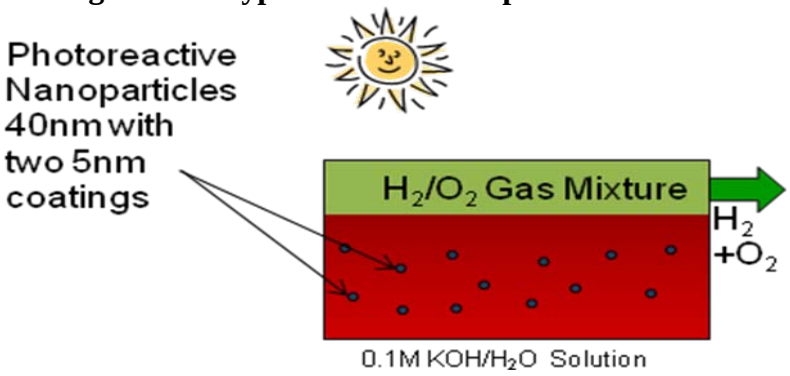

Several reactor bed designs have been examined to determine the most cost effective physical embodiment. For the single and dual bed colloidal suspension reactor systems, the two main designs considered were a plastic film-covered trough and a continuous bag, or baggie, made of plastic film.

The bed area is determined by the available solar flux (see section 3.4) and the effective solar-to-hydrogen conversion efficiency. The depth of the reactor bed and particle concentration are matched to ensure full photon capture and utilization by the PEC nanoparticles. If concentration is too dilute for a given total depth, light will penetrate to the bottom of the bed and photons will be absorbed by the bottom surface. Should the particle concentration be too high, photons will be fully absorbed in only the upper layers of the bed. The particle concentration and bed depth

also impact specifications for other system components such as pumps and valve sizes and type of mixing equipment. For this design, a depth of 10 cm was arrived at through discussions with UCSB as a start towards optimizing the mass transfer, current density, and mixing considerations.

4.1.5 Bed Trough System

The first embodiment considered for the colloidal suspension reactor was a covered pond trough system. It consists of a series of long shallow troughs with transparent film window covers, allowing light to penetrate while containing product gasses. Due to the large area required for a 1 tonne H_2/day system, the total system reactor would be comprised of multiple reactor beds, each measuring approximately 1060 ft long, 40 ft wide, and 10 cm deep. Width is limited by the dimensions of available transparent films and the convenience to carry the rolls on a standard 55 foot length truck. The film is sealed to a frame on the trough so as to maintain a gas-tight seal with respect to the trough. Each reactor bed has inlet ports for the water reactant and outlet ports for the product gases. Driveways are interspersed between troughs to provide vehicular access. For a 1 tonne/day system with 10% STH efficiency, there are 18 troughs needed.

4.1.6 Continuous Bag (Baggie) System

In contrast to the trough system, the baggie system would not need the substantial trough fabrication work and would not need a separate continuous trough-to-window sealing mechanism, reducing reactor cost. Site preparation would still be needed to contour the surface on which the baggies are contained (i.e. make a flat surface), but this will be significantly less involved than the trough system preparation. Baggies will consist of a transparent polyethylene cover that is heat-sealed to an opaque, thicker polyethylene for the bottom. A thicker layer is used on the bottom to provide abrasion protection from the bare ground on which the baggie will sit. The bags will have ports built into them for addition of water and removal of product gasses. Each baggie bed will be of approximately the same dimensions as a trough system bed (~1060 ft x 40ft x 10cm) and will have driveways between them for easy access.

A second option for baggie fabrication is to produce the bag in one long continuous sleeve from transparent polyethylene using a continuous tube extrusion process. This represents simplified manufacturing over the two-piece baggie systems as it requires fewer parts and sealing only at the ends. While such machinery exists for production of much smaller bags, it is not certain how effectively this process can be scaled up for 40 ft wide bags. Consequently, the extruded sleeve baggie was not selected for cost analysis even though that embodiment it quite attractive due to its simplicity. After analysis of engineering issues and costs involved in both bed options, it was determined that the baggies would be substantially less complex and more cost effective than the trough systems. End and top views of the baggie configuration are shown in Figure 4-8 and Figure 4-9.

Figure 4-8: End View of Type 1 Baggie Configuration

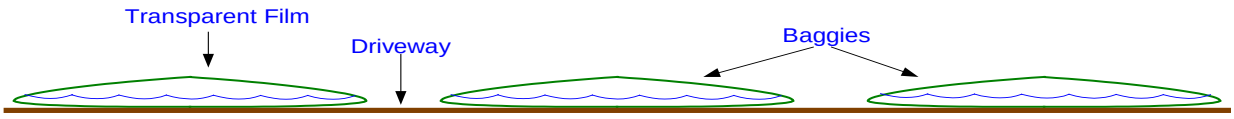

Figure 4-9: Top view of Type 1 Baggie Configuration

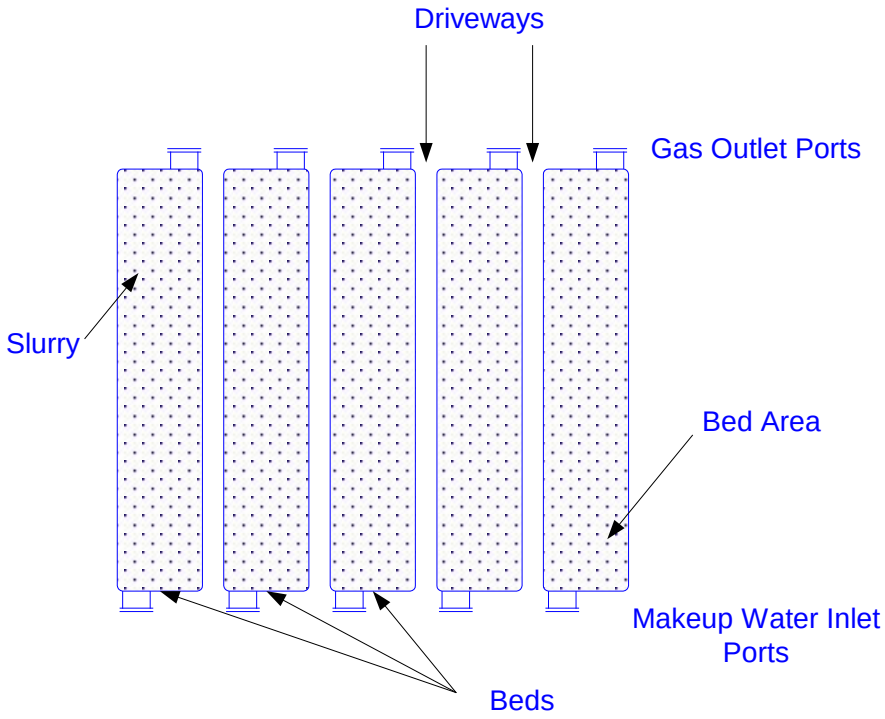

4.1.7 Plastic Films

The baggie top layer will consist of a transparent high density polyethylene (HDPE) film to transmit sunlight and keep the product gases from escaping. This top layer is sealed to a thicker HDPE bottom liner.

An NREL[25] report by Daniel Blake concerning hydrogen reactors indicates that the hydrogen permeability coefficient for high density polyethylene is approximately 156 $cm^3 \bullet mm/m^2 \bullet atm \bullet day$. Using this factor, the volume of hydrogen lost through the 6 mil HDPE film for the Type 1 system is 4.33 kg/day, which is 0.39% of the total output. This could be decreased by increasing HDPE film thickness or by using a less permeable film such as Tedlar, which is significantly more costly than HDPE. This hydrogen loss is minor and therefore ignored in this report.

Based on data from Berry Plastics[26], the transparent HDPE[27] film transmits an average of 90% of incident light. It is available in rolls up to 56 ft wide and more than 1000 ft long and, therefore, a single continuous roll of film is able to serve as the top or bottom layer of a baggie. The flat oval

[25] Blake, Daniel M. "Hydrogen Reactor Development and Design for Photofermentation and Photolytic Processes". NREL Project PD19. May 23-26, 2005.
[26] Agriculture Films by Berry Plastics. http://www.covalenceplastics.com/site/content/agricultural/agricultural. Date Accessed 18 July 2008.
[27] In discussions with Berry Plastics, LDPE was substituted for HDPE. However, volume quotes of the base LDPE and HDPE polymer from polymertrack.com indicate that the prices of the two are comparable, and thus we will use HDPE in the analysis due to its increased hydrogen impermeability

cross-section of the baggie containment package will allow for the volume expansion that occurs due to varying output hydrogen production rate occurring over a full day due to varying solar insolation over the 24 hour period. Thus far it appears that the limiting factor in bed width is the width of the plastic film roll sizes, since it is undesirable to bond multiple sheets of HDPE to increase bed width.

4.1.8 Ports

Ports are installed in the HDPE bag for removal of product gasses and addition of reactant water. For these ports, we have assumed a molded port cost of $15 each and an additional 15 minutes fabrication time for port-to-baggie installation. Given a standard labor cost of $1/minute, this amounts to a $30 total cost per port. The specifications and costs of the ports are shown in Figure 4-10.

Figure 4-10: Port Specs and Installation Costs

Port Costs	
Material cost	$15
Installation labor	15 min
Labor Rate for installation	$1/min
Total installation labor cost	$15
Total port cost	$30
Number of ports needed	
Per bed	12
Width of bed	40 ft
Length of bed	1060 ft

4.1.9 Laminating and Sealing Machines

The physical creation of the baggies involves laminating the edges of the top and bottom polyethylene layers, sealing the ends, and installing the ports. We assume a simple laminating process that thermally melts one HDPE film layer into another upon compression between two heated rollers. We further postulate a laminating speed of 0.5 feet/sec using a $100,000 machine. We additionally assume a 15 minute loading and unloading time. For end sealing, we envision a static laminating machine (i.e., without rollers), that costs $20,000 and can seal three foot lengths at a time, with an 8 second application time, resulting in sealing of the 40 foot width in two minutes. We also assume an extra 10 minutes of sealing for each corner of the bag. The production time for sealing a single bag is shown in Figure 4-11.

Figure 4-11: Production Specifications for Laminating and End Sealing Machines

Laminating Machine		
Speed	ft/sec	**0.5**
Length Baggie	ft	**1060**
Load/Unload Time	min	**15**
Sides/Bag		**2**
Time to Seal	min	160.7
End Sealing Machine		
Seal Length	ft	**3**
Width Baggie	ft	**40**
Time/Seal	min	**2**
Ends/Bag		**2**
Time/Corner	min	**10**
Time to Seal	min	93.3
Bag Production Time	min	254

4.1.10 Bed Headspace Considerations

Over the daily cycle of production, hydrogen production varies from a maximum at noon to zero during the dark hours. It is desirable to size the gas processing system for the average daily output of hydrogen and oxygen rather than for the noon peak. In order to accomplish this, the bed headspace between the water and the HDPE film must be able to lift sufficiently to contain the gases and thereby average out the output gas flow to the gas processing system. Expansion of the headspace with gas production over a day was examined for the Type 1 system for the worst case of the maximum solar day, June 21. Assuming 10% conversion of solar energy to H_2 and O_2 , the volume increase necessary to accomplish this, results in a maximum average lifting of the middle of the cover by 28.9 cm (11.3 inches) when the gas is at 60^{o}C (140^{o}F) to contain the H_2, O_2 , and vapor H_2O outputs. This is well within the expansion capacity of the 40 ft wide bag, which is a flattened oval with a very low aspect ratio, when fully expanded (see Figure 4-12). Note that the baggie does not stretch; rather, it is just becoming slightly more circular in cross section.

Figure 4-12: Headspace Daily Vertical Rise in 40 ft Wide Bed (to scale)– June 21

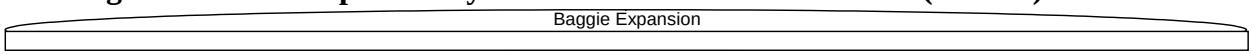

4.1.11 Capital Costs

The hydrogen production system is anticipated to have a 20 year operational lifetime. However, the transparent film is susceptible to UV degradation which causes the film to haze and become less transparent. Thus the capital costs shown below are only for the initial reactor: replacement costs are considered to be an operational and maintenance (O&M) expense. In our cost analysis we assume the baggies are good for 5 years. All other components of this subassembly are anticipated to last the entire plant life of 20 years. We have further assumed that the baggies would be purchased from an outside manufacturer. Assumptions for the Capital Cost Recovery and Capital Costs of this outside manufacturer are shown in Figure 4-13 .

Figure 4-13: Capital Recovery Factor for Baggie Production (1 tonne/day H_2)

Capital Recovery Factor		
Average Machinery Lifetime		**10**
After tax rate of return(discount rate)		***10%***
Corporate Income Tax Rate		***40%***
Capital Recovery Factor		0.205
Capital Cost Repayment		
Laminating Machine Cost	$	**$ 100,000**
"Seal a Meal" Machine Cost	$	**$ 20,000**
Winders Cost	$	**$ 35,000**
Number of Winders Needed		**3**
Installation Factor		**1.4**
Total Capital Cost	$	$ 315,000
Capital Recovery Factor		0.205
Baggies/System		**20**
Hours/Shift	hr	**7**
Shifts/Day		**1**
Working Days/Year	days	**240**
Production Capacity	Systems/year	32
Annual Payment per system to recover capital	$	$ 2,003

4.1.12 Type 1 Reactor Cost Summary

The components and component costs needed for a Type 1 reactor are listed in Figure 4-14. The top transparent material area of the baggies is 70,940 m^2. The 1.3 in. sealing seam width reduces photon capture area to 70,540 m^2.

Figure 4-14: Type 1 Reactor Capital Costs for 1TPD

Reactor Component	Quantity	Unit cost	Overall cost
Reactor H2 Average Production	1,111 kg/day		
Baggie cost total	18 baggies		
bag material-top	70,940 m2	$ 0.54 /m2	$ 38,091
bag material-bottom	70,940 m2	$ 0.47 /m2	$ 33,154
total			$ 71,245
port hardware 12 /baggie	216 ports	$ 15.00 each	$ 3,240
port installation 12 /baggie	216 ports	$ 15.00 each	$ 3,240
assembly labor	18 baggies		$ 9,144
payment for capital recovery			$ 1,849
markup factor			1.5
total baggie cost	18 baggies		$ 133,077
Baggie Roll-unroll system	1	$ 37,000.00	$ 37,000
forklift	1	$ 18,571.00	$ 18,571
Coated PEC nanoparticles	74.598 kg	$ 304.00	$ 22,678
Make-up water pump	1	$ 213.00	$ 213
Make-up water manifold pipes	1,380 ft	$ 0.52	$ 718
Total Baggie Reactor Cost			$ 212,257

4.2 *Type 2 Dual Bed Colloidal Suspension Reactor*

The second type of colloidal suspension reactor is one which employs separate beds for the O_2 gas production reaction and the H_2 gas production reaction, and which are linked together with diffusion bridges. A 0.1M KOH electrolyte is common to both beds and facilitates transport of ionic species. These beds also contain an intermediary reactant denoted "A", which participates in the reactions, but is not consumed. "A" can be iodine, bromine, iron or other elements. A typical set of equations describing the nanoparticle photoreactions is:

Bed I: 4 photons + 4 A + 2 H_2O => 1 O_2 + 4H^+ + 4 A^-
Bed II: 4 photons + 4H^+ + 4 A^- => 2 H_2 + 4 A

4.2.1 Photoelectrode Reactor Bed Particles

In the Type 2 dual bed colloidal suspension reactor, there is a suspension of nanoparticles contained within the water/electrolyte solution within each shallow reactor bed. The nanoparticles are similar to the Type 1 system nanoparticles (see section 4.1.1) in structure and fabrication method. As shown in Figure 4-15, both nanoparticles (i.e. those for the H_2-production bed and those for the O_2-production bed) are modeled as 40 nm photo-active substrate particles onto which 5 nm photo-active coatings have been deposited. Like the Type 1 system, full functionality of the dual-bed water splitting approach has not been demonstrated with 10% efficiency for hydrogen, however, several lower efficiency implementations have been demonstrated (e.g., at Florida Solar Energy Center). Consequently, the material system is ill-defined. While it is likely that different materials will be used for nanoparticles in the two beds, for cost analysis, we have modeled the Type 2 nanoparticles systems as consisting of Fe_2O_3 substrate particles with a deposited photoactive layer. The voltage and associated electrolysis reaction is generated by multiple photons absorbed by the composite particles. The basic research on the fabrication and testing of these particles is ongoing at UCSB and other universities.

Figure 4-15: Type 2 PV Nanoparticle Structures

4.2.2 Nanoparticle Cost for Type 2 System

Nanoparticle fabrication for the Type 2 system is similar to that of the Type 1 system. The exact material system for both systems is not known so we select to model them identically even though in reality they would contain different materials. Because Type 2 systems use two beds and have effectively half the conversion efficiency of Type 1, twice as many particles are needed for the same H_2 output. Type 2 systems therefore require 134.2 kg of particles for a 1 TPD module and would cost $40,798 at $304/kg.

4.2.3 Type 2 Solar-to-Hydrogen Conversion Efficiency

Because the overall water splitting reaction occurs in two reactions, the bandgap requirements for each reaction are expected to be lower than the nominal 1.4-1.5 V bandgap of single step Type 1 reaction. Consequently, the partial reactions might be thought of as being "easier". However, two beds are required. Thus in the absence of knowledge of the appropriate material system, it is impossible to calculate the expected photon to H_2 (or O_2) conversion and thus the area of the beds. So we make the simplifying assumption that the H_2 and O_2 production beds will be equal in area, and that the H_2 bed will be about the same area as an equivalent production Type 1 bed (even though it only conducts a partial water splitting reaction). Under these assumptions, the Type 2 system will have half the STH conversion efficiency of a Type 1 system. Thus, for cost analysis purposes we use a nominal 5% STH efficiency to reflect the energy of H_2 produced divided by the solar energy incident on both beds.

Figure 4-16 displays the reactor STH bounds used in the cost analysis. Note that these STH conversion efficiencies reflect only reactions within the reactor bed: they do not include hydrogen losses through the HDPE film, hydrogen losses due to gas separation, or lost hydrogen associated with maintenance or plant down-time. The STH value is half that of the Type 1 system because the necessary photon capture area is doubled.

Figure 4-16: Type 2 System STH Bounds

Lower Bound STH	Nominal STH	Upper Bound STH
2.5%	**5%**	**7.5%**

4.2.4 Type 2 Reactor Bed

The Type 2 dual reactor beds are diagrammed in Figure 4-17. Each bed is filled with a dilute electrolyte containing the "A" component and the nanoparticles. It is covered by a transparent plastic film which contains the gaseous products of the reaction and prevents evaporation. O_2 and H_2 are removed from the respective beds. The beds are connected with liquid communication bridges below the waterline, containing fabric mat barriers which allow diffusion of ions in the electrolyte, but not gas bubbles. There is active circulation of solutions within each bed using perforated pipes through which the solution is pumped to maintain a uniform concentration of species within the bed. The ions and atoms are transported across the bridges between the beds by diffusion.

Figure 4-17: Type 2 Dual Bed Colloidal Suspension Reactor

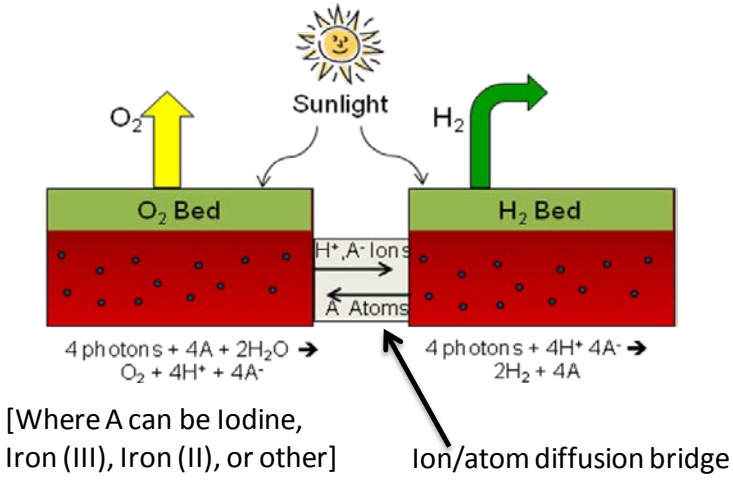

As with the Type 1 single bed system, a baggie system is utilized, but with the added feed-through bridge passages between each pair of beds for ion and "A" atom diffusion between beds. The bags will also have ports in the ends for water addition and removal of product gases.

4.2.5 Dual Bed Reactor Assembly

An end view of one of the Type 2 dual bed assemblies is shown in Figure 4-18. Four bags are combined into one integrated reactor assembly 20 ft wide and comprising 3 dual-bed reactors. In this layout, the bags are sequentially for H_2, O_2, H_2, and O_2 production. The baggies are bonded to one another and are able to diffuse electrolyte and ions via a porous mat communication bridge which runs the length of the baggie below the water line. To facilitate mixing within the bags and diffusion across the bridges, the slurry is continuously circulated from the bed center to the bed edges, using perforated pipes through which the slurry is pumped.

Figure 4-18: Type 2 End View of a Dual Bed Reactor Assembly

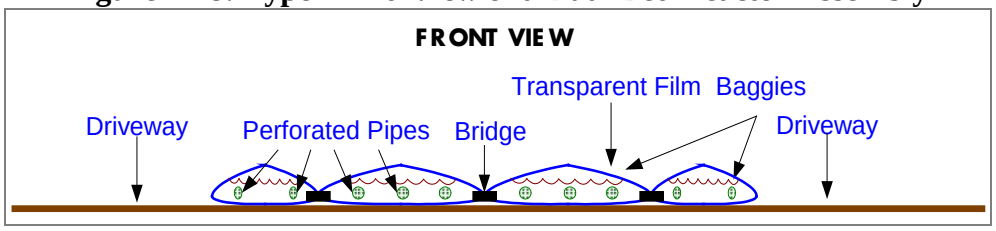

In the initial design, communication bridges were placed every 40 feet down the length of the bed to allow ion diffusion pathways from one baggie to the next. However, system diffusion calculations indicated that the resulting diffusion lengths were unrealistically long. Consequently, a new system was defined wherein individual baggies were abutting one another, with a water/electrolyte/ion bridge for diffusion down the entire length of the baggies.

Figure 4-19 displays a top view of two reactor assemblies. Bed length is limited to 200 feet (as opposed to 1060 foot length of Type 1 beds) due to added complexity of attaching ion bridges.

Figure 4-19: Top View of Two Type 2 Reactor Bed Assemblies

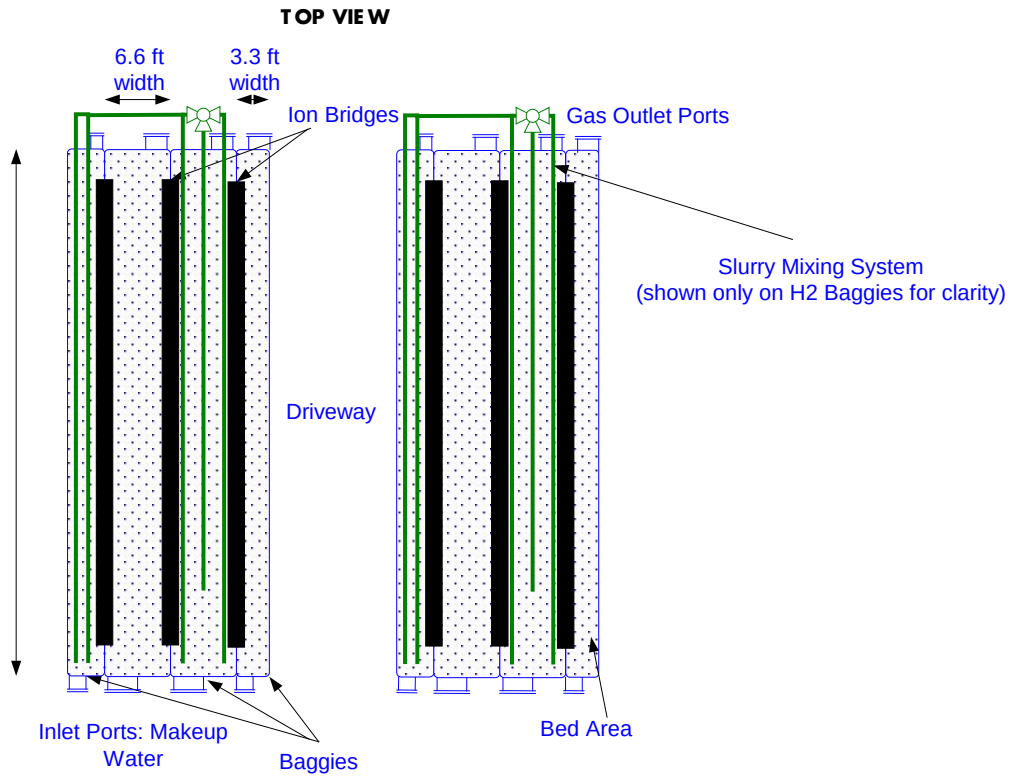

Since the Type 2 Reactors are much smaller than the Type 1 (9.4%), the ports are smaller and the cost of the ports plus installation is about ¼ of that for the Type 1 ($9/port vs. $30/port).

4.2.6 Type 2 Reactor Cost Summary

The components and component costs for a Type 2 reactor are listed in Figure 4-20.

Figure 4-20: Type 2 Reactor Capital Costs for 1TPD

Reactor Component	Quantity		Unit cost		Overall cost
Module H2 Average Production	1,000	kg/day			
Baggie Assembly components - for	347	assemblies			
bag material-top	168,145	m2	$ 0.54	/m2	$ 90,285
bag material-bottom	127,691	m2	$ 0.47	/m2	$ 59,677
porous polypropylene membrane	51,033	ft2	$ 0.66	/ft2	$ 33,682
total					$ 183,644
port hardware 8 /baggie sys	2,776	ports	$ 4.50	each	$ 12,501
port installation 8 /baggie sys	2,776	ports	$ 4.50	each	$ 12,501
perforated PVC pipe-0.5"	691,547	ft	$ 0.24	/ft	$ 162,790
circulation pump	347	baggie sys	$ 175.07	each	$ 60,750
baggie system assembly labor	347	baggie sys			$ 81,811
payment for capital recovery					$ 13,503
markup factor					1.5
total baggie system cost	347	baggie sys			$ 791,250
Baggie Roll-unroll system	1		$ 37,000.00		$ 37,000
forklift	1		$ 18,571.00		$ 18,571
Coated PEC nanoparticles	134.20	kg	$ 304.00		$ 40,798
Make-up water pump	1		$ 213.00		$ 213
Make-up water manifold pipes	9,812	ft	$ 0.52		$ 5,102
Total Baggie Reactor Cost					$ 892,934

The costs for the Type 2 reactor are 4.2 times higher than the Type 1 because of the near-doubling of reactor area and number of nanoparticles, the added porous membrane, the added slurry circulation system, and the additional number of ports.

4.2.7 Type 1 and Type 2 Reactor Bed Technology Summary

The Type 1 and 2 systems are innovative and promising approaches to PEC, but are relatively immature compared with the standard PEC cell approach, thus having greater cost uncertainty:

- Definition and fabrication of the optimal nanoparticle PV materials
- Production costing for fabrication of the particles
- Effective photo-reactive active area (capture area) on a given base nanoparticle
- Nanoparticle density needs in the beds for total photon capture, accounting for reflection and scattering effects
- For the Type 2 reactor: uncertainty in diffusion times across diffusion bridge
- For the Type 2 reactor: uncertainty in whether there is 100% exclusive generation of O_2 on the first side and H_2 on the second side

4.3 *Type 3 and 4 PEC System PV Cell Properties, Fabrication, and Cost*

The currently demonstrated approach for PEC systems utilizes discrete PV cells to generate the electron voltage and current for PEC electrolysis. Two basic types of photocell PV systems that have been demonstrated are fixed planar arrays and steerable concentrator arrays. This sub-section examines the photocell component materials and PEC cell fabrication and cost properties common to Type 3 and 4 configurations. The specific configurations are subsequently discussed in Section 4.4 (fixed planar arrays) and in Section 4.5 (steered concentrator arrays).

4.3.1 Photocell PEC Operation

The photocell PEC system utilizes a PV cell generating sufficient voltage to electrolyze water. The cell generates electrons from incident photons and has either integral electrodes immersed in an electrolyte, or closely connected electrodes immersed in an electrolyte. For the PEC cell, the PV materials absorb photons to generate electrons for electrolysis at a total voltage on the order of 1.6-2.0 volts and conduct electrons between the oxygen gas generating anode and the hydrogen gas generating cathode. The electrolysis gases are separated to create separate outlets for the H_2 and O_2. In the most common embodiment, the front face is illuminated by solar radiation and is a conductive window that functions as the electrolysis anode.

Multiple PV active layers can be used to increase overall voltage and to maximize solar spectrum utilization. A typical multi-layer PEC cell is shown in Figure 4-21, and is characterized by:

- Transparent conductive window anode with anti-reflective coatings
- Multi-junction PV material consisting of thin films deposited onto cathode
- Stainless steel (SS) foil sheet substrate/cathode
- Separation of H_2 & O_2 products

Figure 4-21: PEC Multilayer Cell Configuration

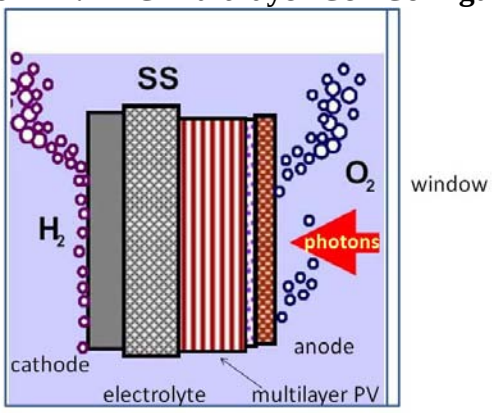

The solar photons are incident on the anode of the multilayer PV section where they generate a voltage corresponding to the PV material's bandgap. The O^{--} ions in the electrolyte release electrons at the anode to form O_2 gas. The electrons are transmitted to the cathode where they combine with the H^+ ions in solution to form H_2 gas. A modified PEC cell configuration is shown in Figure 4-22 from the Gibson, et al, Patent[28] (assigned to General Motors). The vertical glass shield faces the sun and protects the TCO (transparent conductive oxide) from electrolyte corrosion. Corrosion-resistant metal anode surfaces are on the top and bottom of the cell. The configuration also avoids potential bubble interference with incident light. The large distance between anode and cathode enhances gas separation.

Figure 4-22: PEC Configuration from Gibson Patent

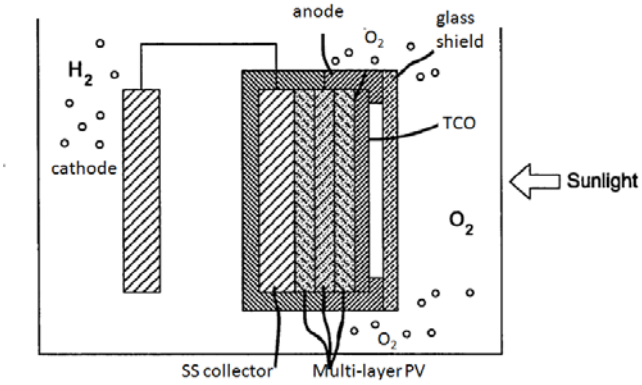

A third PEC cell configuration, shown in Figure 4-23 from the Gratzel, et al, Patent[29] , uses an ion–conducting membrane or glass frit at the cell bottom to prevent potential gas mixing.

[28] Photochemical Device and Electrode, Patent no. 7,052,587, May 30, 2006, Gibson, et al.
[29] Photocatalytic Film for the Cleavage of Water into Hydrogen and Oxygen, Patent no. 7,271,334, Sep 18, 2007, Gratzel, et al

Figure 4-23: PEC Configuration from Gratzel Patent

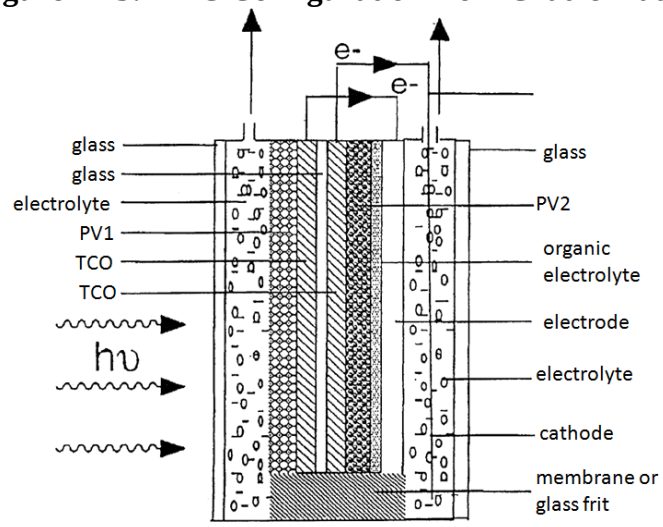

A fourth PEC configuration is shown in Figure 4-24 , from the McNulty, et al, Patent Application[30] (assigned to GE). This configuration uses a membrane to separate anode and cathode compartments. The membrane is impregnated with photoactive particles. (The particles are similar to those used in the Type 1 PEC system described in Section 4.1.) The membrane porosity allows cation and anion transport between the compartments, however, in some embodiments, holes are added to the membrane to enhance ion transport.

Figure 4-24: PEC Configuration from McNulty Patent Application

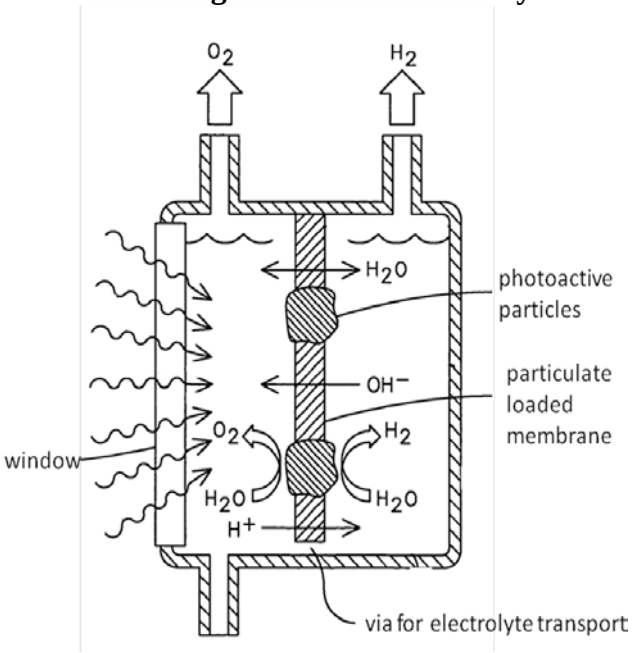

[30] Photochemical Cell and Method of Manufacture, Patent Application no. 2007/0119706 A1, May 31, 2007, McNulty, et al.

Thus there are multiple PEC cell configurations which can be used, some using membrane separation of the gases and others relying solely on gravity separation. For this costing study, we have based our cell design on the simplest generic design of Figure 4-21 , assuming an open electrolyte compartment and gravity separation of gases. However, we have added into the cost a contingency margin that is intended to provide for additional features, such as a simple membrane separator that could be necessary.

Solar-to-hydrogen (STH) conversion efficiency of the PEC system is the product of the PV conversion efficiency and the electrolysis efficiency. The theoretical maximum multi-layer STH conversion efficiency for photoelectrolysis exceeds 40%. PEC systems to date have demonstrated 8%-12.4% conversion efficiencies, with future projections of 25-31%.

Figure 4-25, compiled from multiple references, describes various PEC cell developments and lists experimental and theoretical STH efficiency.

Figure 4-25: PEC Cell Research Descriptions and Performance

Year	Author	Organization	Publication	PV materials	Band Gap eV	Total Volts	Illum suns	Efficiency
1998	Turner	NREL	Science, 17-Apr-98	GaInP2 /GaAs Test 20 hr life add nitrides for corros resist	1.85 / 1.4	3.25	11.6 X	12.4% STH exp
2003	Turner	NREL		GaInP / GaAs calculated	1.8 & 1.4 eV	3.2	1 X	31% STH calc
							500 X	36% STH calc
2008	Turner Leisch	NREL Colo Sch Mines	DOE H2 Prog Rev 2008	CuGaSe2 / Si (CGS / Si) max theoretical	1.72 / 1.1 eV	2.82		28% STH theory
2006	Turner Deutsch	NREL	ICMR Symposium Aug-06	GaPN / Si good corrosion resistance experimental	1.72 / 1.1 eV	2.03		1% STH exp
2005	Licht	U Mass	J.Phys.Chem.B	AlGaAs / Si-RuO2 lab demo separated PV & electrodes -anode/cathode area 45.5:1				18% STH exp
				predicted limit				27% STH theory
2005		multiple sources		TiO2 single layer	3.2	3.2	1	

PV cell efficiency levels have been steadily improving to beyond 40% solar-to-electric efficiency, with the most substantial jumps forward being achieved by multi-junction concentrators, as shown in Figure 4-26. The highest PV efficiencies are predicated on high voltage multi-layer configurations. These are not readily encompassed into PEC efficiencies because additional cell voltage achieved beyond that required for electrolysis does not increase H_2 production, it only heats the electrolyte.

Much of the most recent PV solar cell development is aimed at reducing cell costs through fabrication improvements, while retaining efficiencies in the 10-15% region.

Figure 4-26: PV Cell Efficiencies[31]

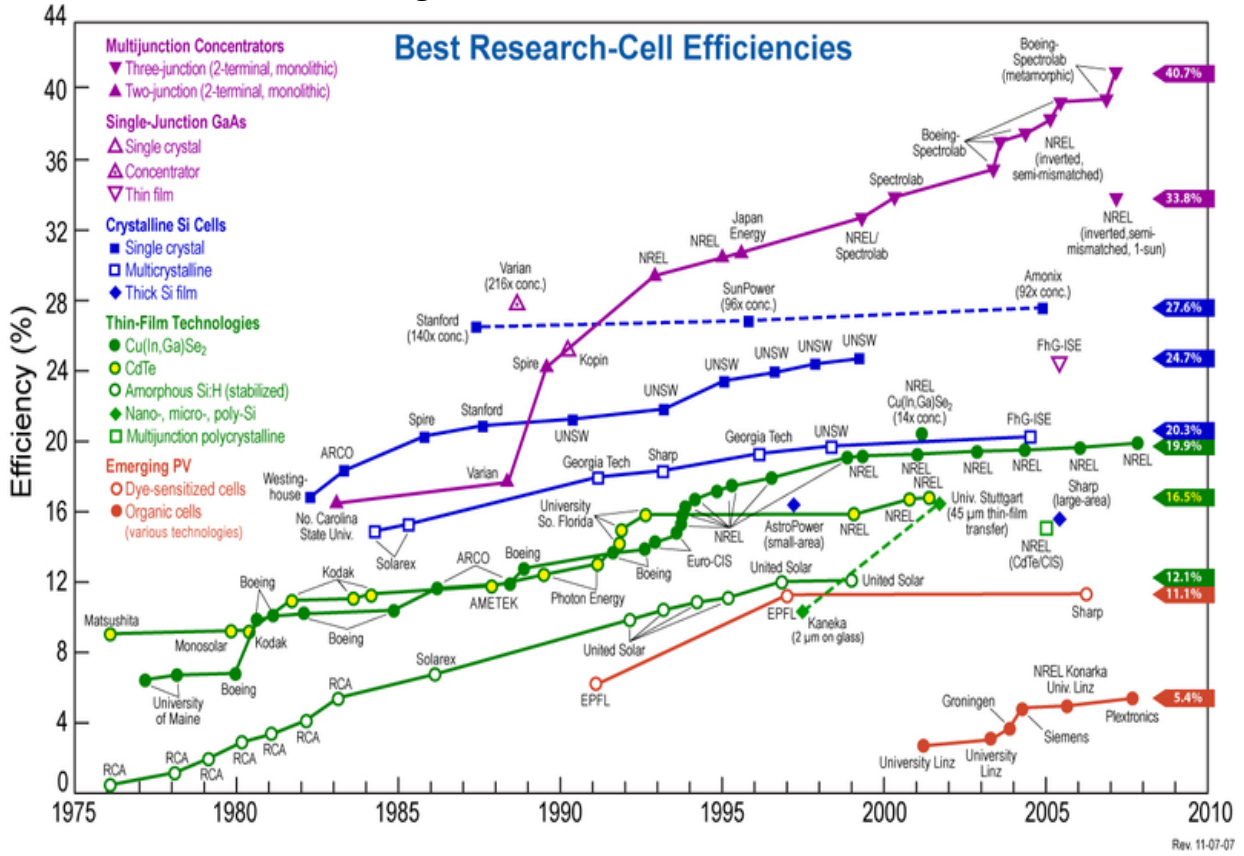

4.3.2 PEC Photocell Cost Factors

A key factor in cost-effectiveness of PEC photocells is the PV component cost, which has been a significant barrier to low cost solar cells and low cost PEC in the past. For the photocell, pathways to reduced cost are:

- Minimizing thickness of individual PV layers
- Use of low cost printing techniques for material deposition
- Use of lower cost PV materials, when possible
- Low cost conductive coatings to protect against corrosion

PV cost per Watt goals of < $1/Watt are designed to bring about commercially viable systems that can compete in the electric power market. In pursuit of this cost goal, First Solar has developed a vapor deposition manufacturing process that can efficiently coat sub micron layers of CdTe and CdS on glass substrates[32]. First Solar is currently selling production solar cell panels utilizing this technology.

Recently, Heliovolt, Nanosolar, and others have developed low cost thin film PV cell fabrication technology using ink deposition in roll-to-roll printing techniques to produce thin film PV cell sheets with CIGS (copper indium gallium selenide) PV material, as described below:

[31] "Solar Cell energy Systems Research," Ertugrul, N., University of Adelaide, 2008, (from NREL Sources)
[32] First Solar, Fast Facts: Company Overview, Aug 2009 accessed at www.FirstSolar.com

- Heliovolt's proprietary FASST printing process[33] cuts prior PV coating times down by a factor of 100, while simultaneously achieving reported STE efficiencies of 12.2%,
- Nanosolar roll-printing technology[34] (Figure 4-27) with printing rate of 100 ft/min, reducing cell costs to \$0.99/peak Watt (~\$100/m^2 at 10% cell efficiency and 1,000W/m^2 insolation). They have commenced commercial production of these cells and predict future developmental cells will reach STE efficiencies near 14%.

Figure 4-27: Nanosolar Roll Printing[35]

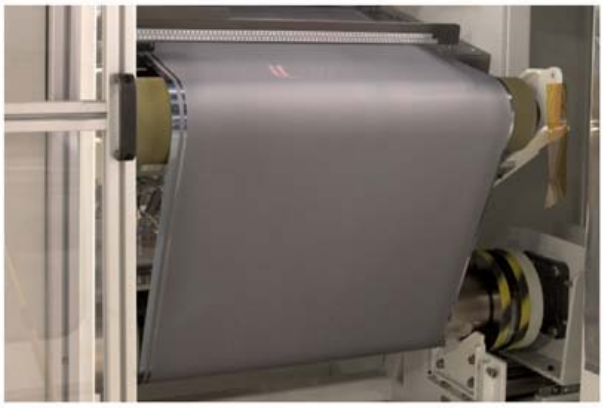

Figure 4-28 displays the Nanosolar PV cell layout described in a recent patent application, with:

211 current carrying conductors
209 Transparent Conductive Oxide (TCO) ZnO window
208 bandgap adjustment layer (<0.10 micron)
206 inked-on active layer, (1-2 micron) e.g., CIGS
204 metal cathode (0.5-1.0 micron)
203 optional adhesion layer
202 substrate metal or plastic

Figure 4-28: Layout of the Nanosolar PV cell[36]

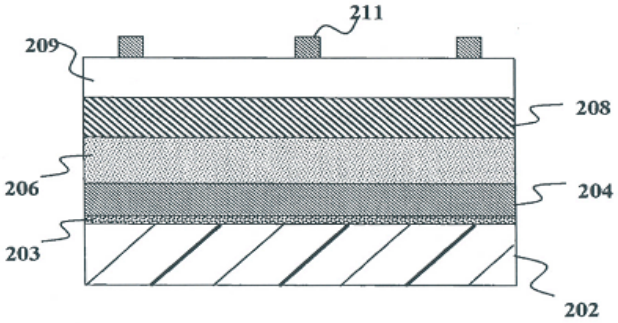

[33] Heliovolt Press Release, Oct 23, 2008
[34] December 18, 2008 announcement by Martin Roscheisen, CEO of Nanosolar
[35] Ultra-Low-Cost Solar electricity Cells, Nanosolar, September, 2009.
[36] US patent application 2005/0183767

For a PEC application, we envision that the current carrying conductors would be eliminated and the conductive layer #209 can be substantially reduced in thickness, since current flow will be normal to the cell face rather than laterally across the face as on solar cells.

This printing technology can also be used to fabricate a two or three layer tandem cell with broader solar spectrum utilization and higher voltage. Such higher cost multi-layer cells are not widely used for commercial planar solar cell arrays because lowest cost per watt and per area are the primary commercial objectives. For these single layer CIGS cells, the energy gap is only 1.2 eV, and the resultant voltage generated, by itself, is insufficient to carry out the electrolysis reaction. Therefore, for high utilization of the solar spectrum, multi-junction PV/PEC cells will have to be developed, with total energy bandwidth >1.8 eV. For Type 3 planar array PEC systems, the large number of cells needed requires development of low cost PV materials and fabrication. For the Type 4 concentrator systems, higher cost/higher efficiency materials are viable because of the much lower active PV area required.

Efforts are being carried out at multiple research locations to develop tandem solar cells using low cost thin film fabrication techniques. Some of these tandem cells will have sufficient voltage match for PEC use. Extensive solar cell work at NREL[37] includes Mg-Cd-Te/Cd-Te dual cells and GaInP/GaAs/GaInAs triple cells. Current solar cell work at ASU[38] is exploring utilizing thin film technology with lower cost active element materials and also fabrication of these multi-junction cells with advanced printing techniques.

4.3.3 PEC Photocell Cost Prediction

From this current ongoing work, it can be predicted that low cost tandem cells having adequate cell voltage for PEC could be developed in the lab within the next 1-5 years, with potential initial production within 6-8 years. With this technology, PV STE efficiencies at 20-30% levels will be achieved with low cost materials, and > 40% with higher cost materials. For PEC applications, the STH efficiencies will be lower, but could reach 20-25% in the future.

Most high efficiency solar cells use gallium as a key component of the photoactive material. Since pure gallium is an expensive material, ~$500/kg, its use in low cost PV cells is predicated on extremely thin layers, less than a micron. (A 1 micron layer of Gallium would cost only $0.03 per m^2.) An advantage of the Ga-based cells (such as Ga As) over Si cells is that they are direct bandgap semiconductors which require much less material (thickness) in a PV layer.
Extensive development in printing techniques over the past 10 years on low cost single-layer CuInGaSe (CIGS) cells has shown that printed-on Ga compound layers at 100-200 nanometer thickness can be effective and affordable. While previously Ga-based PV cells were too expensive for commercial terrestrial applications, with the newly developed low cost printing technologies, some manufacturers are looking at future terrestrial commercial market applications for high efficiency triple layer Ga-compound cells.

Fraunhofer ISE has fabricated laboratory-grade triple-layer solar cells at 41.1% efficiency (~30 deposition layers on Ge substrate) and plans to enter the commercial market with spinoff

[37] "CdTe - Progress and Roadmap Alignment", National Center for Photovoltaics, Gessert, T. , NREL, 2008 Solar Annual Review Meeting.
[38] ASU Press Release on January 23, 2008.

Concentrix Solar GmbH to produce concentrator systems at competitive costs based on this research. Concentrating solar panels under development at Concentrix are reported to achieve a peak efficiency of 27.2% after packaging losses. Current DOE, NASA, and DARPA programs to produce nano-thickness high efficiency solar cells using GaAs, GaInP, and other III-V materials have already had measurable success at realizing the low cost efficient multi-junction cells needed for future PV cells.

Spectrolab has developed maximum-efficiency[39] (40.7%) triple-layer solar cells with concentrators, and is currently marketing these triple-layer cells at a high price level[40] (~$100,000/m^2 for the bare cell without interconnects, with an additional $40,000/m^2 for the interconnects), focusing on fabrication small quantities of very high performance cells rather than low cost. However, we have assumed that the dual layer cells needed for the PEC application can use the nano-thickness fabrication techniques being developed and utilized for mass production by First Solar, Nanosolar, Heliovolt, and others to dramatically reduce production costs.

A manufacturing advantage of PEC over pure solar cells is that the anode reactant face replaces the face conductor grid in the solar cell package. The face conductor grid also partially obscures the active PV face, and is a particular issue in concentrator PV systems. Consequently, by eliminating the face conductor, PEC panels are able to both reduce some cost components and improve photon capture of the PV component. Of course, the PEC cell also includes the electrolyte cavity, water feed, and H_2 take-off lines, so overall package complexity would be greater than for PV cells.

Since there is no current PEC commercial industry to use as a guideline, the costs used in this study for the active PV/PEC module for the Type 3 and Type 4 cells have been calculated based on a combination of solar cell open literature cost reports, an NREL cost projection for solar cells, and a DFMA (Design for Manufacturing and Assembly) style cost analysis.

As reflected in the open literature and by high levels of patent activity, much attention has been recently directed to the rapid/low-cost manufacture of thin film PV active components. With printing and vapor deposition techniques, cells can be manufactured with very thin active layers, less than a micron. Figure 4-29 lists, in the first 2 rows, a cost breakdown for current and future PV cells from an NREL study[41], which was in turn based on actual First Solar costs. The NREL cost breakdown shows that for thin film solar cells, the inactive material components and labor and assembly components are the heavily dominant manufacturing cost items, approaching 95% of the total cost. Thus cost impact of the use of more expensive photo-active materials is minimized. In Figure 4-29 , we have added analogous costs relevant to advanced PEC cells, based on the NREL study findings, with additions and deletions to reflect the differences

[39] Question #23 of Spectrolab's FAQ 2009 website, www.spectrolab.com/prd/terres/FAQ_terrestrial.htm

[40] Based on $10/cm^2 cell cost and $14/cm^2 cell with interconnect, as reported in Question #8 of Spectrolab's FAQ 2009 website, www.spectrolab.com/prd/terres/FAQ_terrestrial.htm

[41] "Thin film PV manufacturing: materials costs and their optimization", Zweibel, K., Solar Energy Materials & Solar Cells, 2000, Elsevier.

between PV and PEC cells. We then added a mark-up of 50% to the PEC module cost to account for non-direct manufacturing business costs[42].

Figure 4-29: Baseline PEC Cell Cost Model based on NREL Solar Cell Cost Study

Cost model	Cell descr	Yr	Parameters		Module Cost												Cost/ Capture area
					materials costs								mfg costs	total cost/ cell	cost with 50% mark -up	
			base effic	cell aperture area	PV cell components			PEC cell unique				total matls				
					active		inactive	encapsulation	Plexiglass Window							
					PV	other	& margin		edge angle	thickness	cost/ aperture					
				m2	$/m2	$/m2	$/m2	$/m2	deg	in	$/m2	$/m2	$/m2	$/m2		$/m2
PV NREL/ Zweibel*	CdTe /CdS	2000	10.0%	0.72	$3.00	$2.00	$39.00	-	-	-	-	$44.00	$56.00	$100.00	$150.00	$150.00
		2010	15.0%	0.72	$1.50	$0.50	$18.00	-	-	-	-	$20.00	$28.00	$48.00	$72.00	$72.00
PEC Type 3	CIGS/Ge	2010	10.0%	2.0	$4.50	$1.50	$14.00	$14.00	0	0.060	$12.03	$46.03	$56.00	$102.03	$153.05	$153.05
Type 4	GaAs/Ge 10:1 concen 300 psi	2015	15.0%	1.8	$6.50	$1.50	$14.00	$39.00	45	0.500	$93.84	$154.84	$56.00	$210.84	$316.27	$31.63

PEC cell: no electrical conductor grid
no electrical connection assembly

* "Thin film PV manufacturing: Materials costs and their optimization", Zweibel, K., Solar Energy Materials & Solar Cells, 2000, Elsevier (based on manufacturing data from first Solar)

For Type 3 and Type 4 PEC cell costing, we have used the above PEC cell cost projections as the baseline level for a PEC production plant in the near term.

For our far term projection of PEC cell cost, we examined the most recent PV cell printing techniques that have been developed for PV cells and are currently in production for that application. We subsequently carried out a DFMA-style analysis of PEC cell fabrication to adapt this PV manufacturing technology to PEC cell manufacture, and to establish a future cost projection. Recent capability advances of ink printing technique of PV cell fabrication have been outlined in a series of Nanosolar press releases:

June 18, 2008:

- "solar industry's first 1 gigawatt (GW) production tool"
- "1GW CIGS coater cost $1.65 million".
- "At the 100 feet-per-minute speed ..... that's an astonishing two orders of magnitude more capital efficient than a high-vacuum process"
- "same coating technique works in principle for speeds up to 2000 feet-per-minute"

September 9, 2009: (Manufacturing capacity)

- "European panel-assembly factory - fully-automated factory processes"
- "one panel every ten seconds, or an annual capacity of 640MW when operated 24x7" (i.e., 5.8 million m^2/year assuming 11% solar conversion effic) (total capacity with 430MW San Jose factory equals 9.7 million m^2/year)
- "Production is presently set at approximately one MW per month" (109,000m^2/yr)

September 9, 2009: (Efficiency)

- "NREL independently verified several of our cell foils to be as efficient as 16.4%"
- "current baseline production process, our best production rolls now achieve higher than 11% median efficiency"

[42] A 50% mark-up, consistent with a 33% gross margin, is considered a typical level for a mature energy product in a competitive market.

The Nanosolar cell layers are depicted in Figure 4-30 and consist of both printed-on layers (blue 50 nm thickness labels) and vacuum deposition layers (red 25 and 50 nm thickness labels).

Figure 4-30: Nanosolar PV Cell Diagram

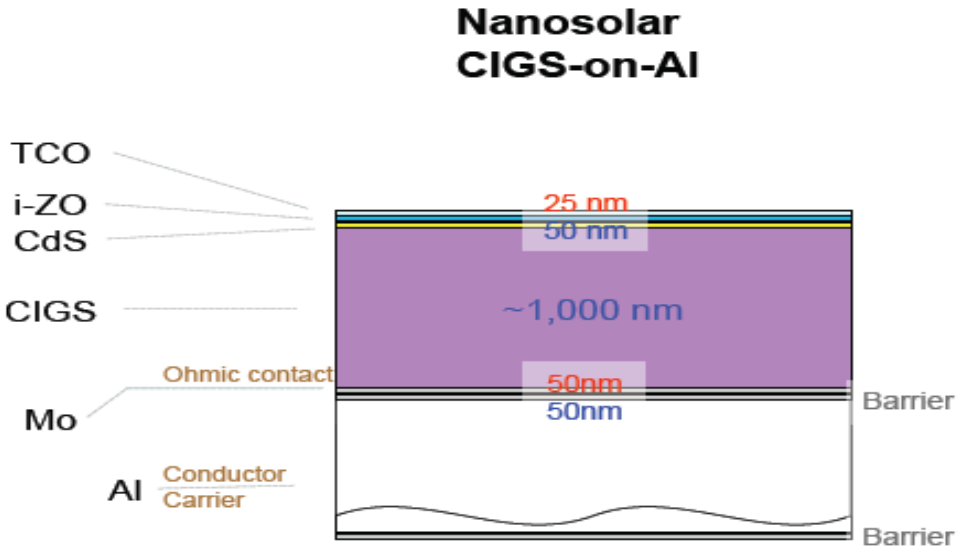

Application of the Nanosolar cell manufacturing expertise to the manufacture of dual layer PEC cells would significantly reduce the costs of PEC cell manufacture from the baseline described in Figure 4-29.

The DTI DFMA (Design for Manufacturing and Assembly) analysis is a projection of potential PEC cell manufacturing costs into the future, given a comparable level of cell photoactive layer ink development and print-on manufacturing technology as is currently practiced by Nanosolar. Insofar as PV cell costs are concerned, we have focused on future manufacturing and materials costs rather than the current actual sales prices. For the current non-mature solar cell industry, the sales price reflects the current inelastic supply/demand situation and the need for fast fabrication plant amortization. Figure 4-31 lays out the results of this future DFMA cost projection analysis.

Figure 4-31: Future Projected PEC Cell Cost Model based on DFMA Analysis

Item	units	Projected Type 3		Projected Type 4	
Plant Total Annual Production	m2/yr	6,144,468	based on First Solar 20MW plant at 8% efficiency, with capacity increased to 100ft/min, 14hrs/day, 240day/year	6,144,468	based on First Solar 20MW plant at 8% efficiency, with capacity increased to 100ft/min, 14hrs/day, 240day/year
Material Costs (based on First Solar Costing)					
Glass/TCO	$/m2	$5.00	Manufacturing advances.	$5.00	Manufacturing advances.
Modularization parts	$/m2	$0.00	PEC segmentation not needed.	$0.00	PEC segmentation not needed.
Panelization	$/m2	$0.00	Included under water cell hardware.	$0.00	Included under water cell hardware.
Back glass or metal	$/m2	$7.05	Inflation adjusted.	$7.05	Inflation adjusted.
EVA	$/m2	$0.00	Not needed.	$0.00	Not needed.
most expensive semi-conductor (Te, Ga In, Ge)	$/m2	$5.23	Incr. to reflect multi-layer, inflation	$10.46	Incr. to reflect higher efficiency.
Shipping carton	$/m2	$1.32	Reduced	$1.32	Reduced
Remaining active matls (semiconductors, metals)	$/m2	$2.82	Inflation adjusted.	$2.82	Inflation adjusted.
Other process expendables	$/m2	$1.00	Reduced complexity.	$1.00	Reduced complexity.
Waste processing	$/m2	$1.41	Inflation adjusted.	$1.41	Inflation adjusted.
Urethane (potting)	$/m2	$0.00	Not needed.	$0.00	Not needed.
Bypass diode	$/m2	$0.00	Not needed.	$0.00	Not needed.
Al target	$/m2	$0.00	Not needed.	$0.00	Not needed.
Miscellaneous and Margin	$/m2	$1.50		$1.50	
Water cell hardware	$/m2	$13.86	Hardware to manifold water/gases.	$35.57	Higher pressure.
Plexiglass window	$/m2	$11.91	Optically clear solar window.	$77.52	Higher pressure.
Total Materials Cost	$/m2	**$51.11/m2**		**$143.66/m2**	
Capital					
Total Uninstalled Capital Cost		$25,390,778	Based on 20MW/year First Solar analysis with escalation (3.5%yr)	$25,390,778	Based on 20MW/year First Solar analysis with escalation (3.5%yr)
Equipment Installation Factor		1.4	Standard DTI DFMA factor.	1.4	
Discount Rate (real, after-tax discount rate)		10%	Standard DOE H2A assumption.	10%	
Average Equipment Lifetime	years	15		15	
Corporate Income Tax Rate		40%	Standard DOE H2A assumption.	40%	
Annual Capital Recovery Factor		0.175		0.175	
Annual Payment to Cover Capital Cost		$6,209,313		$6,209,313	
Total Capital Repayment per m2	$/m2	**$1.01/m2**		**$1.01/m2**	
Utilities (Heat, Electricity, Water)		**$3.00/m2**	From First Solar analysis (consistant with 37.5kWh/m2 of electricity at $0.08/kWh)	**$3.00/m2**	From First Solar analysis (consistant with 37.5kWh/m2 of electricity at $0.08/kWh)
Labor					
Simultaneous Laborers	FTE	26	Deduced from First Solar analysis	26	Deduced from First Solar analysis
Fully Loaded Labor Rate	$/h	60	Consistant with other First Solar assump.	60	Consistant with other First Solar assump.
Operating Days per Year	days/yr	240	Typical mfg work days/year.	240	Typical mfg work days/year.
Production Hours per Day	hrs/day	14	Two shifts of 7 hours/shift	14	Two shifts of 7 hours/shift
Annual Labor Cost		**$5,241,600**		**$5,241,600**	
Total Labor Cost per m2	$/m2	**$0.85/m2**		**$0.85/m2**	
Maintenance of Equipment					
Annual Maintenance as % of Uninst. Capital		4%	First Solar analysis assumption	4%	First Solar analysis assumption
Annual Mainenance Cost		$1,015,631		$1,015,631	
Annual Mainenance Cost	$/m2	**$0.17/m2**		**$0.17/m2**	
Total Variable Cost before Markup		**$56.14/m2**		**$148.69/m2**	
R&D					
Annual R&D as % of Variable Cost		2%	Deduced from First Solar analysis.	2%	Deduced from First Solar analysis.
Annual R&D Cost	$/m2	**$1.12/m2**		**$2.97/m2**	
Warranty					
Annual Warranty as % of Sales		3%	First Solar analysis assumption	3%	First Solar analysis assumption
Annual Warranty Cost	$/m2	**$4.50/m2**		**$9.00/m2**	
Rent & Factory Overhead					
Annual OH as % of Variable Cost		5%	Deduced from First Solar analysis.	1.9%	Dollar value equal to Type 3 since production plants virtually identical.
Annual OH Cost		**$2.81/m2**		**$2.81/m2**	
Scrap					
Annual Scrap as % of Variable Cost		3%	DTI estimate.	3%	DTI estimate.
Annual Scrap Cost	$/m2	**$1.68/m2**		**$4.46/m2**	
Profit					
Annual Profit as % of Variable Cost		15%	DTI estimate.	15%	DTI estimate.
Annual Profit Cost	$/m2	**$8.42/m2**		**$22.30/m2**	
G&A					
Annual G&A as % of Variable Cost		5%	DTI estimate.	1.9%	Dollar equal to Type 3 value since operations are virtually identical.
Annual G&A Cost	$/m2	**$2.81/m2**		**$2.81/m2**	
Advertising/Misc.					
Annual Misc. as % of Variable Cost		5%	DTI estimate.	5%	DTI estimate.
Annual Misc. Cost	$/m2	**$2.81/m2**		**$7.43/m2**	
Computed Total Gross Margin		30.1%		25.8%	
Computed Total Mark-up from DFMA Variable Cost		38%		32%	
Expected Sales Price	**$/m2**	**$80.28/m2**		**$200.47/m2**	
Annual Sales	$/year	$493,303,251		$1,231,792,257	

4.4 *Type 3 Planar Array System*

Planar PEC arrays are similar to planar solar cell PV arrays, except that the cell electrodes are in direct contact with the PEC electrolyte and output is H_2 and O_2 gas rather than an external electric current. Arrays are fixed in place and inclined toward the sun at an optimum tilt angle for the latitude to maximize the average insolation over a year. Incident solar energy is the direct solar component normal to the array face plus the diffuse radiation from the atmosphere.

4.4.1 PEC Planar Array Design

Figure 4-32 shows a diagram of the planar PEC Panel. Each panel is made up of multiple cells, with the cell size being as large as can be readily manufactured. Hydrogen from the panel manifold is ducted to a hydrogen compressor. For this design, the oxygen is vented, but it could also be separately collected and stored. Each individual panel is 1 m wide and 2 m in length. Peak hydrogen output per $2m^2$ panel, with a peak input solar intensity of 927.6 W/m^2 and 10% STH efficiency, is 0.12 g/min (1.11 liters/min).

Figure 4-32: Layout of Type 3 PEC Panel

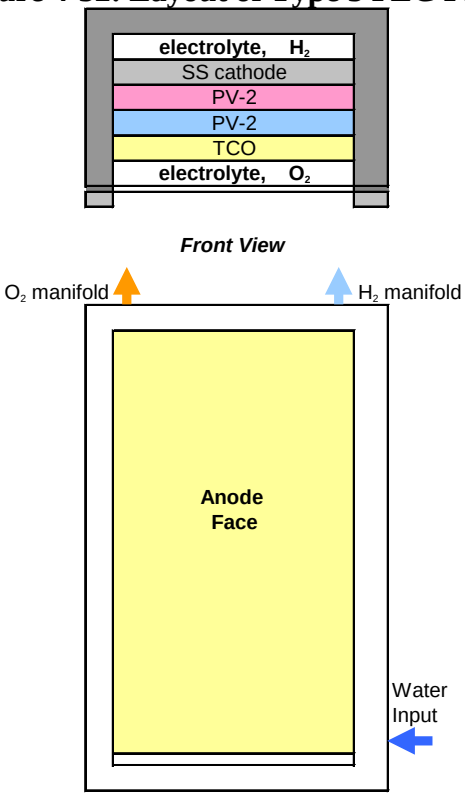

The planar array is characterized by:

- Array facing south at angle from horizontal equaling local latitude
- Arrays spaced apart in the North/South direction to reduce shadowing at low sun angle
- Electrolysis separation of H_2 and O_2
- Buoyant gas collection
- O_2 released to atmosphere
- 0.1M KOH Electrolyte Solution
- Plexiglas window with 95% max photon transmission in PV band
- Transparent anode,
- Multilayer PV cell
- Stainless steel cathode
- 10% baseline STH efficiency, with future increase to 15% (for low cost cells)

Planar Array Cost Issues are:

- 10 year transparent window life
- 10 year PEC cell life
- PEC cell cost ~$153 /$m^2$ for 10% efficiency

The PEC panel array would be similar to the PV array shown in Figure 4-33. The array tilt angle for the location chosen (Daggett, CA) is about 35^o.

Figure 4-33: Analogous PV Array Structure

The Baseline PEC panel array cost is based on the PEC Panel component costs listed in Figure 4-29. A typical layout of a planar array field is show in Figure 4-34.

Figure 4-34: Type 3 Planar Array Field Layout

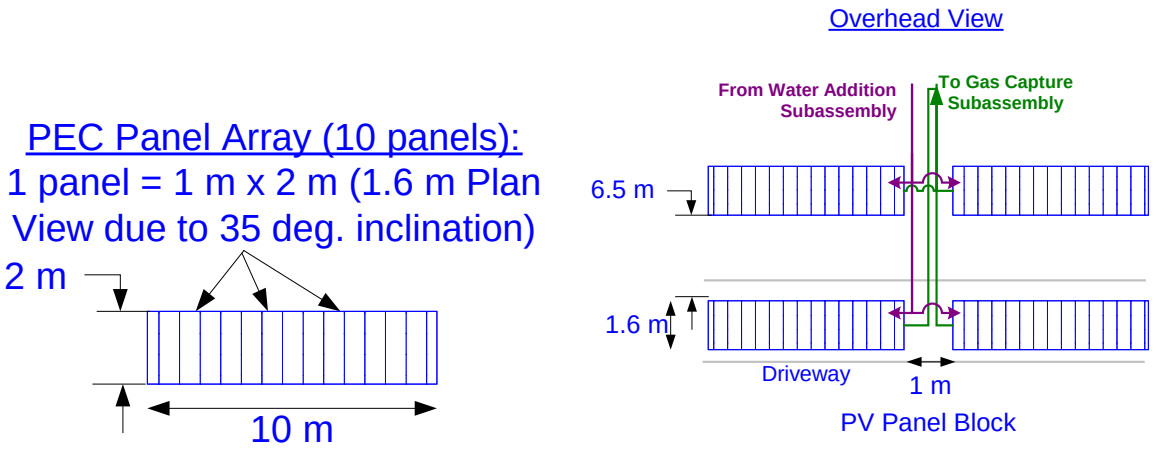

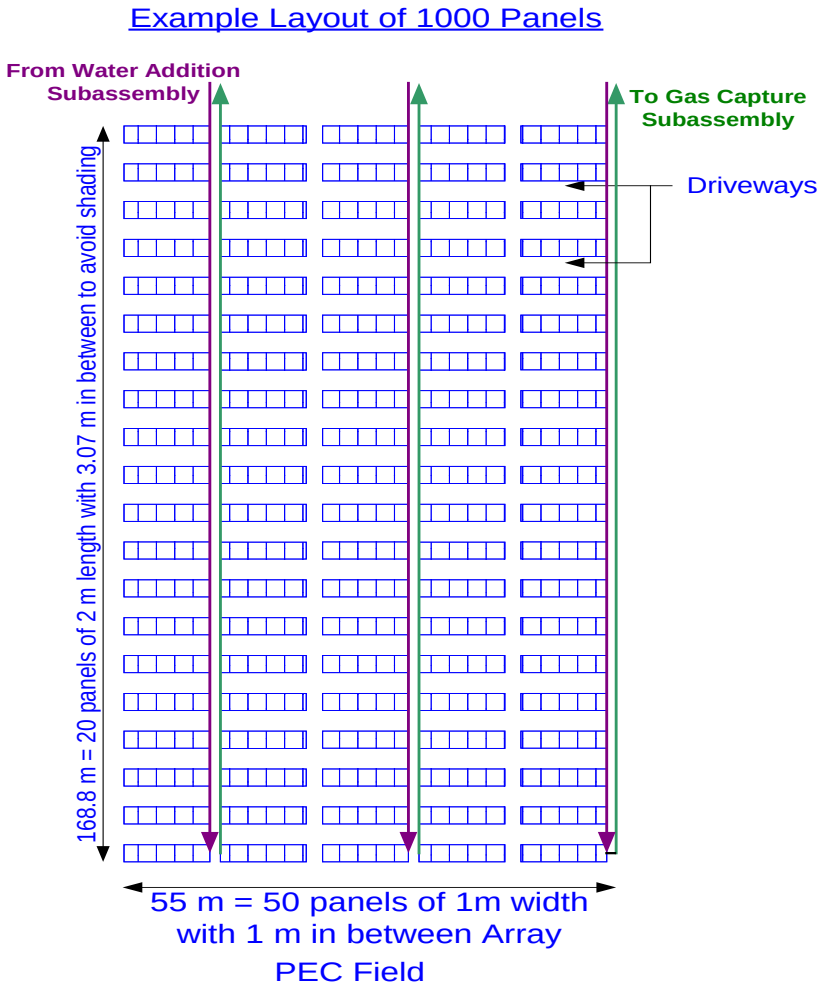

4.5 *Type 4 Solar Concentrator System*

The Type 4 system uses a solar concentrator reflector to focus solar direct radiation onto the PEC cell and uses a solar tracking system to maximize the direct radiation. Solar concentrators, which can use reflectors or lenses to focus solar energy onto PEC cells in a receiver unit, substantially reduce the cost impact of the PV component of the system, but add the costs of the concentrators and steering systems. Since the PV components comprise only a fraction of the Type 4 total system costs, more costly cells (i.e., GaAs/GaInAs) with high efficiencies, are cost effective. Steerable concentrating solar systems have been extensively used for PV electric systems and for solar/thermal systems.

4.5.1 Concentrator PEC Cell Technology

A PEC concentrator system can potentially use a concentration ratio of 10-50 suns, and the NREL world-record PEC cell used 11.6:1 concentration (Figure 4-25). This is substantially less than most concentrating PV/electric systems which are routinely between 20:1 and 100:1.

Spectrolab as of 2004 had demonstrated concentration ratios up to 1000:1[43], with peak efficiency at that time being achieved at about 200:1, as shown in Figure 4-35 from this reference. For Type 4 systems, the major cost components are the large area of concentrators and tracking systems rather than the PV cell component. Therefore, higher cost PV components with higher efficiency can reduce the overall area and cost of the system. In a PEC concentrator system, the PV cell efficiency could also be expected to improve with increased solar irradiation up to a max concentration ratio dependent on the selection of active PV material.

Figure 4-35: Variation of PV Efficiency with Concentration[44]

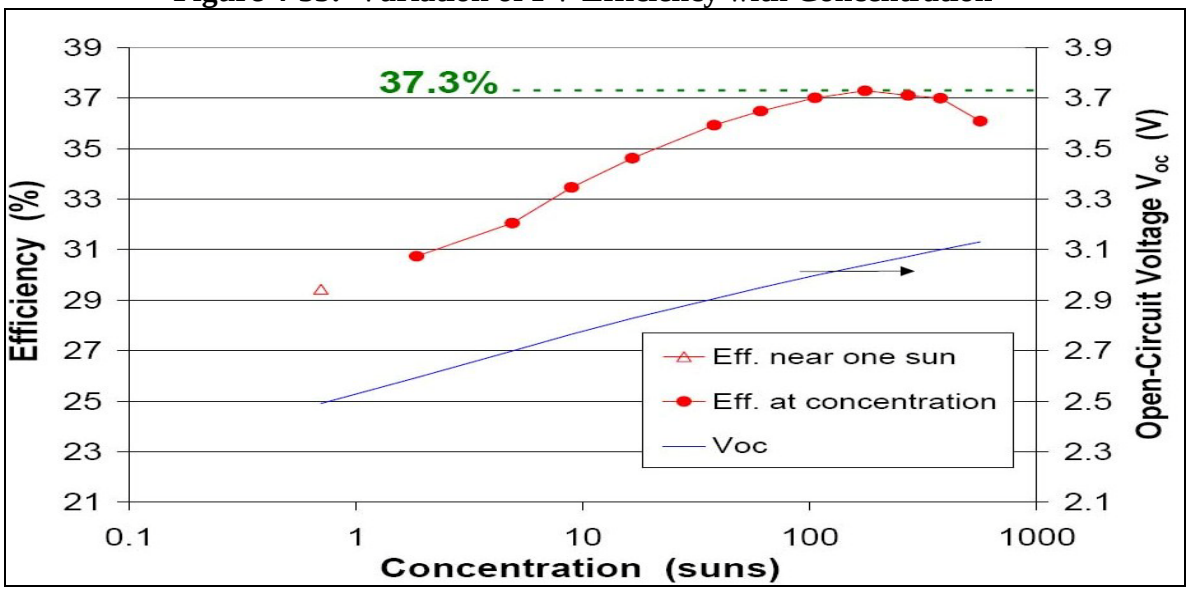

In concentrator PV systems, the PV receiver is generally air-cooled. For the concentrator PEC system, the receiver is inherently water-cooled by the water reservoir and this would prevent high temperatures in the cell.

A different configuration for a concentrator cell has been used by Solar Systems P/L of Australia, separating the IR from the visible light, and using the IR energy to separately heat the electrolyte and enhance electrolysis (see Thompson, McConnell, Mosleh[45]).

Since the PEC receiver is relatively small, the water reservoir and the H_2 and O_2 collectors can be pressurized by the inlet water pump at relatively low added cost. Pressurization to about 300 psi obviates the need for a separate compressor, minimizes water vapor loss by the reactor, and reduces O_2 gas bubble size, which will minimize bubble scattering of incident photons at the anode face.

[43] "Commercialization .of Concentrator Multijunction Photovoltaics", Spectrolab, Inc., Intl Conference on Solar Concentrators, Scottsdale, 2005.
[44] "Commercialization .of Concentrator Multi-junction Photovoltaics", Spectrolab, Inc., International Conference on Solar Concentrators, Scottsdale, 2004.
[45] Cost Analysis of a Concentrator Photovoltaic Hydrogen Production System, J. Thompson, R. McConnell, (NREL), M. Mosleh, International Conference on Solar Concentrators, May 1, 2005.

For solar concentration, an alternative to a reflector array is a solar lens, as used by Entech[46] for their concentrator PV / electric system. One advantage of the system is less sensitivity to wind loads. Figure 4-36 shows the Entech system, steerable in azimuth and elevation, with a 22:1 concentration ratio. The unit uses multi-layer PV cells.

Figure 4-36: Entech PV Refractor System 22:1 concentration ratio

4.5.2 Solar/Thermal Concentrators

A second area of widespread experience with solar concentrators is in the development of solar/thermal power. A typical full parabolic trough array currently used for solar/thermal power generation with one-axis tracking (East-West) is the Kramer Junction System, shown in Figure 4-37.

Figure 4-37: Junction Tracking Solar Thermal Trough Array[47]

[46] "ENTECH's 20-Year Heritage and Future Plans in Photovoltaic Concentrators", O'Neill, Mark, International Solar Concentrator Conference., Nov 10-14, 2003.

[47] "Need for Regulatory Revisions to Successfully Secure CSP Projects in the US: Lessons from Spain", NREL's Trough Workshop 13 Feb 2006 Incline Village, NV , Rainer Aringhoff, Solar Millennium AG, Erlangen, Solar Millennium LLC, Glendora, Los Angeles, & Berkeley, Feb 13, 2006

4.5.3 PEC Solar Concentrator Design for this Study

The Concentrator PEC baseline design for this analysis uses an offset parabolic cylinder array to focus radiation on a linear PEC receiver. The offset parabolic array has advantages of structural weight reduction, aperture blockage elimination, and location of the active receiver components, water feed, and hydrogen collection piping in the reflector base assembly. The PEC receiver component is a linear array of PEC cells at the reflector focal point. The concentrator has 2-axis steering to track the solar direct radiation. The arrays are spaced apart sufficiently to avoid shadowing of solar radiation when the sun is above 10^o from the horizon (East-West) and above 26^o from the horizon (South). Because it uses a concentrator, the array will receive only a small amount of the solar diffuse radiation, as was discussed in Section 3.5.3.

Characteristics of the 2 Dimensional Offset Parabolic reflector, diagramed in Figure 4-38, are:

- No reflector aperture blockage
- 2-axis steerable structure to track sun in azimuth and elevation
- Mounted like an offset feed radar antenna, but with much simpler/lighter structure because of very slow movement.
- Reduced manufacturing cost/weight
- Water feed and gas ducting located on base structure
- Reflector structure of molded composite with a mirror facing surface
- Radiation on PEC receiver confined to a 90^osector

Figure 4-38: Offset Parabolic Cylinder Reflector PEC

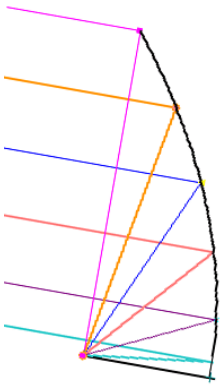

The linear PEC receiver units are mounted at the cylindrical reflector focal line, on the reflector base, with water feed and H_2 ducting through the base structure. The receiver has a cylindrical sector Plexiglas window to minimize structural stress due the 300 psi internal pressure and to focus the radiation onto the PEC cells. Specific receiver characteristics are:

- 10 cm span window, cylindrical to reduce stresses
- Receiver internal refraction by cylindrical water-filled lens
- Cells Pressurized at 300 psi to:
    - eliminate compressor system
    - reduce H_2O vapor in reactor output gas by factor of ~300
    - reduce gas duct sizes
    - reduce gas bubble sizes

- prevent water boiling under high local temperatures

The PEC receiver unit is diagramed in Figure 4-39, with internal details shown in Figure 4-40.

Figure 4-39: Receiver Solar Input Diagram

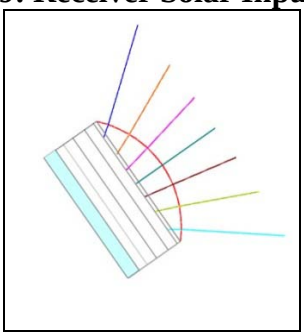

Figure 4-40: Receiver Details

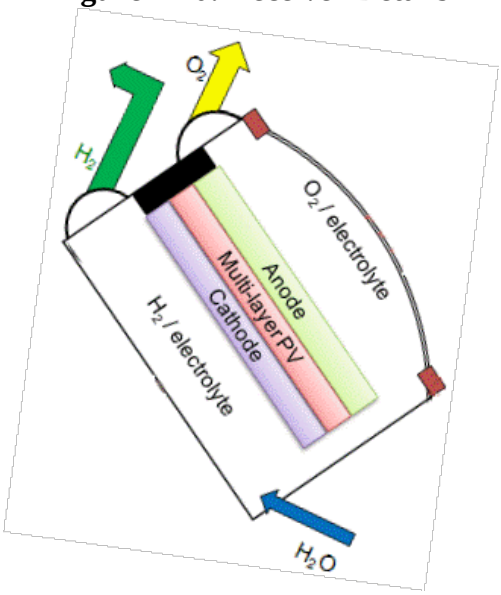

The Type 4 Reactor System Layout for a 1TPD output is shown in Figure 4-41.

Figure 4-41: Type 4 Baseline 1 TPD System Layout[48]

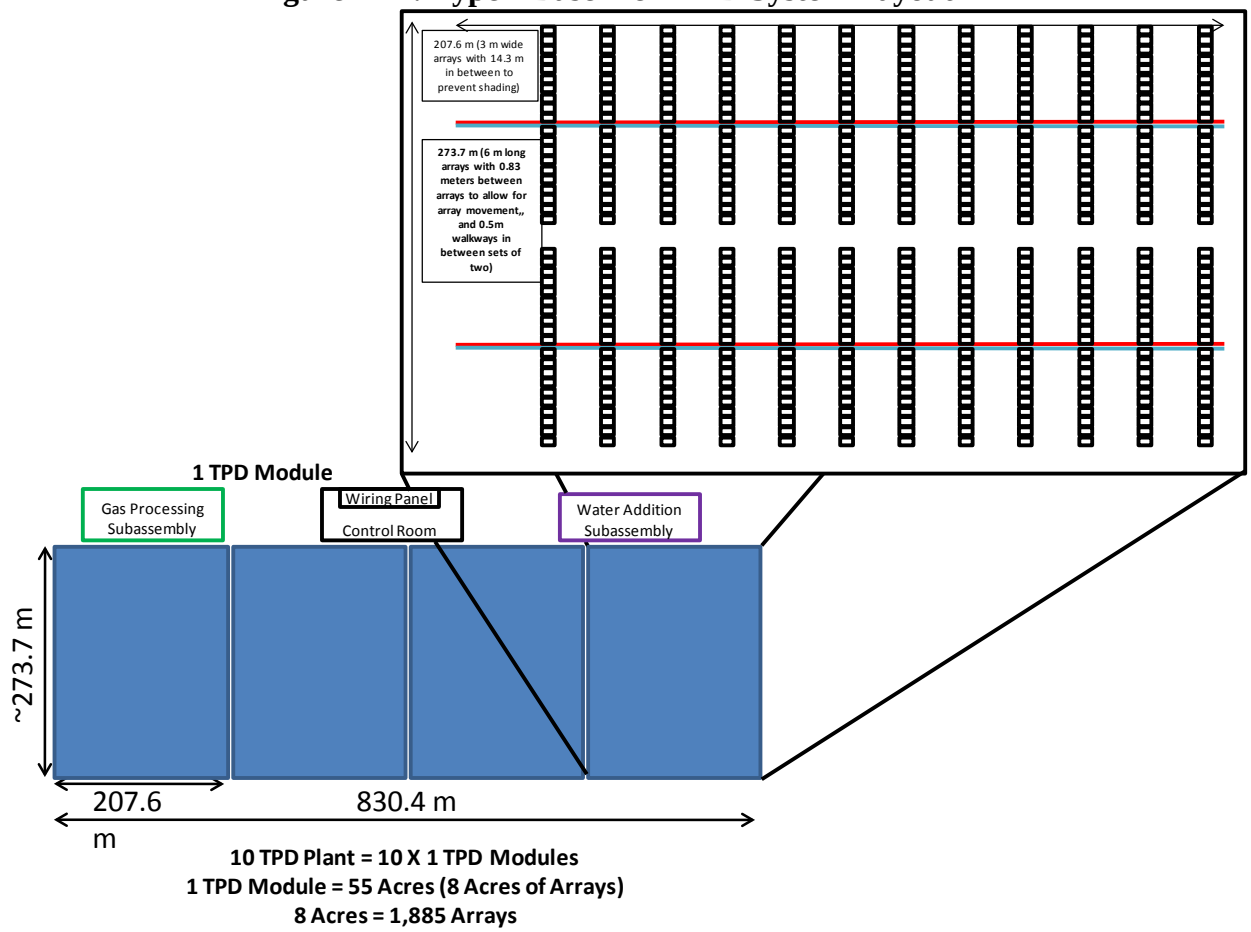

4.5.4 Solar Collector Costs

In estimating reflector collector costs for the Type 4 system, we have used for reference an NREL study of parabolic trough solar thermal power systems[49] for which the collector is a two dimensional parabolic reflector and the receiver at the focal line is a linear thermal energy conversion element. The structures are designed to survive moderate winds in operation and to survive occasional high wind storms by rotating downward in place to reduce drag forces. Costs predicted by this study for year 2020 are listed in Figure 4-42 .

Though the solar collectors in the Parabolic Trough Reference track in one axis, the drive mechanism is only 8% of the hardware cost. We have assumed that the cost increase for two axis tracking is balanced by a saving in structural cost of the offset reflector vs. the symmetrical parabolic reflector of the solar thermal collector. For the PEC Type 4 system, the solar concentrator and tracking hardware by itself is estimated at $60/m^2 (uninstalled) vs. $155/m^2 for the complete Type-3 planar array, however, it allows use of a much smaller amount of PEC cells. For a 10:1 concentration ratio system, the reactor cost per capture area is $120.63/m^2.

[48] This table is approximate and contains slightly more than the number of arrays for a 1TPD plant.
[49] Assessment of Parabolic Trough and Power Tower Solar Technology Cost and Performance Forecasts, NREL/SR-550-34440, Oct. 2003, Sargent & Lundy Consulting Group, Chicago, Ill

Figure 4-42: Type 4 Solar Collector Cost Estimate[50]

COLLECTOR COSTS - Year 2020 based on Trough 400 NREL/SR-550-34440		
Component:		$/collector area
Concentrator	mirror	16 $/m2
	structure	36 $/m2
	drive & controls	8 $/m2
	total basic collector	60 $/m2
Installation	erection	10 $/m2
	foundations	12 $/m2
	total	22 $/m2
Piping	interconnection	2 $/m2
	headers	5 $/m2
	total	7 $/m2
Overall Collector including installation	Equal to cost from NREL/SR-550-34440	89 $/m2

The baseline system uses a concentration ratio of 10:1. Figure 4-43 shows the reduction in receiver cost (per solar capture area) which could be achieved with an increase in concentration ratio from 10:1 to 30:1. Reduction in PEC cell breadth reduces the window span, with a thinner/lower-cost window, and also reduces the PV surface area/cost and cell encapsulation area/cost. A doubling of the concentration ratio from 10:1 to 20:1 could reduce the basic reactor cost by about 17%.

Figure 4-43: Type 4 Cost Reduction with Increased Concentration Ratio

RECEIVER COSTS vs CONCENTRATION RATIO						
Design	Concentration ratio		Baseline	Increased Concentration		
			10	15	20	30
Parameters	Pressure		300 psi	300 psi	300 psi	300 psi
Materials	PV components	$/m2	$22.00	$22.00	$22.00	$22.00
	Window	aperture W edge angle thickness $/m2	0.300 in. 45 deg 0.500 in. $93.84	0.200 in. 45 deg 0.375 in. $71.17	0.150 in. 45 deg 0.250 in. $36.73	0.100 in. 45 deg 0.187 in. $32.87
	Encapsulation	$/m2	$39.00	$39.00	$39.00	$39.00
	TOTAL	$/m2	$154.84	$132.17	$97.73	$93.87
Assembly and markup			$161.42	$150.09	$132.87	$130.93
Receiver Cost / receiver aperture		$/m2	$316.27	$282.26	$230.60	$224.80
Receiver Cost / capture area		$/m2	$31.63	$18.82	$11.53	$11.24
Collector plus Receiver Cost - Installed		$/m2	$120.63	$107.82	$100.53	$100.24
COST RATIO			0%	-11%	-17%	-17%

[50] Assessment of Parabolic Trough and Power Tower Solar Technology Cost and Performance Forecasts, NREL/SR-550-34440, Oct. 2003, Sargent & Lundy Consulting Group, Chicago, Ill.

4.6 *Summary of All PEC Reactor Systems*

Figure 4-44 summarizes the PEC Reactor System sizes and costs.

Figure 4-44: Summary of Reactor Parameters for 1TPD PEC Systems[51]

Reactor Subassembly (incl. feedwater pumps and manifold pipe)		**Type 1** Single-Bed Colloidal Suspension	**Type 2** Dual-Bed Colloidal Suspension	**Type 3** Panel at latitude angle	**Type 4** Solar concentrator 10:1 ratio
Reactor Description		1060' x 40' x 0.3' bed	200' x 19.7' x 1.2' bed	2m x 1m panel	3m x 6m reflector
ft2		42,400	3,937		
m2	m2	3,941	366	2	18
Number of Reactors		18	347	26,923	1,885
Bed area	m2	70,940	126,983		
Photon Capture Area	m2	70,540	126,969	53,845	33,924
Reactor Cost	$	$212,257	$892,934	$8,343,345	$3,135,209
Cost/capture area	$/m2	$3.01	$7.03	$154.95	$92.42
Hydrogen Production					
Baseline Conversion Efficiency	%	10%	5%	10%	15%
Average incident solar energy	kWh/m2/day	5.25	5.25	6.19	6.55
Average photon energy reacted	kWh/day	37,034	33,329	33,330	33,330
LHV of hydrogen	kWh/kg	33.33	33.33	33.33	33.33
Average H2/day	kg	1,111	1,000	1,000	1,000

[51] Though the average daily output from the complete systems is 1,000 kg H_2, The Type 1 reactor must produce an additional 11.11% to make up for H_2 lost in the H_2/O_2 separation process carried out in a PSA (pressure swing adsorption) system. Conversation with UOP regarding PSA losses indicates an expected 90% H_2 recovery in the PSA with a 2:1 molar mix of H_2 and O_2.

5. Gas Processing Subassembly

The function of the gas processing subassembly is to collect, compress, and separate out the product hydrogen and deliver it to the production facility limits. The components of this subassembly, along with pertinent parameters, are listed in Figure 5-1.

Figure 5-1: Gas Processing Components

Components	Type 1 System	Type 2 System	Type 3 System	Type 4 System
Piping	Water inlet, Gas outlet 14.7 psi	Water inlet, Gas outlet, Electrolyte circulation 14.7 psi	Water inlet, Gas outlet, 14.7 psi	Water inlet, Gas outlet, 300 psi
Compressor (2-stage)	305 psi, H_2, O_2, VH_2O	300 psi, H_2, VH_2O	300 psi, H_2, VH_2O	Not needed
Condenser & Intercooler Units	Reactor outlet, condenser, Dual intercoolers	Reactor outlet, condenser, Dual intercoolers	Reactor outlet, condenser, Dual intercoolers	Reactor outlet condenser
PSA - O_2 Removal	PSA needed, 33 % molar O_2	PSA not needed,	PSA not needed	PSA not needed

The outlet pressure of hydrogen at the plant gate is 300 psi. This pipeline pressure was selected to provide a system comparable to other DOE H2A Production Plants, for which outlet pressure is specified at a uniform 300 psi. At the exit of Type 1, 2, and 3 reactors, the gas is at atmospheric pressure. At the exit of Type 4 reactors, the gas is at 300 psi. The Type 1 compressor compresses the gas mixture to 305 psi to accommodate a slight pressure loss in the PSA.

A Hydrogen Flow Meter is physically located at the reactor exits but it is accounted for in the control system subassembly.

5.1 *H_2-O_2 Gas Mixture Safety*

In all of the PEC systems, oxygen and hydrogen are produced. In the Type 1 single bed colloidal suspension system, the product gas within the headspace of the reactor bed (and subsequently fed to the gas processing systems) is a stoichiometric mixture of oxygen and hydrogen with a small amount of water vapor. Over a wide range of ratios, these gases will be a combustive mixture. For the Type 2, 3, and 4 systems, the H_2 and O_2 are inherently separated in the PEC reactor and combustibility issues don't arise.

Explosion limits for H_2/O_2 mixtures have been examined by Shroder et al.[52]. Figure 5-2, below, taken from that reference, shows the Lower Explosive Limit (LEL) and Upper Explosive Limit (UEL) for various mixture fractions of H_2 and O_2.

[52] "Explosion Limits of Hydrogen/Oxygen Mixtures at initial Pressures up to 200 bar", Schroder et al., Chemical Engineering Technology 27 (2004) 847-851.

Figure 5-2: Explosion Limit Pressure/Mixture Dependence for H_2/O_2 Mix

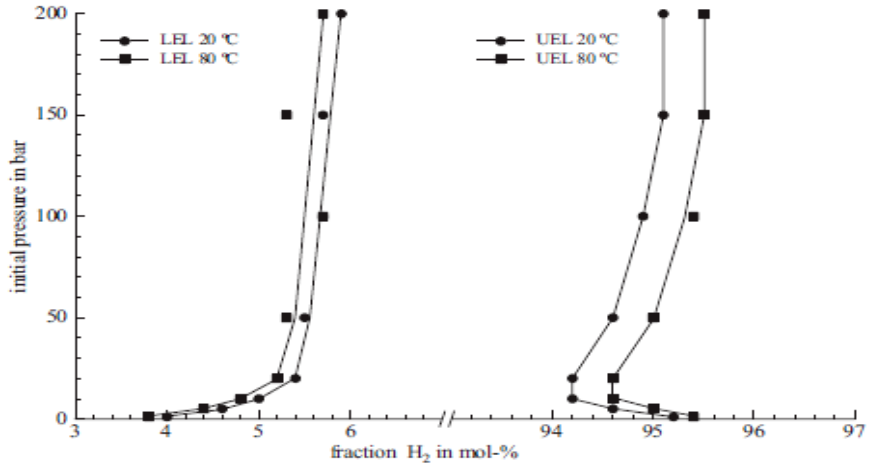

In the Type 1 system, headspace gas temperature is generally equal to 20°C or greater, as corresponds to the curve with circular markers in Figure 5-2. The reactor operates at atmospheric pressure, 1.01 bar. From the graph we see that any molar fraction of hydrogen between 4% and 95.2% where pure oxygen is the other gas is within the explosive limits of the gas mixture. In the Type 1 system, the mole fraction is well within these limits, thus the Gas Capture and Compression components in those systems must be carefully designed to safely handle the product gas.

Storing this flammable mixture in the baggie headspace and piping it to compression and separation poses safety concerns. For this analysis it is assumed that the safety issues are overcome, although to obtain the appropriately safe equipment the capital costs may rise somewhat. Additional investigation is required to determine the exact cost implications.
From the standpoint of compressor safety, Norwalk Compressors of Norwalk, CT, suggest that an oil-free, balanced-opposed, piston compressor can safely compress a hydrogen/oxygen gas stream to 300 psi (20.7 bar) prior to gas separation. Particular care must be taken when compressing the flammable gas mixture to avoid sparking or exceeding per stage temperature limits. However, compression of flammable mixtures using intercooling to hold temperatures down is a fairly routine industrial process and can be conducted safely.

5.2 *Compressors*

The pure H_2 gas, separated from impurities, is delivered to the plant gate at 300 psi (20.4 atm., 20.7 bar). A compressor with intercooling is used in Type 1, 2, and 3 systems. For Type 1 systems, the compressor compresses an H_2/O_2 mix to 305psi prior to input into the H_2 separation unit to allow for a 5 psi pressure loss in the separation. For Type 2 and Type 3 systems, the compressor compresses nominally pure H_2 to 300psi for delivery to the plant gate. For Type 4 systems, no compressor is needed as the pure H_2 gas is already at 300psi coming out of the reactor.

Pursuant to the modular plant concept, the compression system is scaled for the gas flows of a 1 Tonne H_2/day output module. Because hydrogen production peaks during periods of peak solar

intensity, the compression module is sized for the day of the year with highest solar input. For Types 1 and 2, this is the averaged daily output on the summer solstice (June 21). As discussed earlier, the bed headspace for Types 1 and 2 is designed to expand to allow gas accumulation over a day by rising during peak production and falling during low or no production, as solar input increases and decreases, such that the flow rate to the compressor is constant over the day. For Type 3, the maximum output is the noon instantaneous peak output rate on June 21. On all other days, the compressors are operated at reduced capacity. Since the Type 2 and 3 reactors separate the O_2 from the H_2, the compressor volume flow is only about 2/3 of the volume flow of the Type 1 system.

Power for the compressor is based on the gas + vapor flow rate, compression ratio (21:1 overall), fluid specific heat, gas temperatures with intercooling, and 75% compressor efficiency relative to isentropic compression. These are modest requirements by industrial standards. Consequently, compressor power is moderate, with variations depending on the specific reactor system outputs. However, since inlet pressure is 1 atm, compressor first stage cylinder volume will be quite large. For this reason, diaphragm compressors, which would normally be attractive for their long life, inherent non-leak attributes, and positive sealing are not viable candidates, and we have selected oil-free piston compressors for the module design.

For the 21:1 compression ratio, a 2 stage compressor is used, with an intercooler between the first and second stage to reduce interstage gas temperature to about 40^o C (in summer) and condense much of the water vapor. At the compressor exit, a second intercooler is used at the compressor outlet to condense most of the remaining water vapor. The amount of water removed is discussed in the next section addressing condensing and gas separation.

Since the PEC compressors are similar in type and compression ratio to the compressors used in the DOE's H2A forecourt analyses[53], we have based the cost on the H2A compressor cost algorithm of \$4,580/(kgH_2/hr). However, since this algorithm is based on pure hydrogen compression and the PEC systems produce a mixture of gases, we converted the costing algorithm to a molar basis: \$9,233/ (kgmol gas/hr).

5.3 *Gas Cooling and Water Vapor Removal*

For the atmospheric pressure Type 1, 2 & 3 reactors a cooler/condenser is used to cool the gases to 40^oC before the compressor inlet and condense water vapor. This has the inter-related benefits of reducing the vapor input to the compressor, reducing compressor mass flow, reducing compressor inlet temperature, and substantially reducing compression power. A sump and water trap is used to draw the water out of the cooler/condenser. For Type 1, 2 & 3, an intercooler (IC-1) is used after first stage compression and a second intercooler (IC-2) is used after second stage compression. Second stage compression of the gases to 300-305 psi will allow removal of most of the water vapor in the intercoolers before the PSA inlet, thus reducing the input to the PSA and greatly reducing the needs for silica gel water absorption.

[53] The standard DOE H2A forecourt analysis assumes a 4-stage, piston compressor, 300psi inlet, 6250psi outlet, and approximate 1500kgH2/day flow rate.

Since the Type 4 system has high reactor pressure, water vapor pressure, and thus water molar fraction, is a very small fraction of the outlet gas mixture. Consequently, only a condenser is needed for the Type 4 system.

Normally, the reactor product gas is saturated with water. The water vapor molar percent of the exit gases is determined by the water's vapor pressure at the gas temperature, which is the water partial pressure of the gas mixture at reactor outlet. For all the reactors operating in the summer, the bed or water reservoir can reach temperatures exceeding 60°C. Water vapor pressure will increase with increasing PEC reactor outlet gas temperature (which depends on the season) and the water molar fraction at reactor outlet will increase accordingly as shown in Figure 5-3, which shows the vapor fractions at the condenser exit and the two intercooler exits (IC-1 and IC-2):

Figure 5-3: Water Vapor Fractions

Reactor Temperature	Vapor Pressure	Water Molar Fraction (40°C coolant)					
		Type 1, 2, 3				Type 4	
		reactor exit (1 atm)	condenser exit (1 atm)	IC-1 exit (10 atm)	IC-2 exit (21 atm)	Reactor exit (21 atm)	condenser exit (21 atm)
40°C	0.073 atm	7.26%	7.26%	1.69%	0.36%	0.36%	0.36%
50°C	0.125 atm	12.53%	7.26%	1.69%	0.36%	0.61%	0.36%
60°C	0.202 atm	20.20%	7.26%	1.69%	0.36%	0.99%	0.36%
70°C	0.313 atm	31.26%	7.26%	1.69%	0.36%	1.53%	0.36%

The heat exchangers are cooled by coolant water with input temperature of 20°C. Water removed in the condensers and ICs is recycled back into feed water storage.

5.4 *Hydrogen Separation from Contaminants*

There are several commercial means available for separating hydrogen gas from a gas mixture. In this analysis we have focused our attention on Pressure Swing Adsorption (PSA), which has the best properties for this application. Other potential means are Temperature Swing Adsorption (TSA), membranes, electrochemical pumps, and combinations of these methods. While only the PSA system is selected for use in the cost analysis, all separation methods are discussed below. Descriptions of these separation methods are drawn heavily from previous DTI reports[54].

5.4.1 Pressure Swing Adsorption (PSA)

A pressure swing adsorption (PSA) system is selected as the best H_2 separation system for this application. PSA technology takes advantage of a materials affinity to preferentially adsorb a particular gas species at high gas pressure. PSA systems are commonly used in the petroleum industry to purify a variety of gases. Separation of hydrogen gas from steam methane reforming (SMR) product gases (H_2, CO, CO_2, H_2O, CH_4) is common. Use of a PSA to separate hydrogen

[54] James, Brian et al., "Technoeconomic Boundary Analysis of Biological Pathways to Hydrogen Production", NREL/ AFH-8-88601-01, August 2009.

from a H_2, O_2, H_2O mixture is a much less frequently encountered application. Dialogue with Adsorption Research, Inc. indicated that it is practical to use PSA to separate such a mixture.[55]

PSA operates by flowing a pressurized stream of gases (e.g., at 300 psi) across a multi-component adsorbent bed (commonly layers of activated carbon, zeolite, silica gel, etc.) to preferentially capture an undesired gaseous species on the surface of the adsorbent. By careful selection of adsorbent materials, all undesirable species may be captured in the bed so that only high purity gas (often greater than 5 nines purity) exits the absorbent bed. PSA systems are inherently cyclic with a series of beds (typically 4, 6, 8 or 12) operating out of phase. After a bed is "full" (i.e. the adsorbent material no longer has open sites on which to further adsorb contaminant gases), the bed with absorbed gases goes into a "vent' cycle where pressure is decreased (typically to 1 atm) to desorb the contaminants. This vent gas stream is typically vented to the atmosphere, or fed to a burner if it contains residual fuel gases. After venting, the bed is purged with a small amount of the pure H_2 gas stream from the exit of the PSA to drive any residual containment out. After purging, the bed is reconnected to the feed gas and enters an "equalization" cycle where gas pressure is raised to full operating pressure (305 psi in this case) in preparation for the resumption of contaminated gas flow.

Hydrogen recovery is a key metric of PSA performance. Hydrogen recovery is defined as the fraction of inlet gas hydrogen that is ultimately recovered in the pure gas exit stream. There are two main sources of hydrogen loss. The first is hydrogen that is contained in the absorption bed at the beginning of the vent cycle. As the bed is depressurized, this hydrogen is expelled and lost out the vent. The second source of loss, during the purge cycle, is the pure hydrogen that is used to actively vent the system of impurities. By summing these two losses, an accurate measure of hydrogen recovery can be attained.

To determine H_2 recovery for an H_2/O_2 mixed gas system, we have ascertained the packing density and adsorption performance of carbon (for O_2 adsorption) and silica gel (for water adsorption). By modeling the desired flow rates and calculating the hydrogen contained in the bed during the various cycles, the hydrogen recovery is calculated.

Key parameters of the absorbent properties of a typical generic PSA system are shown in Figure 5-4. For the PEC application, the parameters of interest are only those for the adsorption of water and oxygen. For each adsorbent there are two values of principal interest: the amount of gas that adheres to the adsorbent at high pressure, and the amount of gas that adheres to the absorbent at low pressure. It is the difference in adsorption levels between the two pressures that is of interest. Although not strictly linear, we have assumed that the adsorption data varies linearly between the two data points listed.

[55] Private communication with Kent Knaebel of Adsorption Research, Inc., 20 Oct 2008.

Figure 5-4: PSA Sizing for Absorption of Oxygen Contaminant Gas

PSA Adsorbent Parameters			
Gas adsorbed			**O2**
Adsorbent			**Zeolite**
bed void fraction		%	36.0%
bed usage fraction		1/LUB	76.9%
adsorption uptake	pressure	psi	305
	uptake fraction	g O2/g adsorbent	0.0390
adsorbent purge	pressure	psi	14.7
	purge fraction	g O2/g adsorbent	0.00188
	residual at venting		4.8%

The base PSA system cost used is based on an H2A 1500kgH_2/day SMR PSA having 6,065L of total absorbent and a $100,000 total price and then scaled in the manner described below.

Capital costs for the individual PSA systems are estimated based on the performance model described above and the H2A data base, using a scaling factor approach. The performance model is used to calculate the approximate bed size of the PSA vessels for the particular flow rates and gas compositions of each system. Once this PSA bed volume is determined, a scaling factor is used to determine the PEC PSA cost relative to the H2A Model PSA System cost data. An 0.5 exponential scaling factor is assumed resulting in the following equation:

$$\frac{\text{PEC PSA Cost}}{\text{H2A PSA Cost}} = \left[\frac{\text{PEC PSA Bed Volume}}{\text{H2A PSA Bed Volume}}\right]^{0.5}$$

5.4.2 Other Separation Methods

There are multiple other techniques for contaminant separation from the product gases. PSA has been used for the baseline system as the superior option for this application; however the other techniques are described below.

5.4.2.1 *Temperature Swing Adsorption*

Temperature Swing Adsorption (TSA) systems are analogous to PSA systems except they use differences in temperature rather than pressure to preferentially adsorb and desorb contaminant species. While used industrially, TSA systems are not as prevalent in process plants as PSA systems. The main advantage of a TSA system is that it would not require compression of the H_2-rich gas potentially lowering electrical requirements and also avoiding the Type 1 safety concerns of compressing H_2/O_2 gas mixture. However, separation of H_2 and O_2 via TSA requires a significant temperature swing with a refrigeration system typically required to achieve the lower temperature bound. Were "waste" cooling or heating to be available from an adjacent process, TSA would be an attractive option. However, as currently configured such "waste" thermal energy is not readily available, and thus the refrigeration system would be a substantial energy and cost element. Additionally, conversations[56] with Kent Knaebel from Adsorption Research Incorporated, a gas separation consulting company, indicated that PSA was a far

[56] Private communication with Kent Knaebel of Adsorption Research, Inc., 20 October 2008.

superior option, given its vastly reduced cycle time. The cycle for a TSA system would be measured in hours, as opposed to minutes for PSA, necessitating a much larger bed volume in order to separate the same amount of gas. This increased capital cost of the beds and cooling system makes TSA less economically practical than PSA. Consequently, the TSA system was not pursued further.

5.4.2.2 *Palladium Membrane Separation*

Membrane separation units are of two main types: metallic membranes and nano-porous membranes. Metallic membranes typically use palladium (Pd), Pd-alloys, or layered Pd/alloy to allow the diffusion of H+ ions through the membrane. Pd membranes are characterized by very high hydrogen selectivity (typically <10,000), high cost (due to the inherent Pd material cost), and moderate hydrogen permeability that is primarily a function of temperature and membrane thickness. Hydrogen flux through the membrane follows Boyd's Law and is proportional to the difference of the square root of the upstream hydrogen partial pressure and the square root of the permeate (downstream) hydrogen partial pressure. Consequently, Pd-membrane systems work best with highly pressurized inlet streams and low pressure H_2 product streams. While a few small scale Pd-membrane commercial products are on the market (e.g. IdaTech), large scale Pd-membrane hydrogen purification systems are not employed industrially due to performance and cost concerns. Based on membrane system modeling for a 20atm (300psi) hydrogen mixture with 60% H_2 and a 1 atm permeate (pure H_2) outlet pressure, hydrogen recoveries in excess of 90% are theoretically possible.

Drawbacks of Pd-membrane separation systems include:

- the necessity to heat the membrane (and hydrogen) to 250-350^{o}C to ensure adequate hydrogen permeability
- the requirement to compress the H_2-rich feedstream to high pressure thereby raising safety concerns related to H_2/O_2 compression
- the low pressure of the pure H_2 product stream thereby requiring additional H_2 compression to achieve a pipeline transport pressure
- uncertainty of using Pd membrane with H_2/O_2 gas mixtures (the Pd may oxidize or be an H_2/O_2 combustion catalyst)
- the general immaturity of the technology.

For these reasons, Pd-membranes are not selected for further analysis.

5.4.2.3 *Nano-porous Material Membrane Separation*

The other broad class of membrane separation systems is based on nano-porous materials. Nano-porous materials function as molecular sieves and use pore size to preferentially pass molecular hydrogen. Figure 5-5, taken from Phair and Badwal[57], shows the range of nano-porous membrane options. Of these, we judge polymeric membrane to be most applicable to hydrogen gas separation due to their low temperature of operation. However, polymer membranes are not highly selective and thus would require additional downstream purification.

[57]"Materials for separation membranes in hydrogen and oxygen production and future power generation", J.W. Phair, S.P.S. Badwal, (CSIRO Manufacturing and Infrastructure Technology, Victoria, Australia) Science and Technology of Advanced Materials 7 (2006) 792–805.

Additionally, hydrogen flow is driven by differences in hydrogen partial pressure across the membrane. Consequently, compression of the unseparated gas is required once again raising safety concern for H_2/O_2 gas mixtures. A detailed analysis beyond the scope of this project is required to optimize pressure level, permeate purity, and H_2 recovery. For these reasons, polymer membranes don't appear to offer superior benefits over PSA systems and are not selected for further analysis.

Figure 5-5: Nano-porous Membranes

	Polymeric	Carbon	Glass	Aluminosilicate	Oxides	Metal
Pore size[a]	Meso–macro	Micro–meso	Meso–macro	Micro–meso	Micro–meso	Meso–macro
Surface area/porosity	Low > 0.6	High 0.3–0.6	Low 0.3–0.6	High 0.3–0.7	Medium 0.3–0.6	Low 0.1–0.7
Permeability	Low–medium	Low–medium	High	Low	Low–medium	High
Strength	Medium	Low	Strong	Weak	Weak–medium	Strong
Thermal stability	Low	High	Good	Medium–high	Medium–high	High
Chemical stability	Low–medium	High	High	High	Very high	High
Costs	Low	High	High	Low–medium	Medium	Medium
Life	Short	Long	Long	Medium–long	Long	Long

[a]Micoporous = pore radius < 1 nm, mesoporous = 1 nm < pore radius < 25 nm, macroporous = pore radius > 25 nm.

5.4.2.4 *Electrochemical Pumps*

Electrochemical purification of hydrogen is possible using an applied voltage to drive hydrogen across a separation membrane. Such systems have been demonstrated at small scale but are not currently in industrial use. In addition to the gas separation function, electrochemical pumps can be used to pressurize the hydrogen stream, thereby eliminating or reducing the need for mechanical H_2 gas compression. In theory, a mixed gas stream could enter the electrochemical pump at 1atm and a high H_2 purity gas stream could exit at pressure (10-100atm).

Conversations with Glen Eiseman of Hydrogen Pump, LLC, preliminarily explored the use of electrochemical pumps for hydrogen purification. Current products from Hydrogen Pumps use a PBI membrane, operate at ~160^oC, employ a Pt catalyst, compress the H_2 stream to several atmospheres, and contain a supplementary gas cleanup system, since only 98% pure H_2 is passed across the membrane. For Type 1, exposure of a H_2/O_2 gas mixture to Pt could result in catalytic combustion of the gases. Development of alternate non-Pt catalyst is theoretically possible, but the authors know of no such development efforts.

Electrochemical pumps could be used for separation of non-O_2 or very low O_2 containing gas mixtures. However, the systems would incur the following disadvantages:

- the necessity to heat the membrane (and hydrogen) to 160^oC
- the need for a secondary gas cleanup system (such as PSA) to further purify the H_2 product gas
- the electrical consumption to power the device

For these reasons, electrochemical pumps are not selected for further analysis.

5.5 *Piping*

Transporting the gas mixture out of the reactor bed, through the compressor and heat exchangers, and through the PSA, and then the product hydrogen to the facility limits requires hundreds of feet of piping. Poly Vinyl Chloride (PVC) is the selected primary piping material to minimize

costs. Hydrogen embrittlement and gas diffusion are not judged to be significant problems at the moderate pressures and temperatures experienced by PEC systems. Dimensions and costs of the piping are included as part of the costs of the related subassemblies.

5.6 *Capital Costs of Gas Processing Components*

The gas and vapor heat exchanger flows, compressor flows (condenser outlet flows), and the compressor powers were calculated for each system and are listed in Figure 5-6. The flow into the PSA for Type 1 is the gas output from Intercooler–II for Type 1.

Figure 5-6: Gas Heat Exchanger and Compressor Properties

PEC Heat Exchanger Design Peak Gas Flows				**T1**	**T2**	**T3**	**T4**
Condenser input	Pressure		psi	14.7	14.7	14.7	300
	Design Criteria - Peak Month			flow average on June 21		flow peak on June 21	
	design mass flow	H2	kg/hr	71.1	64.0	153.8	107.8
		O2	kg/hr	564.1	0.0	0.0	0.0
		VH2O	kg/hr	242.4	144.7	347.9	9.6
		Total	**kg/hr**	877.5	208.7	501.7	117.4
	design mole flow	H2	k-Moles/hr	35.3	31.7	76.3	53.5
		O2	k-Moles/hr	17.6	0.0	0.0	0.0
		VH2O	k-Moles/hr	13.5	8.0	19.3	0.5
		Total	**k-Moles/hr**	**66.3**	**39.8**	**95.6**	**54.0**
Intercooler-I input	Pressure		psi	64	64	64	
	mole flow	Total	**k-Moles/hr**	**57.0**	**34.2**	**82.3**	NA
Intercooler-II input	Pressure		psi	305	300	300	
	mole flow	Total	**k-Moles/hr**	**53.8**	**32.3**	**77.6**	NA

PEC System Compressor Powers				**T1**	**T2**	**T3**	**T4**
Flows	design max	stage 1	k-Moles/hr	57.0	34.2	82.3	NA
		stage 2	k-Moles/hr	53.8	32.3	77.6	0.0
	average	stage 1	k-Moles/hr	37.1	22.3	22.3	NA
		stage 2	k-Moles/hr	35.0	21.0	21.0	NA
Pressure ratio				4.35	4.35	4.35	NA
				4.78	4.78	4.78	0.0
Powers	design max power	stage 1	kW	97.6	57.2	136.8	
		stage 2	kW	100.0	60.6	145.0	NA
		total	kW	**197.6**	**117.8**	**281.8**	
	average power	stage 1	kW	63.3	37.1	37.1	
		stage 2	kW	64.9	39.3	39.3	NA
		total	kW	**128.2**	**76.4**	**76.4**	

The compressors, condensers, and intercoolers were sized for the maximum flow conditions as defined in Section 4.

The components of the Gas Processing subassemblies and their cost totals are specified in the costing summaries for each PEC type. For the condenser and intercoolers, separate shell and tube heat exchanger systems, including the water coolant pumps, were defined for each application and priced based on Plant Design and Economics for Chemical Engineers[58]. Costing for gas processing components is based on peak flows. These costs are listed in Figure 5-7.

[58] Plant Design and Economics for Chemical Engineers, Peters, M., Timmerhaus, K., West, R., McGraw-Hill, 2003.

Figure 5-7: Capital Costs of Gas Processing Components (without piping)

Subassembly	Cost Components	Cost			
		Type 1	Type 2	Type 3	Type 4
Compressor	Molar Flow kgMol/hr	57.00	34.21	82.26	
	molar cost $/kgMol/hr		$9,233	/kgMol/hr	NA
	Price	$526,302	$315,884	$759,481	
	Source: H2A Cost guidelines				
Heat Exchangers	Condenser, with cooling pump	$13,765	$10,626	$16,607	$7,098
	Intercooler-1 with cooling pump	$15,103	$11,464	$17,894	-
	Intercooler-2 with cooling pump	$15,552	$11,870	$18,495	-
	Source: Plant Design and Economics for Chem. Engineers				
Gas Separation	Pressure Swing Adsorption	$107,147	-	-	-
	Source: H2A Cost guidelines with scaling factor				
TOTAL		$677,868	$349,844	$812,477	$7,098

6. Control System Subassembly

Plant control systems serve many functions including local and remote monitoring, alarming and controlling of plant equipment and functions. The more functions the system performs, the more costly and complex the system becomes. A very simple system may provide only local indication or monitoring of equipment operation. A complex system would include all three functions for each piece of equipment from a remote facility and some logic for how to operate each piece under a given set of conditions. Automating of plant operations can increase the cost of the control system and needs to be evaluated against the operational labor savings. As described below, we have assumed the lowest level of control sophistication consistent with full functionality and safe operation.

6.1 *Components*

For this subassembly the design approach was to create a basic system which satisfies safety requirements and provides savings in operational labor. Because of the reactors' large area requirements, remote capabilities are essential. This will require electrical wiring to be laid out between the plant components and the primary control area. Monitoring of the primary indicators will be included. Alarming capabilities will be used to draw attention to hazardous conditions. Central controls will be used for flow valves. For the basic control system, the components and instrumentation for each function are listed in Figure 6-1.

Figure 6-1: Control System Components

Components
Programmable Logic Controller (PLC)
Control Room Computer, Monitor, Labview software Control Room Wiring Panel
Bed Reactor Wiring Panels (Type 1 and 2)
Wiring Conduits Power Wiring Instrumentation Wiring
Production Monitoring Instrumentation Water Level Controllers Pressure Sensors Gas Flow Meters
Alarms Hydrogen Area Sensors
Electrical power

While the control system is relatively simple, the subassembly is complicated by the sheer size of the reactor field and the modular nature of the reactors. Each reactor must be individually monitored and controlled, leading to a large number of replicated sensors. Additionally, the instruments are dispersed over the plant area, up to ~108 acres in size, leading to long runs of wiring. To simplify the system, all instrumentation will operate on electricity rather than compressed air, so that an air compressor is not required. Electricity will be treated as a plant operating expense and bought off the grid at the typical $/kWh for the region.

For monitoring and control of the PEC processes, sensors and controls are used to maintain proper, safe system operation. These include water level controllers, pressure sensors, hydrogen sensors, and gas flow meters as described below:

- Water level controllers:
  - Maintains water in reactor at a level to assure electrolyte contact with anode and cathode surfaces.
  - Designed for max make-up water flow for June 21 solar condition
- Pressure sensors:
  - Monitor pressure to sense pressure build-up or loss in system
  - Type 1 and 2: one per reactor bed
  - Type 3 and 4: 18 per PEC module
- Hydrogen sensors:
  - Used as contaminant warning system on small samples of output gases
  - Thermal conductivity sensor – senses large conductivity difference between H_2 and other potential gases (O_2, N_2, H_2O)
  - Can use an input gas dryer to eliminate water
  - Located at reactor gas collector pipes
  - Continuous operation, using very small gas flow samples

- Gas flowmeters:
    - Measures flow of gas mixture (H_2 and O_2 gas plus H_2O vapor)
    - One flowmeter per system module located at the gas processing system inlet

The number of these used in each system depends on the characteristics and needs of the particular PEC reactors. Numbers of sensors and controllers and their capacities are listed in Figure 6-2.

Figure 6-2: Sensors and Controllers

Baseline Systems	Type 1	Type 2	Type 3	Type 4
Water Level Controllers				
number	1 per reactor bed	1 per reactor bed	1 per 10 panel assembly	1 per reactor receiver
max water flow @ L/min	2.174	0.092	0.001	0.008
Pressure Sensors				
number	1 per reactor bed	1 per reactor bed	18 per PEC module	18 per PEC module
Hydrogen Sensors				
number	1 per reactor bed	18 per PEC module	18 per PEC module	18 per PEC module
max gas flow @ L/min	5.90	3.54	3.10	2.04
Gas flow meter				
number	1 per PEC module	1 per PEC module	1 per PEC module	1 per PEC module

6.2 *Wiring*

Because of the large size of the plants, there is significant amount of wiring involved with conveying power to the flow control and instruments as well as wiring for instrumentation sensors. Figure 6-3 shows a possible layout of the production facility for Type 1 systems. Some key dimensions are identified so that approximate lengths of wiring and conduit can be computed. The number of wiring runs required is shown in the Wiring Panel. All panels are assumed to be at the near end of each reactor unit and subassembly center. The hydrogen flow meter has a single signal and power wire. The flow valves have 1 power wire but 2 signal wires; 1 for actuating the valve and 1 for status of valve. Since this is a simple control system, other equipment (pumps, compressor, gas separation unit) will only have local control and monitoring. All monitoring and sensor instrumentation has a single power and a single multiplexed signal wire with the exception of the hydrogen area sensor. It requires two signal wires for monitoring hydrogen and alarming at certain conditions. Water flow control into each individual reactor or panel will be computer controlled from the central controller.

Figure 6-3: Typical Subassembly Design Showing Control System - Type 1

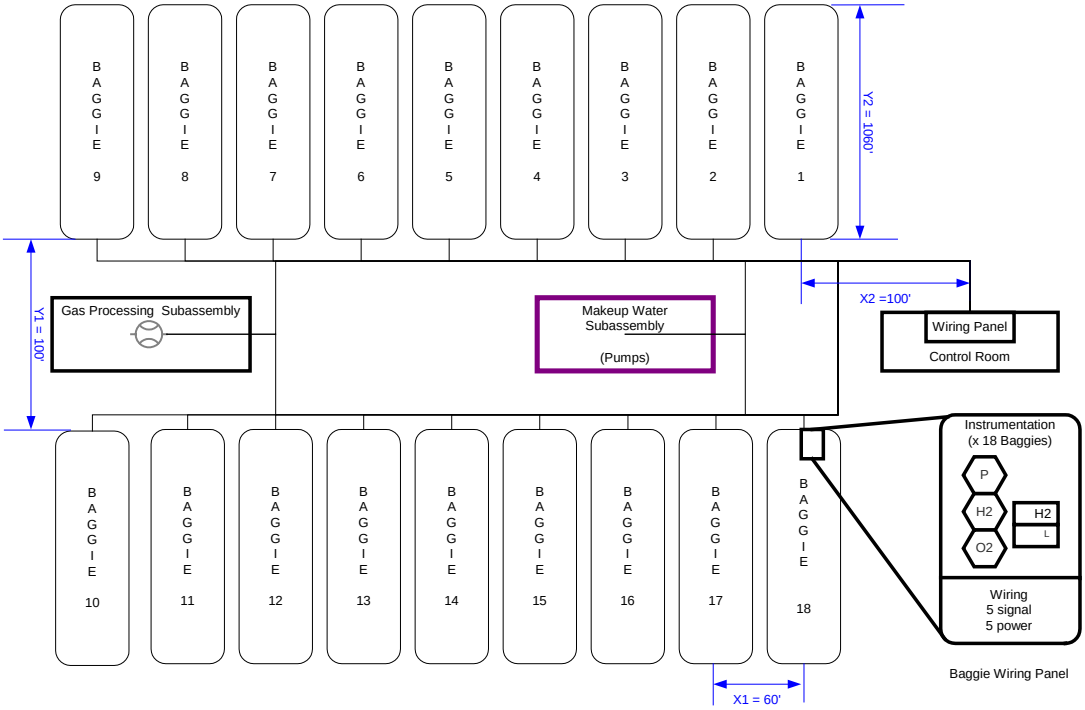

Each of the PEC Types will have different layouts depending on size and numbers of the reactors. Based on this format, the wiring quantities needed for the systems are listed in Figure 6-4 . Signal and power wiring will be run in separate conduits. This is done to ensure that there is no interference in the signal data from the power wiring. In the diagram above, there are two main conduits runs (above and below the gas processing subassembly shown in the diagram). That route will be used for both power and signal wiring. Each individual reactor assembly will have its own conduit run along the length of the reactor for the wiring panel located at the near end. Each subassembly will have its own conduit run off the main horizontal conduit lines for its wiring.

Figure 6-4: Control System Wiring and Conduit Quantities

Components	Signal Wiring Qty (ft)	Power Wiring Qty (ft)	Conduit Qty (ft)
Type 1	21,060	1,404	4,420
Type 2	1,621,190	164,039	76,836
Type 3	23,233	2,323	11,617
Type 4	24,157	2,416	12,079

The flow valve and flow meter wiring requirements are included in the appropriate subassembly line. The additional power wiring in those subassembly lines are for the other equipment (pumps, compressors, etc) that require power. The control system wiring could have been done overhead with cable trays, however, since some level of excavation will already take place to prepare the land, it is assumed that the lines are placed underground. Installation costs of buried conduit in this case will be lower because it is included in the excavation of the reactor area.

6.3 *Capital Costs*

The analysis above provides a fairly extensive list of components for a typical control system. All of the instrumentation, sensors, and wiring is COTS (commercial-off-the-shelf) and readily available. The costs of those components are summarized in Figure 6-5.

Figure 6-5: Capital Costs of Control System Components

Subassembly	Component	Unit Price
PLC	Programmable Logic Controller - Type 1 and 2 Programmable Logic Controller – Type 3 and 4 Source: DTI Estimate	$2,000 $3,000
Control Room	8’ x 20’ trailer (1 trailer for types 1 and 2, 2 trailers for type 3 and 4) Source: http://www.buyerzone.com/industrial/modular_buildings/prefab_guide.html	$50/ft2
Control Room Wiring Panel	Customized to wire count Source: Consultation with Innomation Systems Inc	$3000
Bed Reactor Wiring Panel	Termination panel. Features transmit and, adjustable input/output levels. Available as PC board only or in a case. +6 to 15 mA Tx. Source: Information from Tessco Technologies Inc.	$146
Computer & Monitor	Standard Desktop, Vostro 420 or similar Source: Dell	$1500
Labview Software	Labview 8.6 Professional Edition Source: National Instruments	$4299
Water Level Controllers	DTI design with float valve control Source: DTI	$50
Pressure Sensors	DP transmitter and sensor, displays, 4 to 20 ma output, standard process connection Source: Omega Engineering Inc. PX209 Pressure Transducer + DPi32 Meter	$345
Hydrogen +Oxygen Area Sensors	316 SST components, displays, 4 to 20 ma output, standard process connection Source: Honeywell 7866 Gas Analyzer (http://www.lesman.com/unleashd/catalog/analytical/analyt_hwhydrogengas.htm)	$7,600
Hydrogen Flow Meter	6” vortex type, 316 SST, displays, 4 to 20 ma output, standard process connection Source: Information from Emerson Process Management	$5,500
Instrument Wiring	22 GA Copper wire UL1007/UL1569 Source: Waytek Inc. at www.waytekwire.com @ 500’ qty	$0.02/ft
Power Wiring	14 GA Copper wire UL1007/UL1569 Source: Waytek Inc. at www.waytekwire.com @ 500’ qty	$0.10/ft
Conduit	½”, 100’ pack, flexible PVC tubing, resistant to oil, water, corrosion Source: Waytek Inc. at www.waytekwire.com @ 550’ qty	$0.58/ft

7. General Cost Assumptions and Calculations

This section addresses baseline assumptions made to obtain the estimated yearly capital costs and operating costs for each of the four systems. On assessing yearly costs for each system's capital equipment investment, an appropriate return on investment (ROI) was used. In order to evaluate the ROI, a discounted cash flow (DCF) analysis was performed using the H2A Production Model, Version 2.0.

The H2A Costing Model provides a structured format for a user to enter parameters which impact cash inflows and outflows associated with the construction and operation of a Hydrogen Production Plant. There are numerous plant-specific parameters which must be entered. Additionally, there are H2A Default values for several of the parameters which can be modified to meet specific circumstances. Once all parameters have been entered, the H2A model computes the levelized cost of hydrogen in $/kg$H_2$.[59]

In order to develop levelized costs, several parameters must be defined. Because this analysis focuses on a plant which is still in its conceptual stage, many of the values for these parameters must be assumed. These are for the baseline systems and analyses. Later in this report, certain parameters with significant uncertainty were varied to show hydrogen cost sensitivity to those parameters.

7.1 *Default H2A Parameters*

The standard default H2A financial values and hydrogen plant operating parameters are listed in Figure 7-1 and are applied to all the PEC systems studied. No hydrogen dispensing parameters are listed here because the PEC plants are central type plants and thus dispensing is not factored into the analysis.

Figure 7-1: H2A Default Values used for all PEC Systems[60]

Financial Parameters	Assumptions
Operating Period	20 years
Facility Life Construction Period and Cash Flow	20 years 1 year
CO_2 Capture Credit	Not included in base cases (default value = 0)
CO_2 Production Taxes O_2 Credit	Not included in base cases (default value = 0) Not included in base cases
Depreciation Type and Schedule for Initial Depreciable Capital Cost	MACRS: 20 years for H2A central model
Inflation Rate	1.9%, but with resultant price of hydrogen in reference year constant dollars
Installation Cost Factor	1.3 (when not specifically calculated)
Land cost	$500/acre

[59] For further description of the H2A Model please consult reference:, D. Steward, T. Ramsden, and J. Zuboy. H2A Production Model, Version 2 User Guide. NREL/TP-560-43983. Golden, CO. September 2008.

[60] D. Steward, T. Ramsden, and J. Zuboy. H2A Production Model, Version 2 User Guide. Appendix 3: Default Values and Assumptions. NREL/TP-560-43983. Golden, CO. September 2008. p. 60.

Financial Parameters	Assumptions
Property Taxes and Business Insurance	2%/year of the total initial capital cost
Reference Financial Structure	100% equity funding with 10% IRR; Incl. levelized H_2 price plot for 0%–25% IRR; Model allows debt financing
Internal Rate of Return	10% after tax
Working Capital Rate	15% of the annual change in total operating costs
Income Taxes	35% Federal, 6% State, 38.9% effective
Sales Tax	Not included - facilities and related purchases are wholesale and through a general contractor entity
Decommissioning	10% of initial capital
Salvage Value	10% of initial capital
Operating Parameters	**Assumptions**
Hydrogen Pressure at Central Gate	300 psig
Hydrogen Purity[61]	98% minimum; CO < 10 ppm, sulfur < 10 ppm
Production Facility Maintenance & Repair	0.5% of direct capital cost (per year)
Burdened Labor Rate for Staff	$50/hour
G&A Rate	20% of the staff labor costs

7.2 *System Common Parameters*

In addition to the financial parameters defined by H2A, there are other project inputs which must be quantified in order to carry out the DCF Analysis. All inputs can be found on the following worksheets in the H2A model;

- Input_Sheet_Template
- ReplacementCosts
- CapitalCosts

Many of these parameters are specific to the location, operation, and type of plant. In the case of these PEC systems, there are some parameters that are the same for all systems and some that vary by system. The parameters in Figure 7-2 are common to all systems.

Figure 7-2: Parameters Common to All Systems

Parameter	Assumed Value	Worksheet
Operating Capacity Factor	90%	Input_Sheet_Template
Reference Year Dollars	2005	Input_Sheet_Template
Site Preparation	1% of direct costs minus unique excavation costs	Input_Sheet_Template
Engineering & design	7% of direct costs	Input_Sheet_Template
Process Contingency	20% of direct costs	Input_Sheet_Template
Project Contingency	$0	Input_Sheet_Template
Up-Front Permitting Costs	0.5% of direct capital costs	Input_Sheet_Template
Annual Maintenance & Repairs	0.5% of direct capital costs	Input_Sheet_Template

[61] Purity levels are driven by H_2 vehicle consumption requirements.

7.2.1 Operating Capacity Factor

The operating capacity factor can be found on the Input_Sheet_Template Worksheet of the model. This analysis assumes that the plant and dispensing station have a 90% operating capacity consistent with H2A baseline assumptions for a large plant. This capacity factor takes into considering things such as planned maintenance outages, forced outages, etc. Thus, if the plant is capable of producing 1,000kgH_2/day, only 900 kgH_2 will be output and economic benefit analysis is based on the amount output or sold. Since each plant's operational output is cyclical with the day and seasons, routine maintenance, such as for pumps, valves, compressors, and PSAs, can be carried out the during off-peak portion of the cycles. This would require some cross-piping of the gas and liquid lines.

7.2.2 Reference Year Dollars

The reference year dollars parameter refers to the year dollars for which the cost of hydrogen is reported. The H2A standard is to report out hydrogen costs in 2005 dollars. The model expects capital costs to be entered in 2005 dollars. In this analysis Reference Year 2005 was selected.

7.2.3 Site Preparation Parameter

The site preparation parameter can be found on the Input_Sheet_Template Worksheet of the model. In central plants, H2A defaults this value to 1% of direct costs– i.e., total initial capital, installation, and setup costs. This analysis uses the same default value however, the cost basis is slightly altered.

For the Type 1 and 2 systems, the direct costs include land excavation for baggies. We excluded that from the cost basis since excavation itself is a site preparation cost. Excavation is not all inclusive as site preparation is still required for things such as driveways, compressors, PSAs, and control buildings.

7.2.4 Engineering & Design Parameter

The engineering & design parameter can be found on the Input_Sheet_Template Worksheet of the model. While the H2A central plants default value is 13% of initial direct costs, we have reduced this value to 7% due to the modularity of the design.

7.2.5 Process Contingency Parameter

The process contingency parameter can be found on the Input_Sheet_Template Worksheet of the model. In H2A central plants default value is 15% of direct costs. This analysis uses 20% of direct costs due to the greater uncertainties in the system configuration.

7.2.6 Project Contingency Parameter

The project contingency parameter can be found on the Input_Sheet_Template Worksheet of the model. In our analysis we have chosen to include all contingency factors in the Process Contingency Parameter, thus the project contingency is set to $0.

7.2.7 Up-Front Permitting Costs

The up-front permitting cost parameter can be found on the Input_Sheet_Template Worksheet of the model. The H2A default for this parameter is 9% of initial direct costs. This analysis uses 0.5% of initial direct costs due to the modularity of the design and its environmental benefits.

7.3 *System Specific Parameters*

The second type of parameters are those which are specific to the system analyzed. Figure 7-3 lists these parameters and rules of thumb applied in computing their values. These are system specific because they are associated with feedstock, process design, and plant design.

Figure 7-3: System Specific Parameters

Parameter	Rule Applied	Worksheet
Land Required	Type 1 & 2: 30% > reactor site Type 3 & 4: Reactors + inter-reactor spacing + gas processing	Input_Sheet_Template
Production facility plant staff	1 worker per shift per 100 baggies	Input_Sheet_Template
Utility Usage	Electricity and water costs use H2A pricing	Input_Sheet_Template
Feedstock Usage	Water uses H2A pricing	Input_Sheet_Template
Yearly Replacement Costs	Depends on system details	ReplacementCosts

7.3.1 Baseline Uninstalled Costs

Baseline uninstalled costs for facility equipment components are on the Capital Costs Worksheet of the model. There is no H2A default value. These are the capital costs of the equipment that are computed for each system. Those separately calculated values are imported into this area of the H2A Production Model. These costs are listed in the system bill of materials.

7.3.2 Installation Cost Factor

The equipment installation cost factor parameter used on the Capital Costs Worksheet of the model is the default value of 1.3, with the exception of the Type 1 and Type 2 reactor beds. The installation costs of these are specifically calculated in a separate excavation cost calculation.

8. Specific System Capital Costs

This section discusses the capital costs of the unique components of Type 1 through 4 systems.

8.1 *Reactor Costs*

8.1.1 Type 1 and Type 2 Reactor Nanoparticle Costs

The explanation of Type 1 and 2 system nanoparticle costs appears in sections 4.1.2 and 4.2.2.

8.1.2 Baggie Sizing

The reactor baggie is fabricated by laminating an upper transparent film to a lower film. When calculating the size of the High Density Polyethylene (HDPE) film needed for the baggies, it is necessary to add the extra width that will be sealed together in the laminator during baggie

construction. In addition, we allow for sufficient volume so that the baggie can rise vertically to accumulate gas over a daily cycle.

In choosing the dimensions of the baggies, polyethylene manufacturers were consulted to determine the manufacturing constraints of polyethylene film production. Since the HDPE is designed to be an impermeable hydrogen gas barrier, it is desirable to avoid seams between sheets as these are potential leak paths. To minimize total sealing areas, the baggies are sized based on the largest single sheet of HDPE commercially available. Conversations with Berry Plastics indicated that the maximum width for a roll of HDPE film is 56 feet. However, to minimize constraints on truck transportation we used a roll width of 42 feet, allowing a 40 foot wide baggie. Berry Plastics also indicated that roll lengths to over 1000 feet are feasible. To ensure impermeability to hydrogen, Berry Plastics recommended 6 mm thick film. For a manageable bed size, we use a length[62] of 1060 ft.

The clear HDPE cover transmittance impacts overall field bed dimensions because it reduces the full solar insolation reaching the particles. Data from the manufacturer indicates that the average transmission of sunlight is 90% across the film.

The baggies are designed to accumulate generated gas so as to average the output of the collection system over a day. To calculate gas production, we used sun position data from the NREL SOLPOS model combined with data from the NREL monthly solar ground measurements to calculate the amount of hydrogen gas being produced during June 21, when solar insolation and corresponding hydrogen production peaks[63], With the rate of gas production and the area of the baggie, we computed the total height required of the film to accommodate the gas volume. We then determined the average rate of gas removal needed to remove the gas accumulated over the 24 hour cycle. Approximately 29 cm of vertical headspace is required to account for this gas accumulation. The average gas flow rate was used to size the compressor and PSA.

8.1.3 Quantity of Baggies

The dimensions of the baggies are determined largely by the constraints of the HDPE film production and practical considerations such as ease of truck transport. However, with these numbers relatively constrained, the determining factor for quantity of baggies is the area of beds required to produce an average of 1,000kg of usable hydrogen gas per day. According to PSA modeling and conversations with PSA manufacturer UOP, PSA systems operating on a stoichiometric H_2/O_2 gas mixture can achieve approximately 90% hydrogen recovery. As mentioned earlier, the HDPE film is only 90% transparent as well. Thus we must oversize the reactor bed in order to account for both this photon loss and the PSA hydrogen losses to achieve the target net 1,000kgH_2/day. Based on the solar insolation, the assumed conversion efficiency of photons to hydrogen, and efficiencies of other components, we integrated the hourly H_2 production to get a daily average kgH_2/m^2 rate. This, combined with our desired H_2 production level, allowed us to calculate the total production area required, by dividing the total area needed by the size of an individual baggie.

[62] The exact length of the bed was selected such that a integer number of baggies was needed to obtain the targeted H_2 production rate.
[63] NREL MIDS SOLPOS (Solar Position) model.

8.1.4 Excavation of Land for Reactor Bed Placement

Because of the considerable footprint area of the baggies, detailed attention was given to calculating an accurate cost for the preparation of the reactor area. Consultation with Mark Dormsteader from Metro Earth Works[64], a company that focuses solely on earth moving projects, suggested that our project would require a loader/dozer and a roller. He said that medium sized equipment would be adequate for such a project. The project would also require a foreman and two laborers on foot. Assuming a standard 8 hour work day, it was estimated to take one day to level the area for one baggie.

To calculate the wages of the workers, we used the Department of Labor's Davis-Bacon Wage Determinations for 2008 which provides a state by state breakdown of average wages for various jobs[65]. We also used equipment rental costs referenced by this report taken from The Blue Book of Building and Construction. The costs for equipment rental and the wages vary widely, causing substantial variability in the construction price depending on location. Figure 8-1 shows some examples of wages and rental costs in the American Southwest.

Figure 8-1: Davis-Bacon Hourly Wage Rates

TABLE 1 – HOURLY WAGE RATES

JOB CLASSIFICATION	AZ	CA	CO		ID		KS	NE	NV	
ZONE			1	2	1	2			LV	CAR-SON CITY
Foreman	44.44	78.84	43.87	45.46	45.73	47.91	23.89	23.84	71.06	63.33
General Laborer	25.69	49.97	22.15	28.63	39.75	41.93	13.76	13.06	50.89	38.71
Chainsaw Operator	26.05	52.97	25.98	29.69	40.26	42.44	15.20	17.63	51.28	39.09
Powderman	28.71	52.97	40.88	40.65	40.04	42.23	17.74	18.26	51.48	39.46
Wagon Drill Operator	40.02	69.43	40.88	41.10	43.55	45.74	17.01	18.26	51.35	39.09
Asphalt Spreader Operator	41.57	67.40	40.65	40.65	43.06	45.24	19.55	19.44	62.10	56.12
Backhoe Operator	40.80	69.51	29.00	29.00	43.42	45.61	18.10	15.50	66.45	57.48
Dozer Operator (1)	35.33	71.38	40.65	40.65	43.51	45.69	18.10	18.26	66.95	56.23
Dozer Operator (2)	40.02	71.38	40.65	40.65	43.51	45.69	18.10	20.15	66.95	58.55
Front End Loader Operator (1)	40.02	71.38	40.65	40.65	43.06	45.24	18.10	17.94	66.45	58.01
Front End Loader Operator (2)	41.57	73.50	40.88	40.88	43.31	45.49	18.10	19.04	67.13	58.65
Grader Operator	41.57	75.77	28.73	40.88	43.51	45.69	19.55	18.93	67.10	58.29
Heavy Duty Mechanic/Welder	35.56	71.38	29.25	41.10	43.51	45.69	21.00	20.38	68.60	57.48
Hydraulic Excavator Operator	41.57	75.77	40.88	40.88	44.09	46.28	19.55	19.75	67.38	61.11
Truck Driver (1)	31.94	56.92	25.01	27.62	41.13	43.31	17.38	15.19	54.29	34.67
Truck Driver (2)	32.83	57.38	25.01	28.12	41.39	43.57	18.10	17.08	55.26	40.48
Roller Operator Compaction	35.33	68.31	40.65	40.65	42.61	44.79	17.38	15.19	54.29	34.67

LOADERS:

Crawler type, diesel powered, with EROPS:

Model	Bucket Size	Hourly Rate ($)		
	Cubic Yards	AZ,NM,UT	CO,ID,KS,NE,NV	CA,SD,WY
Caterpillar 933C	1.30	41.72	43.33	45.42
Deere 555G	1.50	51.52	53.56	56.21
Caterpillar 953C	2.42	84.96	88.76	93.68
Caterpillar 963C	3.20	110.46	115.20	121.34
Caterpillar 973C	4.19	161.25	168.29	177.42

Since the system is in the Mojave Desert, next to Arizona, Arizona labor rates are more appropriate, as the California rates are for primarily urban construction. Based on costs for

[64] Private communication with Mark Dormsteader from Metro Earth Works, George /Kevin: add reference.

[65] Moll, Jeff, Marjorie Apodaca, Ken Goddard, Jon Stites, Andrea Glover. Cost Estimating Guide for Road Construction. US Forest Service, USDA, Washington DC. April 2008.

construction in Arizona, Figure 8-2 shows cost for land leveling for an 18 baggie Type 1 system. Other systems costs were estimated in a similar way based on the particular area of the system. The excavation costs calculated concerned only the leveling of land for the baggie installation. Installation costs of the other system components are computed using H2A methodology.

Figure 8-2: Excavation Cost Estimate for Type 1 and Type 2 Systems using Arizona Costs

Excavation Cost Estimation for Arizona		
Equipment Cost- Dozer		86.4 $/hr
Equipment Cost- Roller		68.36 $/hr
Operator Cost- Dozer		35.33 $/hr
Operator Cost- Roller		35.33 $/hr
Laborer Cost		25.69 $/hr
Foreman Cost		44.44 $/hr
Number of Laborers		2
Number of Operators		3
Total Cost/ Day	$	2,570
Total Cost/ Bed Area	$	2,570
Total Cost/ Type 1 System	$	46,259
Total Cost/ Type 2 System	$	82,237

8.1.5 Type 1 and Type 2 Reactor Costs

The total reactor costs for Type 1 and 2 are shown in Figure 8-3.

Figure 8-3: Type 1 and Type 2 Baseline Reactor Costs

	Type 1	Type 2
Type	Horizontal single bed	Horizontal dual bed
Gross Production (kgH_2/day)	1111[66]	1000
Net Production (kgH_2/day)	1,000	1,000
Reactor bed unit size	40 ft x 1060 ft	20 ft x 200 ft
Unit Capture Area (m^2)	3,919	366
Number of Reactors	18	347
Total Reactor Capture Area (m^2)	70,540	126,969
Total Cost, Reactor Subassembly	$212,257	$892,934

[66] Conversation with UOP indicates 90% H_2 recovery in the PSA with a 2:1 molar mix of H_2 and O_2, so reactor production is increased to achieve targeted 1000 kg/day. PSA H_2 recovery with only 2% O_2 is estimated to be 98%.

8.1.6 Type 3 and Type 4 Reactor Costs

As discussed in Section 3, the Type 3 reactor costs are baselined on the costs of existing solar cell planar arrays, with additional costs to reflect the PEC aspects:

- multi-layer thin film photoactive element to achieve 1.6-2.0V output
- electrolyte reservoir contiguous with anode and cathode
- water input lines and H_2 output lines
- separation of anode O_2 output from cathode H_2 output
- corrosion prevention of cell components
- manifolds for gas production and water feel lines

It was concluded that by using low cost printing techniques to generate thin film cells, the Type 3 panel cost would be between $ 150 and $200/m^2. This compares with low cost solar cell panels that are priced at $1/watt (priced using 1kW/m^2 solar intensity), which is $100/m^2 for 10% efficiency cells. PEC cell STH efficiency of 10% was used for the baseline system. The Type 4 system uses multi-layer photoactive cells with higher efficiencies, 15% STH for the baseline system. With a baseline concentration ratio of 10:1, the Type 4 cell cost is not as dominant as it is in the Type 3 system. The primary cost factors are the solar tracking reflector collectors, which track in azimuth and elevation. Costing of collector component was based on prior reports generated for solar thermal systems[67]. Baseline costs predicted for the 10:1 concentrator system assembly hardware in year 2020, normalized on the basis of collector area are:

- Reflector assembly: mirror, structure, drives, controls: $60/m^2
- PEC receiver assembly: $316/m^2 of cell area or $31.60/m^2 of collector area

Type 3 and Type 4 costs are summarized in Figure 8-4.

Figure 8-4: Type 3 and Type 4 Baseline Reactor Costs

	Type 3	**Type 4**
Type	Planar PEC array	Tracking concentrator array
Gross Production (kgH_2/day)	1,000	1,000
Net Production (kgH_2/day)	1,000	1,000
PEC unit size	Fixed array, 1m x 2m	Tracking reflector, 3m x 6m
Unit capture area	2 m^2	18 m^2
Number of units	26,923	1,885
Total capture area (m^2)	53,845	33,924
Reactor cost per Capture area	$154.95/m^2	$92.42/m^2
Reactor Unit cost ($)	$310	$1,663
Total Cost, Reactor Subassembly	$8,343,345	$3,135,209

PEC reactor sizes and costs are compared in Figure 8-5 for Types 1 through 4.

[67] Assessment of Parabolic Trough and Power Tower Solar Technology Cost and Performance Forecasts, NREL/SR-550-34440, Oct. 2003, Sargent & Lundy Consulting Group, Chicago, Ill.

Figure 8-5: Summary of Reactor Parameters for PEC Systems (1 Tonne H_2/day Module)

	Type 1 Single Bed Colloidal Suspension	Type 2 Dual Bed Colloidal Suspension	Type 3 Fixed Flat PEC Panel	Type 4 Tracking Concentrator
Gross Production (kgH_2/day)	1,111[68]	1,000	1,000	1,000
Net Production (kgH_2/day)	1,000	1,000	1,000	1,000
Reactor Parameters				
Dimensions of reactor	1060'x40'x0.3' bed	200'x20'x1.2' bed	2m x 1m panel	6m x 3m reflector
Number of Reactors	18	347	26,923	1,885
Reactor Capture Area (m^2)	70,540	126,969	53,845	33,924
Total Cost, Reactor Subassembly	$212,257	$892,934	$8,343,345	$3,135,209

8.2 *Piping Costs*

Pipe sizing was determined through the use of the continuity equation: $\dot{m} = \rho A v$ (mass flow equals fluid density multiplied by pipe cross-sectional area multiplied by fluid velocity). For gas piping, we assumed a maximum gas velocity of 100 ft/second to limit pressure loss due to pipe flow. For water piping, we assumed a maximum velocity of 15 ft/second. An exact physical layout of the piping systems would need to be performed to fully assess the velocity and pressure drop relationships in all of the piping components. Consequently, the calculations performed are simplified scoping values but are considered adequate for preliminary costing considering the relatively low cost of the piping system and the low costs associated with small changes in pipe diameters. We rounded pipe diameter to the nearest nominal size for cost analysis purpose.

Three different pipe sizes were used for the various stages of water transfer. The pipes that input the water to the individual reactors are sized for individual reactor requirements. Each of these pipes is connected to a manifold sized for half of the overall volume. Finally, one pipe connects the two manifolds to the feedwater reservoir. For the Type 2 system, there is an additional pipe network to circulate the nanoparticle slurry within each baggie to facilitate the ion and solution diffusion process. This network consists of perforated pipes through which the slurry is pumped. Similarly, gas piping was sized both for individual outlets on each reactor, and the main collection lines that lead to the Condenser and Compressor Subassemblies. Pipe sizes for each system are listed in Figure 8-6.

[68] Based on 90% PSA hydrogen recovery consistent with input stream of 2:1 molar mix of H_2 and O_2, so reactor production is increased to achieve targeted 1000 kg/day.

Figure 8-6: Piping Sizes and Unit Costs for PEC Systems

System	Type 1	Type 2
Water Piping:		
Reactor Feed	1/2”	1/2”
Cost/ft	$0.52	$0.52
Gas Piping:		
Reactor Outlet Piping	1 1/2”	1/2”
Cost/ft	$1.00	$0.52
Main Collection Piping	4 1/2”	2 1/2”
Cost/ft	$6.18	$2.80
Final Collection Piping	6”	3”
Cost/ft	$8.51	$4.31
System	**Type 3**	**Type 4**
Water Piping:		
Water Manifold Piping	1/2”	1/2”
Cost/ft	$0.52	$0.52
Water Collection Piping	1”	1/2”
Cost/ft	$1.00	$0.52
Water Column Collection Piping	4”	2”
Cost/ft	$6.18	$2.12
Water Final Collection Piping	5”	3”
Cost/ft	$8.51	$4.31
Gas Piping:		
Manifold Piping	1/2”	1/2”
Cost/ft	$0.52	$0.52
Collection Piping	1”	1/2”
Cost/ft	$1.00	$0.52
Column Collection Piping	4”	2”
Cost/ft	$6.18	$2.12
Final Collection Piping	5”	3”
Cost/ft	$8.51	$4.31

8.3 *Pump Costs*

The make-up water pumps for the reactors will only run during H_2 production and for several hours after the H_2 production period is over. The water consumed every day is primarily, 99%, for hydrogen production, with the remaining 1% being evaporation. This flow is 15,325 kg/day for the peak day for the Type 1 system. The water feed can be handled with an inexpensive pump.

Slurry circulation pumps for the Type 2 system are included in the baggie assembly. 3700 GPH pumps are used.

Larger pumps are needed for the cooling water for the condenser and two intercoolers. Cooling water flow for each of these heat exchangers varies from 1,089 to 16,703 kg/hr for cooling 60^{o}C

product gases, as is shown in Figure 8-7. The costs for these pumps are integrated with the heat exchanger costs.

Figure 8-7: Cooling water needs for Heat Exchangers

Cooling Water Flow for 60C day, June 21		T1	T2	T3	T4
Condenser	kg/hr	9,924	5,948	14,301	1,089
Intercooler-I	kg/hr	11,864	6,947	16,703	NA
Intercooler-II	kg/hr	9,280	5,393	12,967	NA

Much of the cooling capacity is used to condense the water vapor present at the heat exchanger inlet. The small condensor cooling flow for the Type 4 system is due to the minimal amount of water vapor at the reactor exit due to the high pressure.

8.4 *Compressor, Heat Exchangers, and PSA*

The compressor, heat exchangers, and PSA were sized differently for the different PEC systems, depending on molar flow and gas mixture. Type 2, 3, and 4 reactors separate the H_2 and O_2, and a PSA in not needed. Since the Type 1 and Type 2 systems store the output gas in the beds over a daily cycle, their compressor and heat exchangers were sized for the expected average output on the peak day (June 21), assuming clear sky conditions. Since the processed gas output from Type 1 includes O_2, the gas system must have 3/2 the molar capacity of the Type 2 system. For the Type 3 system the compressor and heat exchangers are sized for the instantaneous peak H_2 production at noon on June 21, the max solar input day. For the Type 4 system, which has no separate compressor, the condenser is sized for the instantaneous peak H_2 production at noon on June 21. Gas flow system sizing requirements and costs are listed in Figure 8-8.

Figure 8-8. Gas Processing Major Component Cost

Subassembly	Components		Flows and Pricing			
			Type 1	Type 2	Type 3	Type 4
Design Max Molar Flow rate		kgMol/hr	52.9	31.7	76.3	53.5
Compressor	Two stage	price factor			$9,233 /kgMol/hr	-
		price	$488,276	$292,966	$704,366	-
Heat Exchangers	Condenser	with cooling pump	$13,765	$10,626	$16,607	$7,098
	Intercooler-1	with cooling pump	$15,103	$11,464	$17,894	-
	Intercooler-2	with cooling pump	$15,552	$11,870	$18,495	-
Gas Separation	Pressure Swing Adsorption		$107,147	-	-	-
TOTAL			$639,842	$326,926	$757,362	$7,098

8.5 *Land Required*

The land required parameter can be found on the Input_Sheet_Template Worksheet of the model. For the Type 1 and 2 horizontal beds, the reactor area equals the emplaced land area. For the Type 3 and 4 reactors, the panels and concentrators are spaced apart to minimize inter-reactor shadowing, as discussed in Section 3.6. Thus Type 3 emplacement area was increased by a factor of 4.07 relative to reactor area and Type 4 emplacement area was increased by a factor of 6.57 relative to reactor area. The additional area encompasses space requirements for pumps, compressors, heat exchangers, a small control room, and access roads.

For the Type 1 and 2 systems, the analysis assumes that the total land required for these is 30% greater than the reactor bed. The 30% factor is encompasses area requirements for pumps, compressors, heat exchangers, gas separator, a small control room, and access roads. The total land requirement for each system is shown in Figure 8-9.

Figure 8-9: Land Requirements

System	Type 1	Type 2	Type 3	Type 4
Reactor collection area (m^2)	70,540	126,969	53,845	33,924
Reactor emplacement area (m^2)	70,540	126,971	219,149	222,881
Shading factor	0	0	4.07	6.57
% increase for auxiliaries, roads	30%	30%	0%	0%
Total Land Required (m^2)	91,702	165,060	219,149	222,881
Cost/acre	$500	$500	$500	$500
Total cost	$11,330	$20,393	$27,075	$27,537

8.6 *Capital Cost Summary*

Capital costs for each system are shown in Figure 8-10.

Figure 8-10: Capital Cost Summary

Component	Type 1	Type 2	Type 3	Type 4
Reactor assy.	$212,257	$892,934	$8,343,345	$3,135,209
Gas Processing	$684,283	$356,654	$917,338	$33,771
Controls	$173,944	$440,826	$319,862	$279,774
Hardware total	$1,070,484	$1,690,414	$9,580,545	$3,448,754
Land	$11,330	$20,393	$27,076	$27,537
Total cost	$1,081,814	$1,710,807	$9,607,621	$3,476,291

Especially in the Type 2 system, the control system makes up a substantial percentage of the total capital cost. Much of these costs come from hydrogen/oxygen sensors which monitor the gas stream for any leaks or potential contamination. Since there are few baggies in the Type 1 system, we have allocated one sensor per baggie. The Type 2, Type 3, and Type 4 systems, however, have considerably more individual hydrogen producing modules than Type 1. Thus, to help alleviate the high cost of these sensors for the Type 2, Type 3, and Type 4 systems, we have decided to use the sensor on the combined gas stream of multiple reactors. We use enough sensors to monitor the gas stream from a hydrogen-producing area equal in size to the baggie in Type 1. We feel that this is adequate to allow workers to localize a leak and stop it before it contaminates much of the system. The leak can be further isolated by workers using simpler hand-held devices. Future work should more closely address the issue of the control system cost, however, a detailed design was beyond the scope of work for this report.

9. Specific System Operating Costs

While ideally the hydrogen production reactor would operate all days of the year, there is a average capacity reduction due to scheduled maintenance, unscheduled maintenance, and periodic reductions in H_2 demand. For these PEC systems, most scheduled maintenance can be carried out at night when there is no H_2 production. The H2A design program automatically imposes a 90% Operating Factor on H_2 central production systems. With these simple PEC H_2 production systems, achievement of a 95% Operating Factor appears feasible. However, since the H_2 demand factors have not been defined for this study, we used the default value of 90% Operating Factor.

9.1 *Electricity Consumption*

Electric power consumption is primarily for the Gas Processing Subassembly. Items consuming power are the PSA, compressor, water pumps, slurry circulation pumps, and control systems.
The gas compressor, the largest power user, is a 2-stage piston compressor with interstage cooling. Its power was calculated by assuming isentropic compression of the gas mixture from 40^{o}C ambient temperature and multiplying that result by an efficiency of 75%. Overall pressure ratio is 20.7 for the Type 1 outlet pressure of 305psi. The power for each stage was calculated after adjusting the gas mix for water vapor removal and temperature reduction in the condensers and intercoolers. Pressure ratio is approximately 4.6 in each stage.

PSA power is minimal as it is only needed for compressed air actuation of valves. The power consumption of the compressed air pump comes from Grainger Industrial Supply.

Power consumption of the total control system was assumed to be 6.5 kW for each of the PEC systems. This includes the control room environmental control system as well as the various control devices. Figure 9-1 lists the electricity usage anticipated for each of the components previously described and provides a total consumption value to be used in further analysis. The previously mentioned duty cycles and operational cycle have been taken into account in these computations.

Figure 9-1: Electrical Power Consumption (average power over year)

Power Consumer		**Type 1**	**Type 2**	**Type 3**	**Type 4**
Average hydrogen/day		1111.11	1000	1000	1000
Compressor	kW	128.6	76.3	76.3	-
Heat exchanger cooling pumps	kW	0.9	0.5	0.5	0.02
PSA	kW	1.0	-	-	-
Make-up water pumps	kW	0.2	0.2	0.2	0.2
Slurry circulation pumps	kW	-	0.2	-	-
Control System	kW	6.5	6.5	6.5	6.5
Total Average Power	kW	137.2	83.7	83.5	6.7
Utilization	%	100%	100%	100%	100%
Yearly consumption	kWh/yr	1,201,872	733,212	731,460	58,867
Consumption per kg H2	kWh/kg H2	3.29	2.01	2.00	0.16

9.2 *Utility Usage*

The usage of utilities, feedstocks, and creation of byproducts is an entry on the Input_Sheet_Template Worksheet of the H2A model. In the case of utilities, the utility of interest (electricity, natural gas, water, or steam) is selected from a drop-down box. There are no byproduct costs associated with the PEC systems, however, the produced O_2 could have some value. For the net 1,000kgH_2/day systems, the utilities consumed are shown in Figure 9-2. The model has a cost rate for each utility and thus computes the total costs of utilities.

Figure 9-2: Utilities Usage

Utility Usage			T1	T2	T3	T4
Average Gross H2/day		kg/day	1111.11	1000.00	1000.00	1000.00
Average Net H2/day		kg/day	1000	1000	1000	1000
Electricity		kWhr/kg H2	3.29	2.01	2.00	0.16
		kWhr/day	3,293	2,009	2,004	161
Water	Electrolysis	kg/day	9,928.8	8,935.9	8,935.9	8,935.9
	Vapor loss	kg/day	53.1	31.9	31.9	31.9
	total usage	kg/day	9,981.9	8,967.8	8,967.8	8,967.8
		gal/day	2,637.0	2,369.0	2,369.0	2,369.0

9.3 *Yearly Replacement Costs*

The specified yearly replacement costs can be found on the Replacement Costs Worksheet of the model. For Type 1 and 2 systems, the transparent film that makes up the baggies will need periodic replacement. The film is made of HDPE and over time will degrade in transmissivity, thereby lowering plant efficiency. This analysis assumes that a 5-yr replacement cycle for the baggies is sufficient to keep system performing at acceptable levels. Additionally, replacement of PEC nanoparticles and PEC cells will be necessary to maintain high system efficiency. We have assumed a baseline five year lifetime for the Type 1 and 2 PEC nanoparticles, which will be replaced along with the baggies. We have further assumed a ten year lifetime for PEC cells in systems Type 3 and 4. Cell replacement will include the complete PV component with Plexiglas window and seals. All other components are anticipated to operate for 20 years. There are no other specified replacement costs over the twenty year analysis period. Figure 9-3 lists specific costs associated with replacement components.

Figure 9-3: Replacement Costs

System		Type 1	Type 2	Type 3	Type 4
Baggies	Life (yrs)	5	5	NA	NA
	number	18	347	NA	NA
PEC Nanoparticles	Life (yrs)	5	5	NA	NA
	kg	75	134	NA	NA
Costs (yrs. 5, 10, 15)		$191,423	$1,399,812	NA	NA
PEC cells	Life (yrs)	NA	NA	10	10
	m^2	NA	NA	53,845	3,392
Costs (yr. 10)		NA	NA	$9,315,170	$1,072,904

9.4 *Yearly Maintenance Costs*

Yearly equipment maintenance costs are calculated by H2A as 0.5% of the direct capital costs. The reactor baggies and PEC cells are replacement items, replaced at 5 and 10 year intervals respectively.

9.5 *Production Facility Plant Staff*

The production facility plant staff parameter can be found on the Input_Sheet_Template Worksheet of the model. For our analysis, we assumed that each worker can oversee 100 acres of baggies. We have also assumed that there are three shifts per day to ensure 24 hrs/day operation of the plant.

Our analysis for each of the systems is shown in Figure 9-4. For the Type 3 and Type 4 systems, which do not have baggies, we have assumed that a worker can monitor a similar area of panels similar to the area of baggies. Thus the worker requirement for these systems is based on the overall area of the system. Additionally, for the 10 TPD plant, and for potential future 50 TPD and 100 TPD plants, we have added three shifts with a supervisor, due to the large size of these plants. Finally, for the 100 TPD plant, we have added one shift of an assistant supervisor for additional support.

Figure 9-4: Plant Staff Requirements for Baseline Plants

Type 1				**Type 2**			
1 ton	10 ton	50 ton	100 ton	1 ton	10 ton	50 ton	100 ton
1	**10**	**50**	**100**	**1**	**10**	**50**	**100**
18	**180**	**900**	**1800**	**31**	**314**	**1569**	**3138**
100	**100**	**100**	**100**	**100**	**100**	**100**	**100**
3	**3**	**3**	**3**	**3**	**3**	**3**	**3**
3	6	27	54	3	12	48	96
0	3	3	3	0	3	3	3
0	0	0	1	0	0	0	1
3	9	30	58	3	15	51	100
3	**0.9**	**0.6**	**0.58**	**3**	**1.5**	**1.02**	**1**
Type 3				**Type 4**			
1 ton	10 ton	50 ton	100 ton	1 ton	10 ton	50 ton	100 ton
1	**10**	**50**	**100**	**1**	**10**	**50**	**100**
54	**542**	**2708**	**5415**	**55**	**551**	**2754**	**5507**
100	**100**	**100**	**100**	**100**	**100**	**100**	**100**
3	**3**	**3**	**3**	**3**	**3**	**3**	**3**
3	18	84	165	3	18	84	168
0	3	3	3	0	3	3	3
0	0	0	1	0	0	0	1
3	21	87	169	3	21	87	172
3	**2.1**	**1.74**	**1.69**	**3**	**2.1**	**1.7**	**1.72**

10. PEC System and Hydrogen Production Cost Results

Much of the PEC work on which this study is based has been done in laboratory scale environments under idealized conditions. However, as background for the Type 3 and 4 systems, there has been extensive development and commercialization of PV systems at large scales. After examination of the various inputs and configuration options, we have postulated what we judge to be the most practical means of hydrogen production for each of the four PEC Types. The four PEC system designs have been developed for a 1 TPD module. The H_2 cost estimates reported in this chapter assume a 10 TPD demand and, therefore, 10 of these modules. The primary effect of the increase to 10 TPD output is a reduction in labor costs per kilogram of H_2 produced.

10.1 *Type 1 Single Bed Colloidal Suspension System*

The subassemblies of this system are described in Section 4.1. An end view of three reactor units is shown in Figure 10-1. For 1 tonne/day average output over a year and for 10% STH conversion efficiency, this requires 18 reactors with capture area of 17.4 acres.

Figure 10-1: End View of Three Type 1 Single Bed Baggie Reactors

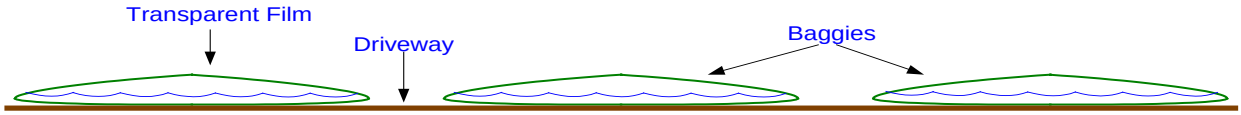

The complete bill of materials and capital costs of the 1TPD production plant are shown in Figure 10-2. The total system cost is $1,070,485 before installation.

Figure 10-2: Bill of Materials for Installed Type 1 Baseline 1TPD System

Description	Unit Size	Units	Unit cost		Qty	Total Cost
Baggie Subassembly						
Baggie	1	assembly	$ 7,393		18	$ 133,077
Roll-Unroll System	1	Roller	$ 37,000		1	$ 37,000
Forklift	1	Forklift	$ 18,571		1	$ 18,571
Coated PEC Microparticles	1	kg	$ 304		75	$ 22,679
Make-up Water Pump	1	pump	$ 212.50		1	$ 213
Reactor Feed Pipe	0.5	in	$ 0.52	/ft	1380	$ 718
Baggie Subassembly Total						**$ 212,257**
Gas Processing Subassembly						
Compressor	57	kgmol gas/hr	$ 9,233		1	$ 526,302
Condensor	1	HX	$ 13,765		1	$ 13,765
Intercooler 1	1	HX	$ 15,103		1	$ 15,103
Intercooler 2	1	HX	$ 15,552		1	$ 15,552
PSA	1	PSA	$ 107,147		1	$ 107,147
Reactor Outlet Pipe	1.5	in	$ 1.57	/ft	36	$ 57
Main Collection Pipe	4.5	in	$ 6.18	/ft	960	$ 5,933
Final Collection Pipe	6	in	$ 8.51	/ft	50	$ 426
Gas Processing Subassembly Total						**$ 684,283**
Control System						
PLC	1	controller	$ 2,000		1	$ 2,000
Control Room building	1	ft2	$ 50		160	$ 8,000
Control Room Wiring Panel	1	panel	$ 3,000		1	$ 3,000
Bed Wiring Panel	1	panel	$ 146		18	$ 2,628
Computer and Monitor	1	computer	$ 1,500		1	$ 1,500
Labview Software	1	program	$ 4,299		1	$ 4,299
Water Level Controllers	1	controller	$ 50		18	$ 900
Pressure Sensors	1	sensor	$ 345		18	$ 6,210
Hydrogen Area Sensors	1	sensor	$ 7,600		18	$ 136,800
Oxygen Area Sensors	1	sensor	$ -		18	$ -
Gas Flow Meter	1	meter	$ 5,500		1	$ 5,500
Instrument Wiring	1	ft	$ 0.02		21,060	$ 409
Power Wiring	1	ft	$ 0.10		1,404	$ 136
Conduit	1	ft	$ 0.58		4,420	$ 2,563
Control System Total						**$ 173,944**
Direct Capital Cost						**$ 1,070,485**
Installation Costs						
Piping Installation	1	ft	$0.11		2,426	$ 267
Levelling of Bed field	1	Bed	$ 2,570		18	**$ 46,259**
Baggie Installation	1	hour	$ 50.00		288	**$ 14,400**
Baggie Reactor Start-up	1	particles,pump			30%	**$ 6,867**
Gas processing Subassembly install	1	gas sys			30%	**$ 203,361**
Control System Install	1	control sys			30%	**$ 52,183**
Installation Cost total						**$ 323,337**
Cost with Installation						**$ 1,393,822**
Reactor Cost/capture area ($/m2) - Uninstalled						**$ 2.21**
System Cost /capture area ($/m2) - Uninstalled						**$ 19.76**

The cost breakdown for the major system capital components is shown in Figure 10-3.

Figure 10-3: Type 1 Baseline 1 TPD System Direct Capital Components

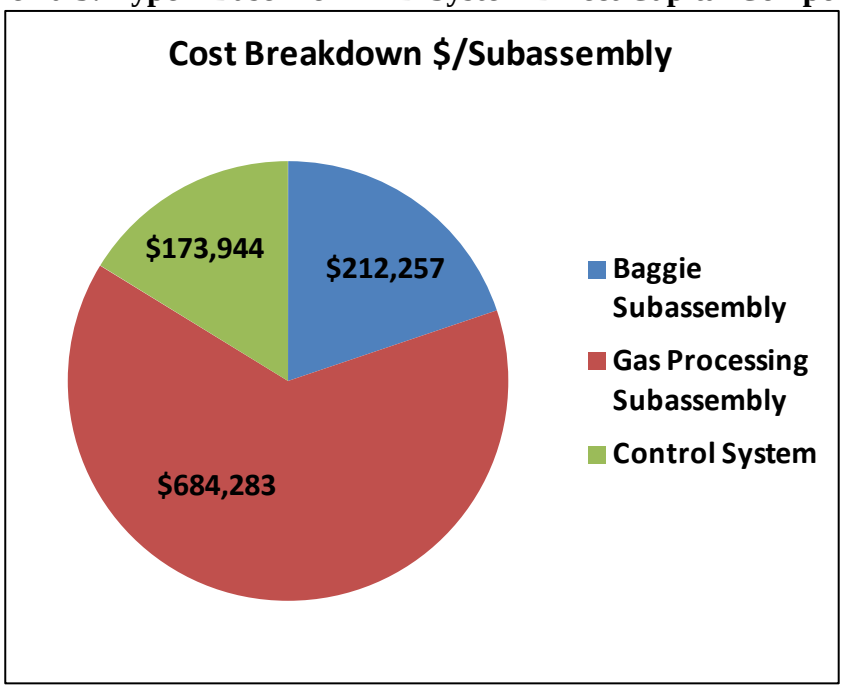

H_2 production cost breakdown for a 10 tonne/day system is shown in Figure 10-4 including capital costs, operating costs, and decommissioning costs. For the baseline parameters, the baseline H_2 cost is $1.63/kg.

Figure 10-4: Type 1 Baseline 10 TPD H_2 Production Cost Elements - $1.63kg

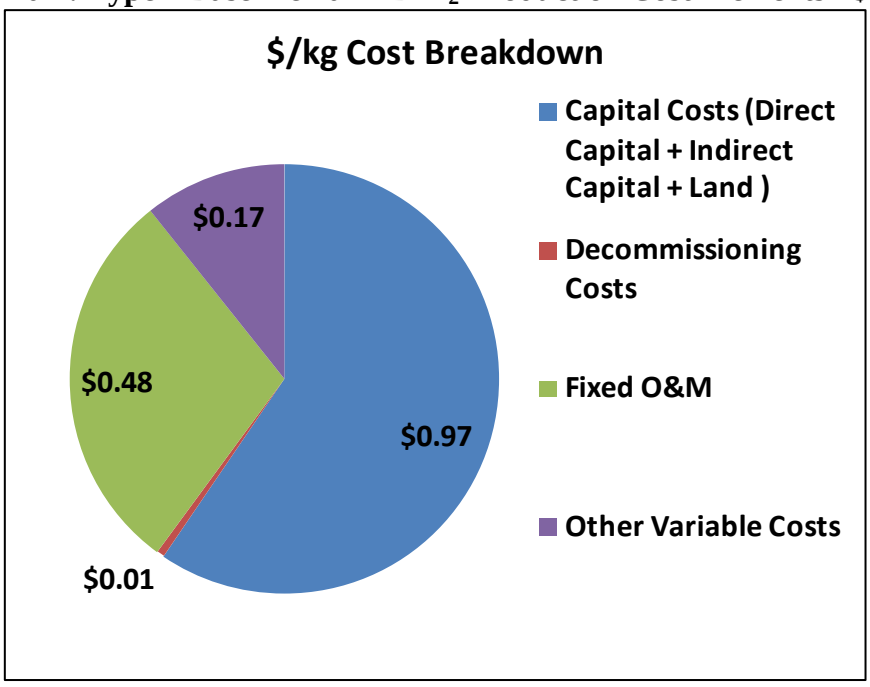

An H_2 production cost sensitivity analysis was carried out to assess variation in H_2 cost as a function of efficiency, cost of particles, and system lifetime. The range of parameters is shown in Figure 10-5 and plotted in Figure 10-6.

Figure 10-5: Type 1 Sensitivity Analysis Parameters

Type 1 Sensitivity Analysis Parameters		
Efficiency	**Particle Cost**	**Particle Lifetime**
5%	0.1x	1 Year
10%	1x	5 Year
15%	20x	10 Year

Figure 10-6: Type 1 H_2 Cost Sensitivity ($/kg$H_2$)

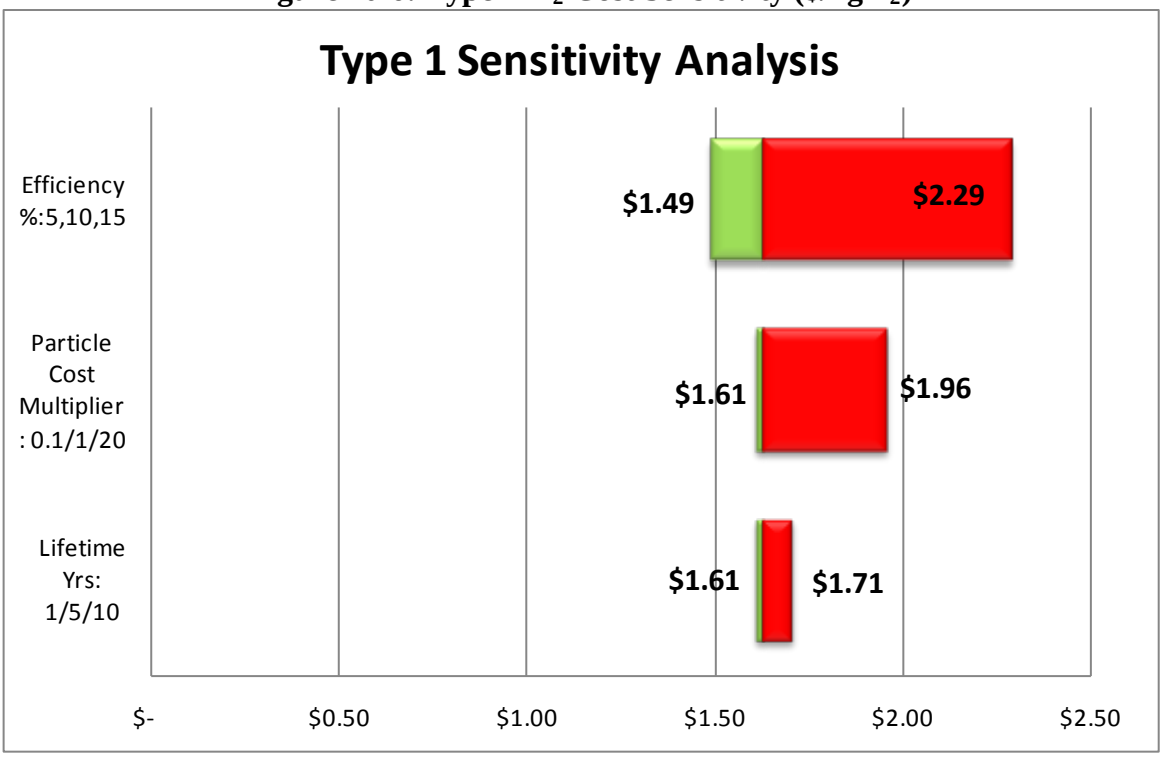

10.2 *Type 2 Dual Bed Colloidal Suspension System*

As described in Section 4.2, the Type 2 system reactor assembly consists of 2 full-size baggies (200 ft x 6.6 ft x 1.5 ft) and 2 half-size baggies (200 ft x 3.3 ft x 1.5 ft) linked together with diffusion bridges as shown in Figure 10-7. For 1 tonne/day average output over a year and for 5% STH conversion efficiency, this requires 347 beds with total capture area of 31.4 acres.

Figure 10-7: Type 2 Reactor Unit

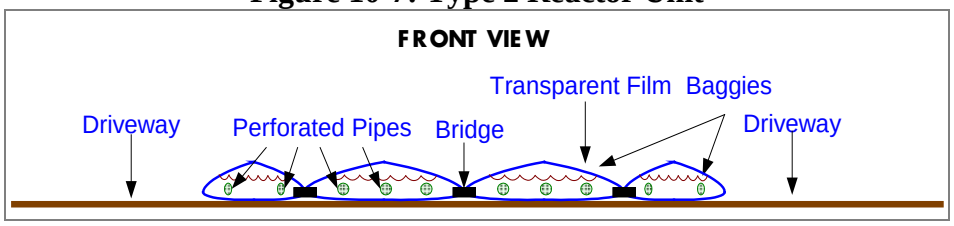

The system layout, with the gas processing modules and control system, is shown in Figure 10-8.

Figure 10-8: Type 2 Total System Layout

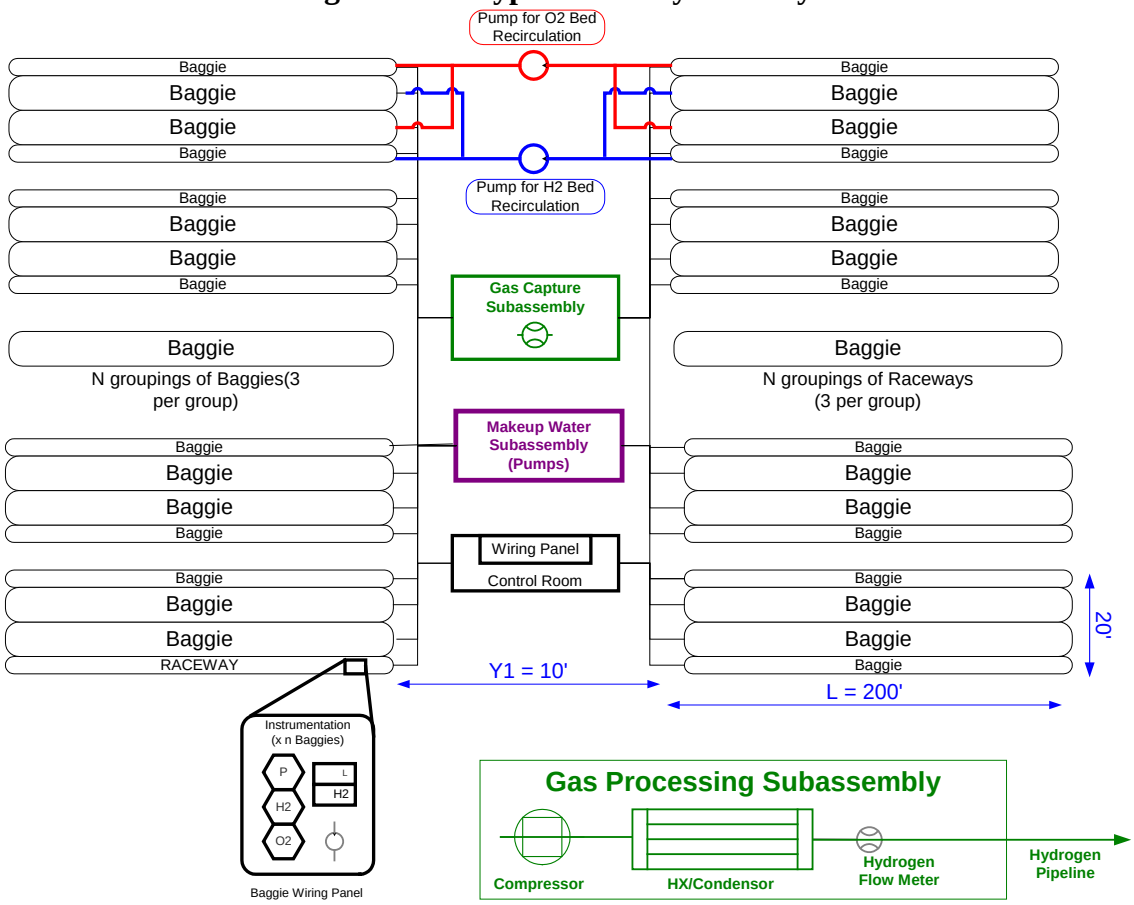

For the 1 TPD system, the Bill of Materials is listed in Figure 10-9. The total initial system cost is $1,690,414 before installation.

Figure 10-9: Bill of Materials for Installed Type 2 Baseline 1TPD System

Description	Unit Size	Units	Unit cost	Qty Req'd	Total Cost
Baggie Subassembly					
Baggie	1	assembly	$ 2,280	347	$ 791,250
Roll-Unroll System	1	Roller	$ 37,000	1	$ 37,000
Forklift	1	Forklift	$ 18,571	1	$ 18,571
Coated PEC Microparticles	1	kg	$ 304	134	$ 40,798
Make-up Water Pump	1	pump	$ 213	1	$ 213
Reactor Feed Pipe	0.5	in	$ 0.52 /ft	9,812	$ 5,102
Baggie Subassembly Total					$ 892,934
Gas Processing Subassembly					
Compressor	34	kgmol gas/hr	$ 9,233	34	$ 315,884
Condensor	1	HX	$ 10,626	1	$ 10,626
Intercooler 1	1	HX	$ 11,464	1	$ 11,464
Intercooler 2	1	HX	$ 11,870	1	$ 11,870
PSA					$ -
Reactor Outlet Pipe	0.5	in	$ 0.52 /ft	694	$ 361
Main Collection Pipe	2.5	in	$ 2.80 /ft	2,265	$ 6,342
Final Collection Pipe	3	in	$ 4.31 /ft	25	$ 108
Gas Processing Subassembly Total					$ 356,654
Control System					
PLC	1	controller	$ 2,000	1	$ 2,000
Control Room building	1	ft2	$ 50	160	$ 8,000
Control Room Wiring Panel	1	panel	$ 3,000	1	$ 3,000
Bed Wiring Panel	1	panel	$ 146	347	$ 50,686
Computer and Monitor	1	computer	$ 1,500	1	$ 1,500
Labview Software	1	program	$ 4,299	1	$ 4,299
Water Level Controllers	1	controller	$ 50	347	$ 17,358
Pressure Sensors	1	sensor	$ 345	347	$ 119,771
Hydrogen Area Sensors	1	sensor	$ 7,600	18	$ 136,800
Oxygen Area Sensors	1	sensor	$ -	18	$ -
Hydrogen Flow Meter	1	meter	$ 5,500	1	$ 5,500
Instrument Wiring	1	ft	$ 0.02 /ft	1,621,190	$ 31,451
Power Wiring	1	ft	$ 0.10 /ft	164,039	$ 15,912
Conduit	1	ft	$ 0.58 /ft	76,836	$ 44,549
Control System Total					$ 440,826
Direct Capital Cost					$ 1,690,414
Installation Costs					
Piping Installation	1	ft	$0.11	12,796	$ 1,408
Levelling of Bed field	1	Acre	$ 3,896	32	$ 124,672
Baggie Installation	1	hour	$ 50.00	5554.6	$ 277,730
Baggie Reactor Start-up	1	particles,pump		30%	$ 12,303
Gas processing Subassembly install	1	gas sys		30%	$ 104,953
Control System Install	1	control sys		30%	$ 132,248
Installation Cost Total					$ 653,314
Cost with Installation					$ 2,343,728
Reactor Cost/capture area ($/m2) - Uninstalled					$ 6.55
System Cost /capture area ($/m2) - Uninstalled					$ 18.46

The cost breakdown for the major system capital components is shown in Figure 10-10.

Figure 10-10: Type 2 Baseline 1 TPD System Direct Capital Components

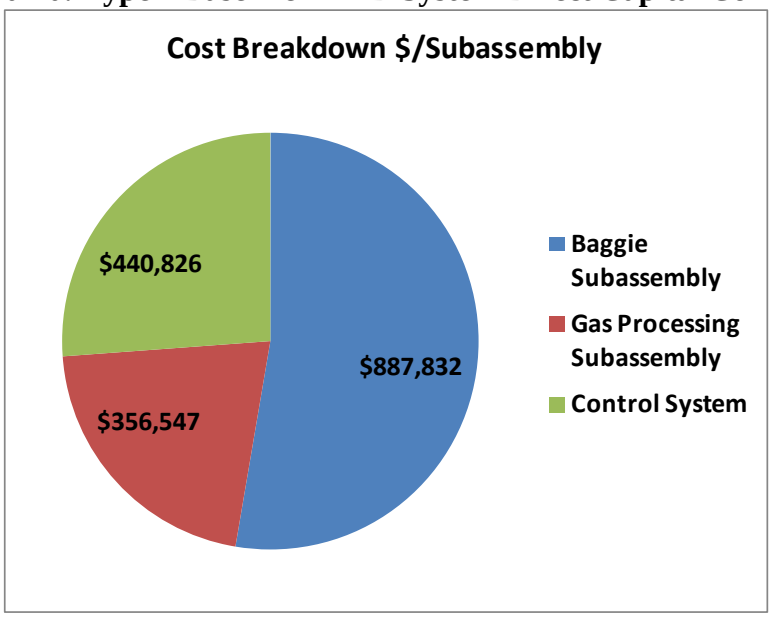

H_2 production cost breakdown for a baseline 10 tonne/day system is shown in Figure 10-11 including capital costs, operating costs, and decommissioning costs. The H_2 cost is $3.19/kg.

Figure 10-11: Type 2 Baseline 10 TPD H_2 production cost elements – $3.19/kg

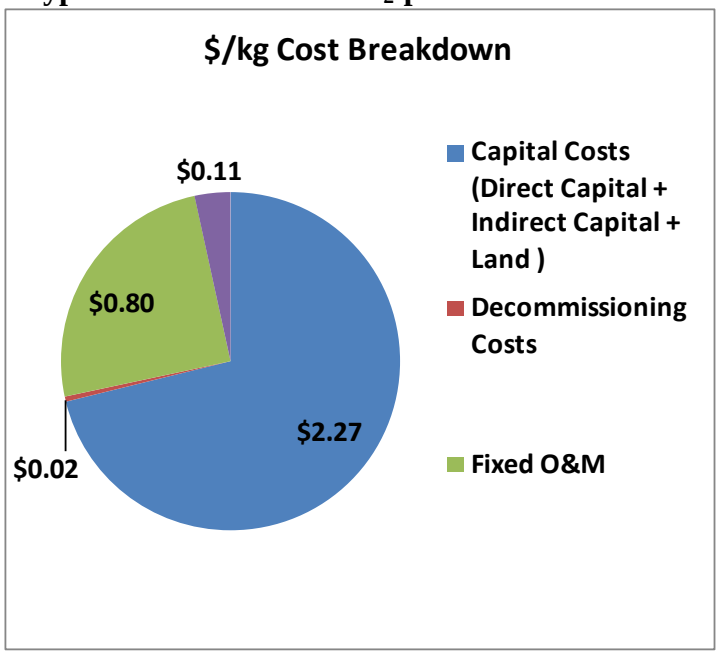

For the Type 2 system there are significant uncertainties with regard to performance parameters, functional operation of the nanoparticles, diffusion mixing, and costs. Therefore, an H_2 production cost sensitivity analysis was carried out to assess variation in H_2 cost as a function of

efficiency, cost of particles, and system lifetime. The range of parameters is shown in Figure 10-12 and the H_2 cost results are plotted in Figure 10-13.

Figure 10-12: Type 2 Sensitivity Analysis Parameters

Type 2 Sensitivity Analysis Parameters		
Efficiency	**Particle Cost**	**Particle Lifetime**
2.5%	0.1x	1 Year
5%	1x	5 Year
7.5%	20x	10 Year

Figure 10-13: Type 2 H_2 cost sensitivity ($/kg$H_2$)

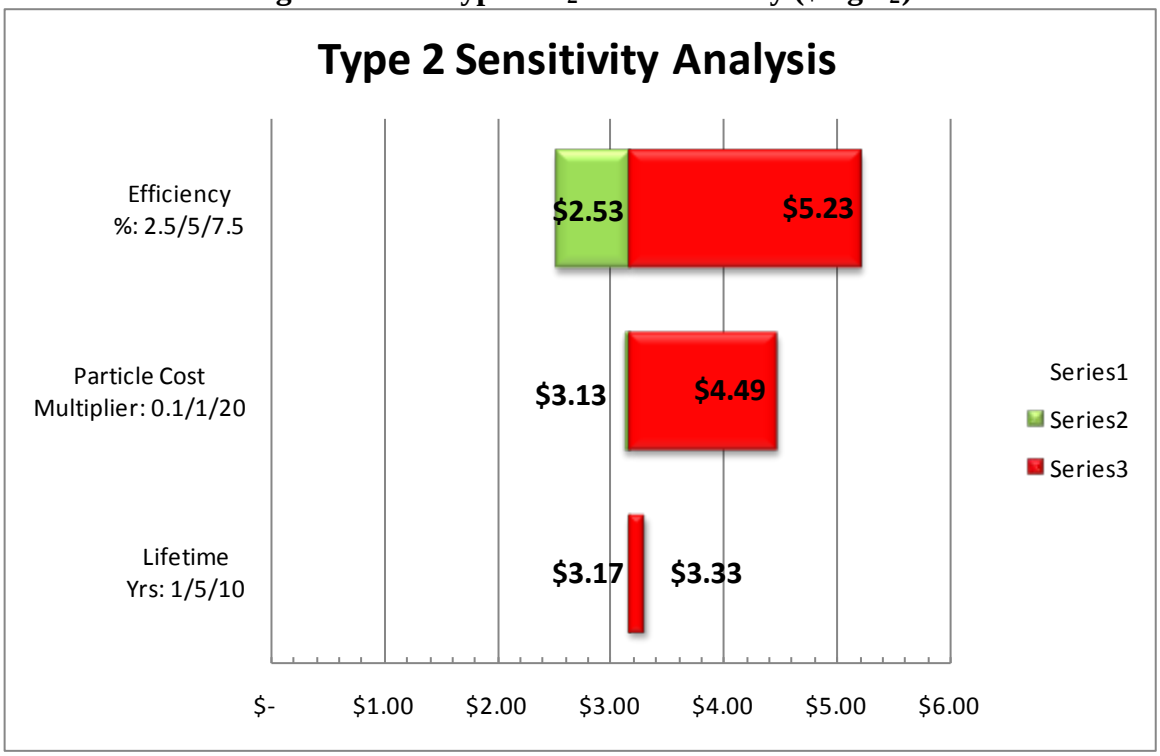

The Type 1 and 2 systems are innovative, promising approaches to PEC, but are relatively immature compared with the traditional PEC cell approach. Greater uncertainties include:

- Definition and fabrication of the optimal nanoparticle PV materials
- Production costing for fabrication of the particles
- Effective photon-reactive active areas (capture area) on a given particle
- Nanoparticle density needs in the beds
- Diffusion times for reactants in Type 2
- In the Type 2 dual bed reactor: uncertainty in whether there is 100% exclusive generation of O_2 on the first side and H_2 on the second side

10.3 *Type 3 PEC Planar Array System*

As described in Section 4.4, the Type 3 system reactor unit consists of self-contained PEC panels. Though this analysis draws on the PEC work done in laboratory environments the solar cell industry has extensive experience at building and fielding PV systems at large scales. Figure 10-14 shows the baseline 1TPD system layout and consists of:

- 26,923 1m x 2m panels
- 53,845 m^2 capture area

Figure 10-14: Type 3 Baseline System for 1TPD[69]

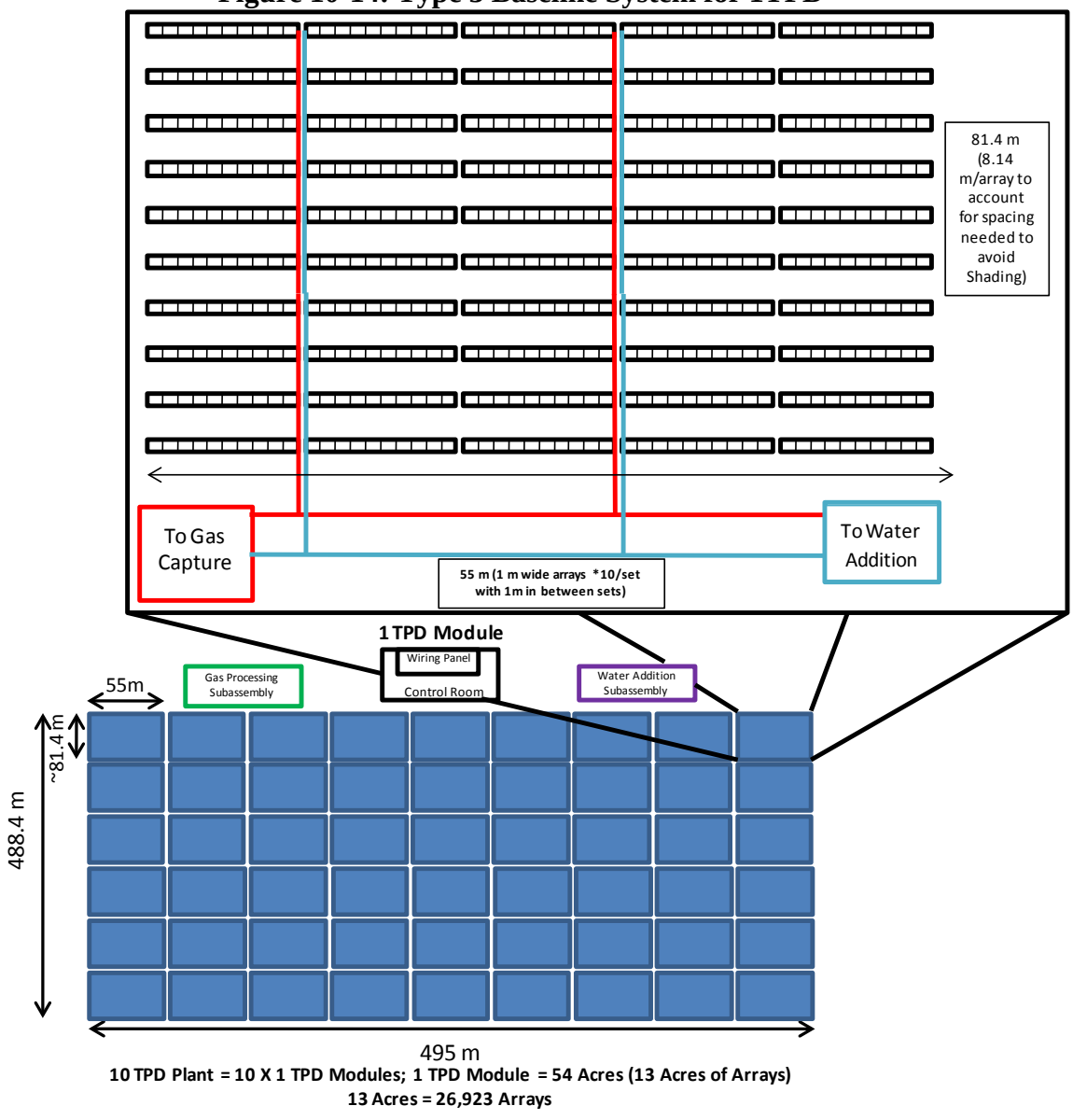

The BOM is displayed in Figure 10-15. Total 1 TPD system cost is $9,580,545 before installation.

[69] This table is approximate and contains slightly more than the number of arrays for a 1TPD plant.

Figure 10-15: Bill of Materials for Installed Type 3 Baseline 1TPD System

Description	Unit Size	Units	Unit cost		Qty Req'd	Total Cost
Reactor Subassembly						
PEC Cell	1	m^2	$ 153.00		53,845	$ 8,238,271
Make-up Water Pump	1	pump	$ 212.50		1	$ 213
Water Manifold Piping	0.5	in	$ 0.52	/ft	86,641	$ 45,053
Water Collection Piping	1	in	$ 1.00	/ft	52,394	$ 52,394
Water Column Collection Piping	4	in	$ 6.18	/ft	1,062	$ 6,563
Water Final Collection Piping	5	in	$ 8.51	/ft	100	$ 851
Reactor Subassembly Total						**$ 8,343,345**
Gas Processing Subassembly						
Compressor	82.26	kg mol gas/hr	$ 9,233		82.26	$ 759,481
Condenser	1	HX	$ 16,607		1	$ 16,607
Intercooler 1	1	HX	$ 17,894		1	$ 17,894
Intercooler 2	1	HX	$ 18,495		1	$ 18,495
Manifold Piping	0.5	in	$ 0.52	/ft	86,641	$ 45,053
Collection Piping	1	in	$ 1.00	/ft	52,394	$ 52,394
Column Collection Piping	4	in	$ 6.18	/ft	1,062	$ 6,563
Final Collection Piping	5	in	$ 8.51	/ft	100	$ 851
Gas Processing Subassembly Total						**$ 917,338**
Control System						
PLC	1	controller	$ 3,000		1	$ 3,000
Control Room building	1	ft^2	$ 50.00		351	$ 17,527
Control Room Wiring Panel	1	panel	$ 3,000		1	$ 3,000
Computer and Monitor	1	computer	$ 1,500		1	$ 1,500
Labview Software	1	program	$ 4,299		1	$ 4,299
Water Level Controllers	1	controller	$ 50		2,692	$ 134,615
Pressure Sensors	1	sensor	$ 345		18	$ 6,210
Hydrogen Area Sensors	1	sensor	$ 7,600		18	$ 136,800
Oxygen Area Sensors	1	sensor	$ -		18	$ -
Hydrogen Flow Meter	1	meter	$ 5,500		1	$ 5,500
Instrument Wiring	1	ft	$ 0.02	/ft	23,233	$ 451
Power Wiring	1	ft	$ 0.10	/ft	2,323	$ 225
Conduit	1	ft	$ 0.58	/ft	11,617	$ 6,735
Control System Total						**$ 319,862**
Direct Capital Cost						**$ 9,580,545**
Installation Costs						
Piping Installation	1	ft	$0.11		280,394	$ 30,843
Panel Installation	1	panel	$ 20.00		$ 53,845	$ 1,076,898
Reactor subassembly install	1	pump			30%	$ 64
Gas processing Subassembly install	1	gas sys			30%	$ 243,743
Control System Install	1	control sys			30%	$ 95,959
Installation Cost Total						**$ 1,447,507**
Cost with Installation						**$ 11,028,052**
Reactor Cost/capture area ($/m2) - Uninstalled						**$ 154.95**
System Cost /capture area ($/m2) - Uninstalled						**$ 204.81**

The cost breakdown for the major system capital components is shown pictorially in Figure 10-16. It can be readily seen that the panel cost dominates the overall capital cost.

Figure 10-16: Type 3 Baseline 1 TPD System Direct Capital Components

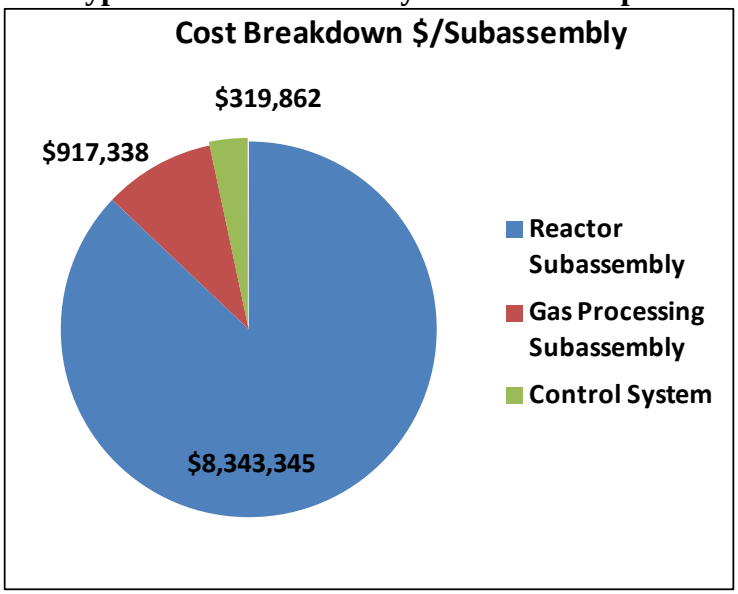

H_2 production cost breakdown for a baseline 10 tonne/day system is shown in Figure 10-17 including capital costs, operating costs, and decommissioning costs. This system is the most mature of the various PEC types so cost predictions are the most reliable. Assuming the baseline parameter values, the H_2 cost is estimated at $10.36/kg.

Figure 10-17: Type 3 Baseline 10 TPD H_2 Production Cost Elements – $10.36/kg H_2

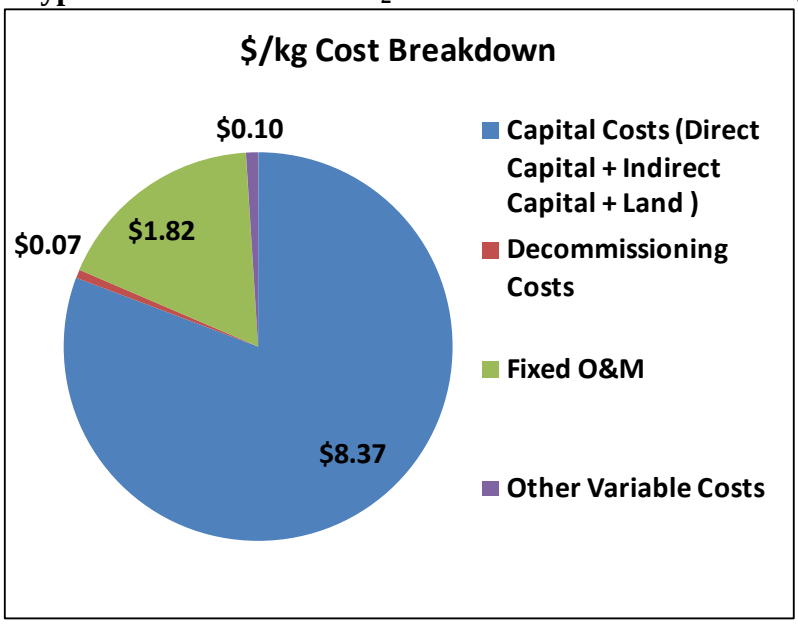

An H_2 production cost sensitivity analysis assessed the variation in H_2 cost as a function of efficiency, cost of PEC cell module, and system lifetime. The range of parameters is shown in Figure 10-18 and plotted in Figure 10-19.

Figure 10-18: Type 3 System Sensitivity Analysis Parameters

Type 3 Sensitivity Analysis Parameters		
Efficiency	**PEC Cell Cost**	**PEC Cell Lifetime**
5%	$80/m^2	5 year
10%	$153/m^2	10 year
20%	$200/m^2	20 year

Figure 10-19: Type 3 Cost Sensitivities ($/kg$H_2$)

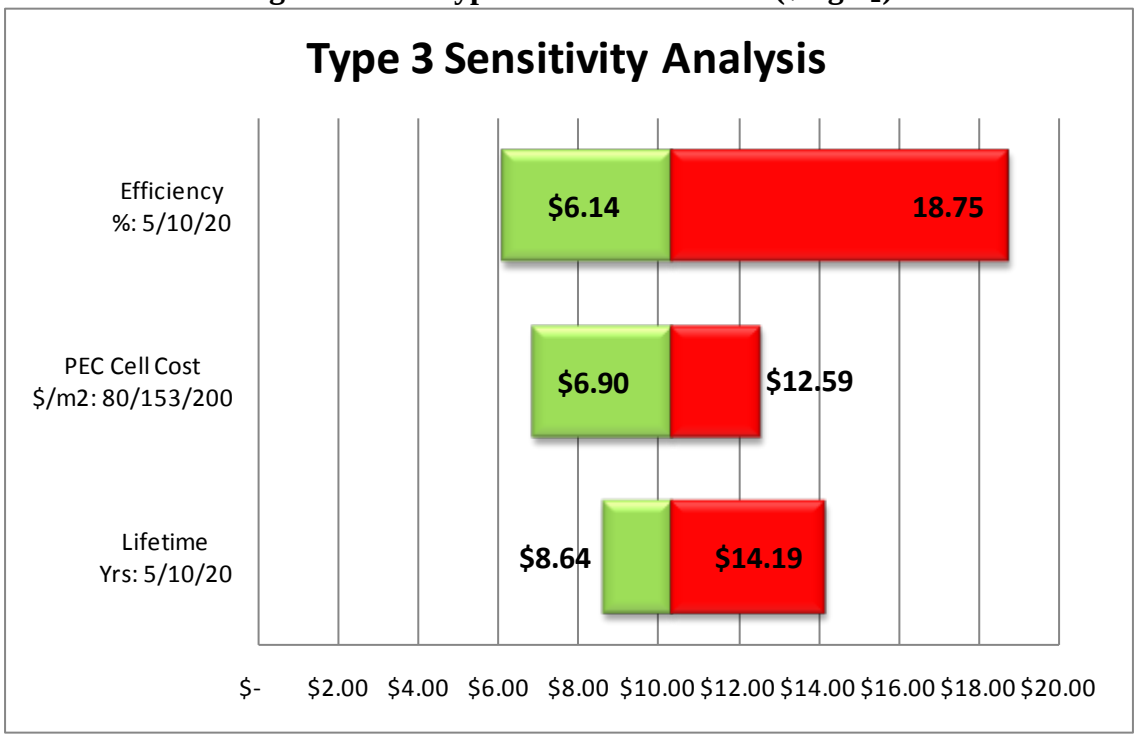

The baseline uses current thin film PV manufacturing costs to estimate the tandem cell costs. There is real potential, as pointed out in Section 4.3, to anticipate future thin film PV cost reduction to 30% of the current level, thus the cost reduction to $6.90/kg appears reasonable.

10.4 *Type 4 PEC Tracking Solar Concentrator System*

As described in Section 4.5 the Type 4 system reactor unit consists of concentrator PEC units that track the sun in two dimensions. The system layout is shown in Figure 10-20[70].

Figure 10-20: Type 4 System Layout

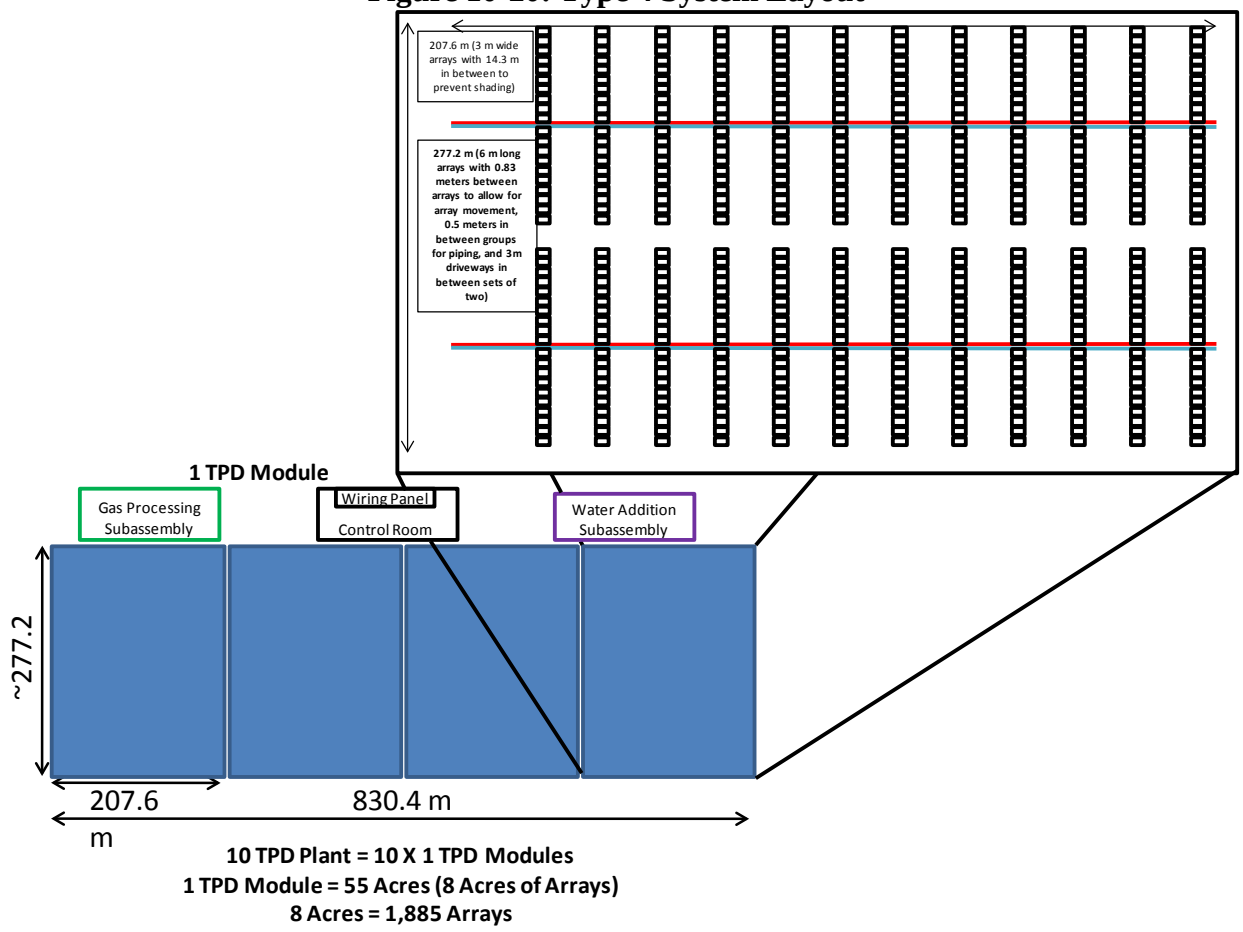

The BOM is listed in Figure 10-21. Total 1 TPD system cost is $3,448,755 before installation.

[70] This table is approximate and contains slightly more than the number of arrays for a 1TPD plant.

Figure 10-21: Bill of Materials for Installed Type 4 Baseline 1TPD System

Description	Unit Size	Units	Unit cost		Qty Req'd	Total Cost
PEC Subassembly Type 4						
Tracking & Concentrating	1	m^2	$ 60.00	/m2	33,923.7	$ 2,035,420
Concentrator ratio	10 :1					
Pressure	300	psi				
PEC Receiver	1	m^2	$ 316.27	/m2	3,392.37	$ 1,072,904
Make-up Water Pump	1	pump	$ 212.50		1	$ 213
Water Manifold Piping (diameter)	0.5	in	$ 0.52	/ft	41,485	$ 21,572
Water Collection Piping (diameter)	0.5	in	$ 0.52	/ft	5,345	$ 2,779
Water Column Collection Piping (dia	2	in	$ 2.12	/ft	892	$ 1,891
Water Final Collection Piping (diam	3	in	$ 4.31	/ft	100	$ 431
PEC Subassembly Type 4 Total						**$ 3,135,209**
Gas Processing Subassembly						
Condenser	1	HX	$ 7,098		1	$ 7,098
Manifold Piping (diameter)	0.5	in	$ 0.52	/ft	41,485	$ 21,572
Collection Piping (diameter)	0.5	in	$ 0.52	/ft	5,345	$ 2,779
Column Collection Piping (diameter	2	in	$ 2.12	/ft	892	$ 1,891
Final Collection Piping (diameter)	3	in	$ 4.31	/ft	100	$ 431
PEC Subassembly Type 4 Total Total						**$ 33,771**
Controls						
PLC	1	controller	$ 3,000		1	$ 3,000
Control Room building	1	ft^2	$ 50.00		351	$ 17,527
Control Room Wiring Panel	1	panel	$ 3,000		1	$ 3,000
Computer and Monitor	1	computer	$ 1,500		1	$ 1,500
Labview Software	1	program	$ 4,299		1	$ 4,299
Water Level Controllers	1	controller	$ 50		1,885	$ 94,232
Pressure Sensors	1	sensor	$ 345		18	$ 6,210
Hydrogen Area Sensors	1	sensor	$ 7,600		18	$ 136,800
Oxygen Area Sensors	1	sensor	$ -		18	$ -
Hydrogen Flow Meter	1	meter	$ 5,500		1	$ 5,500
Instrument Wiring			$ 0.02	/ft	24,157	$ 469
Power Wiring			$ 0.10	/ft	2,416	$ 234
Conduit			$ 0.58	/ft	12,079	$ 7,003
Controls Total						**$ 279,774**
Direct Capital Cost						**$ 3,448,755**
Installation Costs						
Piping Installation	1	ft	$0.11	/ft	95,642	$ 10,521
Reactor Foundation & Erection	1	m2	$ 22.00		33,924	$ 746,321
Reactor feed install	1	pump			30%	$ 64
Gas processing Subassembly install	1	gas sys			30%	$ 2,129
Control System Install	1	control sys			30%	$ 83,932
Installation Cost Total						**$ 842,967**
Cost with Installation						**$ 4,291,722**
Reactor Cost/capture area ($/m2) - Uninstalled						**$ 92.41**
System Cost /capture area ($/m2) - Uninstalled						**$ 126.51**

The cost breakdown for the major system capital components is shown pictorially in Figure 10-22 (the PEC subassembly includes the PEC receiver and the reactant water supply). This figure includes hardware cost without installation cost.

Figure 10-22: Type 4 Baseline 1 TPD System Direct Capital Components

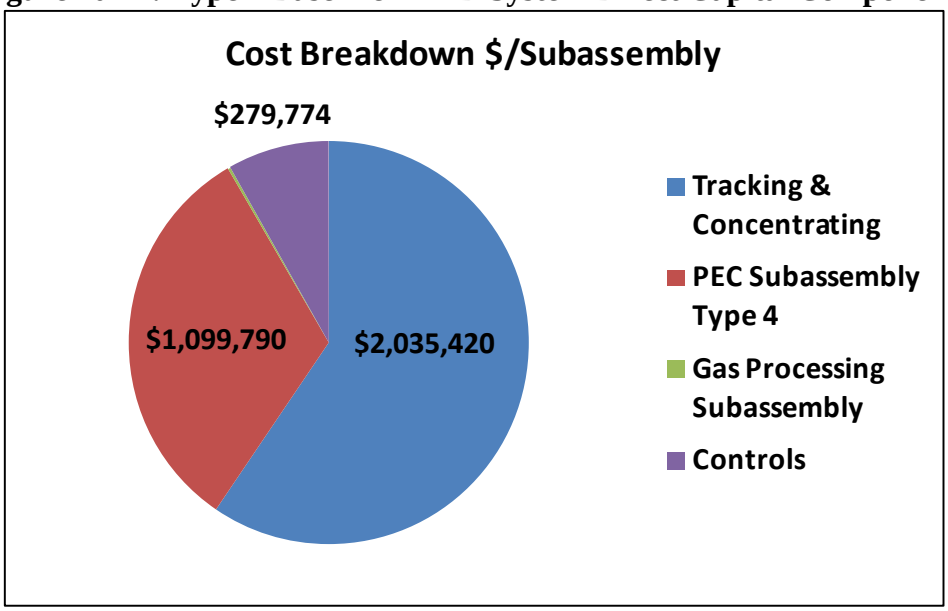

H_2 production cost breakdown for a baseline 10 tonne/day system is shown in Figure 10-23 and includes capital costs, operating costs, and decommissioning costs. Assuming the baseline parameter values, the H_2 cost is estimated at $4.05/kg.

Figure 10-23: Type 4 Baseline 10 TPD H_2 Production Cost Elements – $4.05/kg H_2

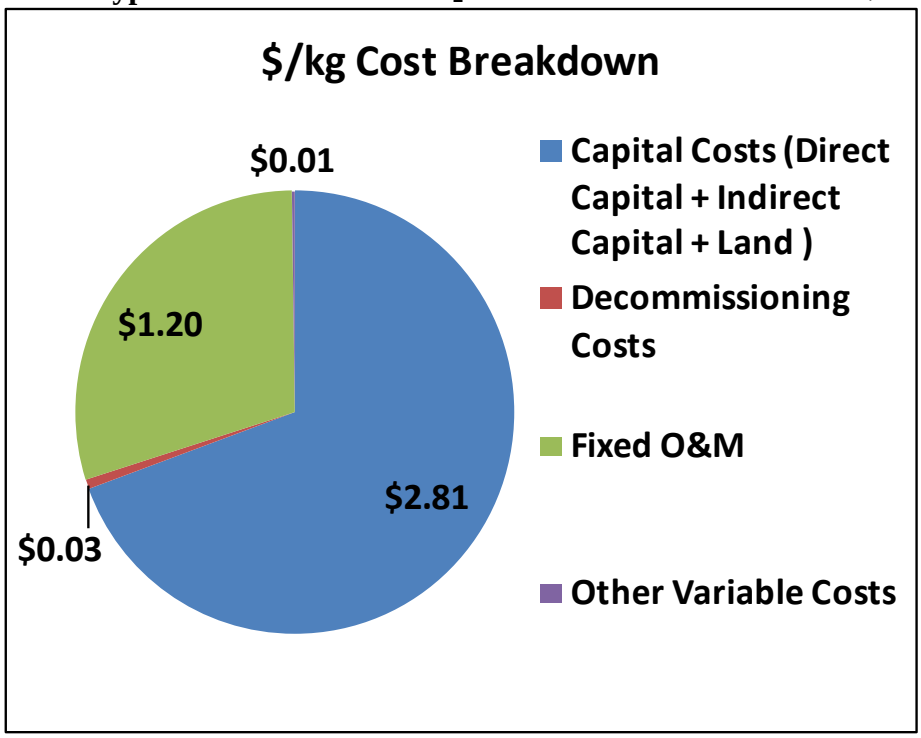

An H_2 production cost sensitivity analysis assessed the variation in H_2 cost as a function of efficiency, cost of PEC cell module, and system lifetime. The range of parameters is shown in Figure 10-24 and plotted in Figure 10-25.

Figure 10-24: Type 4 Sensitivity Analysis Parameters

Type 4 Sensitivity Analysis Parameters		
Efficiency	**PEC Cell Cost**	**PEC Cell Lifetime**
10%	$200/m^2	5 year
15%	$316/m^2	10 year
25%	$450/m^2	20 year

Figure 10-25: Overall Type 4 Cost Sensitivities ($/kg$H_2$)

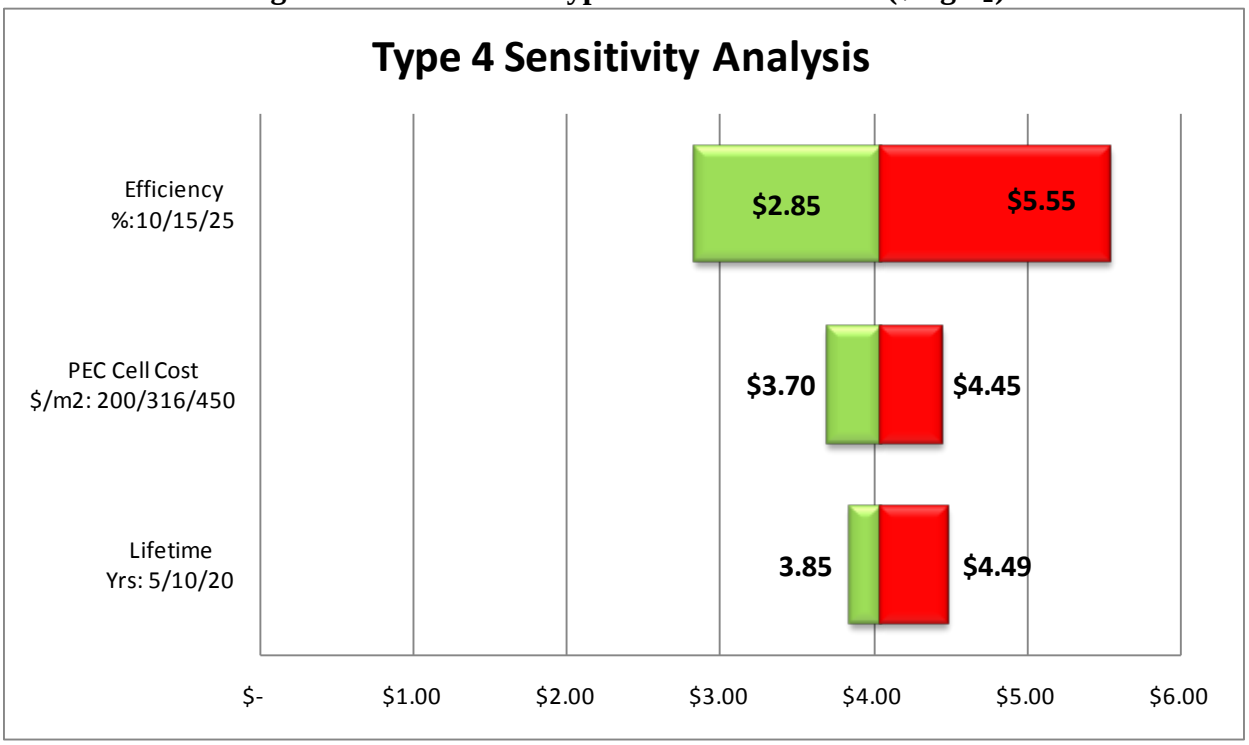

These cost reductions do not include the effects of increasing the solar collection ratio from 10:1 to 20:1, a change that would reduce the PEC receiver subassembly cost, further reducing the H_2 production cost. A higher concentration ratio significantly reduces the PV cost and the Plexiglas window cost. Resultant H_2 costs for 20:1 concentration ratio could be reduced to approximately $3.60/kg for 15% efficiency and approximately $2.60/kg for 25% efficiency.

11. Summary of Results and Conclusions for Levelized Hydrogen Costs

11.1 *PEC Hydrogen Production Systems*

The specific systems types conceptually designed and evaluated in this report are:

1. Type 1: Single electrolyte bed colloidal suspension of PEC nanoparticles producing mixture of H_2 and O_2 product gases.
2. Type 2: Dual electrolyte beds containing colloidal suspensions of PEC nanoparticles, with one bed carrying out the H_2O => ½ O_2 + 2 H+ half-reaction, the other bed carrying out the 2H+ => H_2 half-reaction , and including a mechanism for circulating the ions between beds.
3. Type 3: PEC fixed planar array tilted toward the sun at local latitude , using multi-junction PEC cells immersed in a electrolyte reservoir.
4. Type 4: PEC solar concentrator system, using reflectors to focus the solar flux at a 10:1 concentration ratio onto PEC cell receivers immersed in a electrolyte reservoir and pressurized to 300 psi.

11.2 *Hydrogen Production Cost Comparison*

The hydrogen production cost results calculated from the system designs and the H2A model are graphed in Figure 11-1. The total cost of produced hydrogen in a 10 tonne per day (TPD) plant (composed of ten 1TPD modules) is provided as well as the cost breakdown over several cost components: capital costs, decommissioning costs, fixed O&M, and variable costs. Note that these are the H_2 production costs for production of 300 psi hydrogen at the plant gate. They do not include delivery or dispensing costs.

Figure 11-1: Levelized costs for H_2 Produced by Baseline PEC Systems

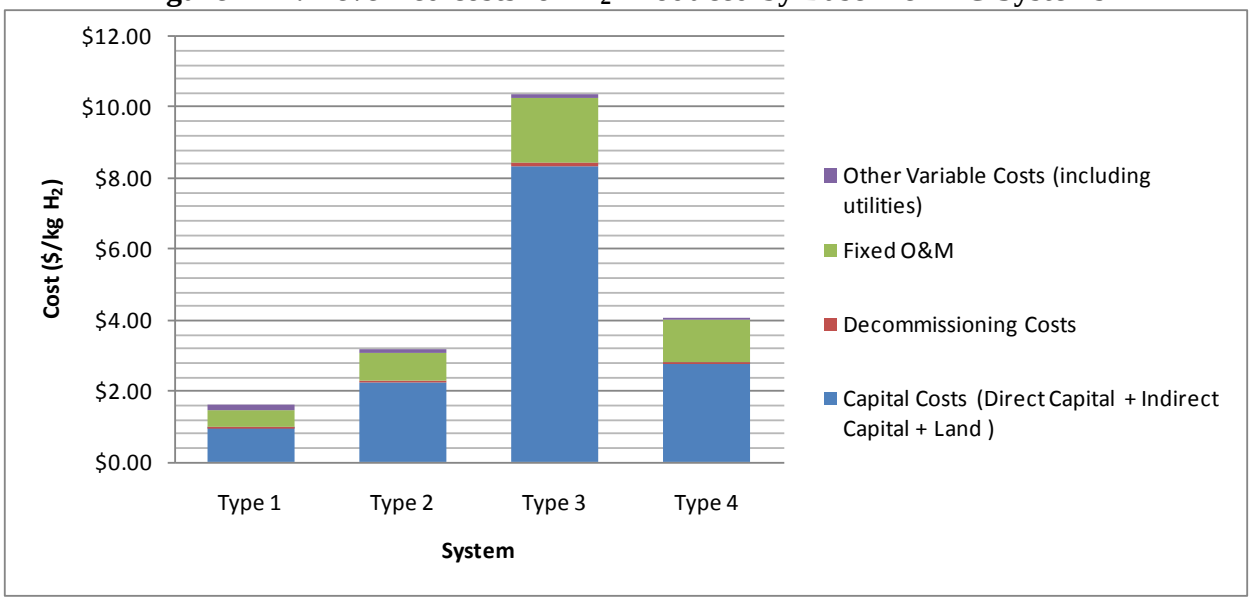

For the Type 1 and Type 2 systems, the levelized cost is quite low, but there is a large amount of development work and uncertainty in producing an operating system having these baseline performance parameters. The Type 3 system is the most mature of the concepts with multiple

examples fabricated, but the substantial capital costs dominate the H_2 production cost. The Type 4 system has been implemented at lab scale with good efficiency. For the Type 4 production system, the costs are moderately low and are dominated by the solar collector structure.

11.3 *H_2 Cost Sensitivity to System Parameters*

Since there is some uncertainty as to the reactor parameters of efficiency, PEC element cost, and PEC element lifetime, a sensitivity analysis was carried out. For the four systems, the sensitivity analysis parameters are listed in Figure 11-2 and the results are shown in Figure 11-3.

Figure 11-2: Sensitivity Analysis Parameters

Type 1 Sensitivity Analysis Parameters		
Efficiency	**Particle Cost**	**Particle Lifetime**
5%	0.1x	1 Year
10%	1x	5 Year
15%	20x	10 Year

Type 2 Sensitivity Analysis Parameters		
Efficiency	**Particle Cost**	**Particle Lifetime**
2.5%	0.1x	1 Year
5%	1x	5 Year
7.5%	20x	10 Year

Type 3 Sensitivity Analysis Parameters		
Efficiency	**PEC Cell Cost**	**PEC Cell Lifetime**
5%	$80/m^2	5 year
10%	$153/m^2	10 year
20%	$200/m^2	20 year

Type 4 Sensitivity Analysis Parameters		
Efficiency	**PEC Cell Cost**	**PEC Cell Lifetime**
10%	$200/m^2	5 year
15%	$316/m^2	10 year
25%	$450/m^2	20 year

Figure 11-3: Sensitivity Analysis Results

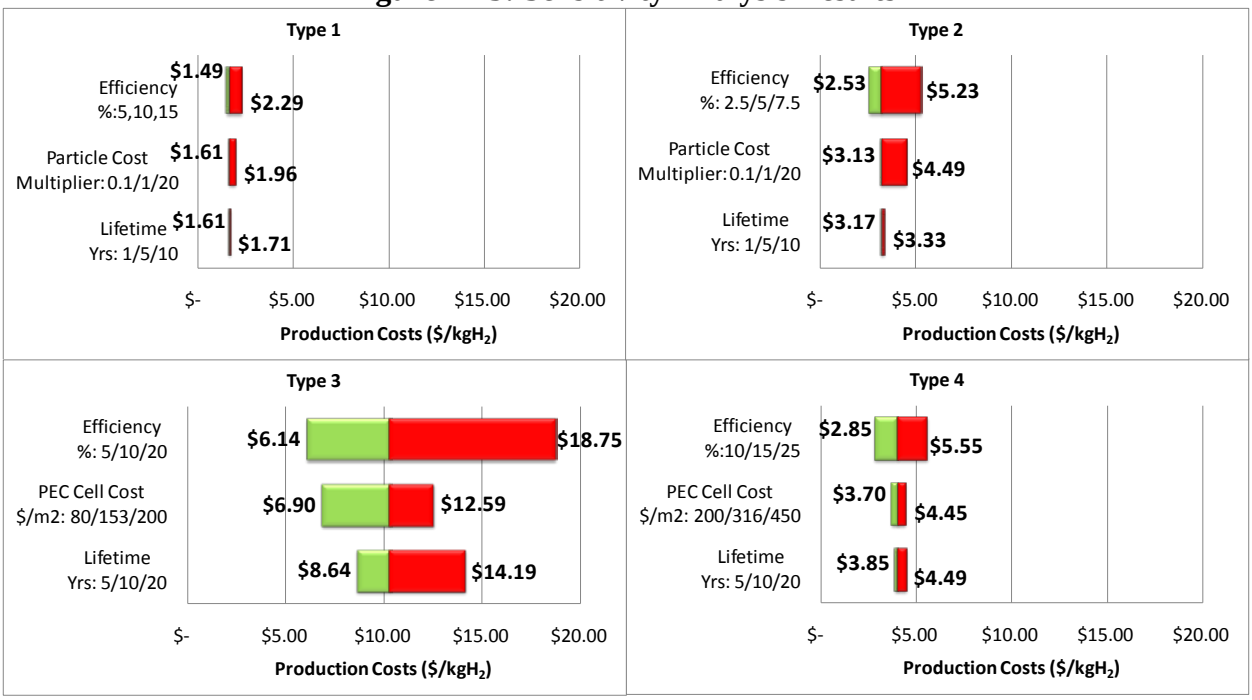

11.4 *Discussion of Results*

This study has shown that, within the cost assumptions used, production of H_2 by PEC systems can be economically viable in several configurations, upon successful resolution of the research challenges. Each system is discussed below

11.4.1 Particle Bed PEC

The Type 1 and 2 particle bed systems are innovative and cost effective PEC approaches, but they are immature and unproven compared with the standard PEC cell approach. Given the study assumptions as to efficiency and nanoparticle effectiveness, the Type 1 and 2 systems yield the lowest cost hydrogen. A unique advantage of these systems vs. the Type 3 panel array is that the gas collection bags are capable of storing the product gas output over a day's production to average out the demands on the gas processing system rather than requiring the processors to handle the peak gas output (as is the case for the Type 3 system).

One issue for these horizontal bed PEC systems is that the H_2 output variation between summer and winter can vary by a factor of 3.2 for a clear environment and by a greater factor in the event of extensive winter cloud cover. Since this study didn't include a monthly hydrogen demand profile, the beds were sized for an average yearly production (averaging 1,000 kg H_2/day over a year) without regard for potential seasional demand varations. The plant size will need to be increased if the winter H_2 demand is greater than 1/3 of the summer demand.

The greater uncertainties in the Type 1 and 2 systems include:

- Incomplete definition and demonstration of the optimal nanoparticle PEC materials, including electrolysis voltage, resistance losses, corrosion effects, lifetime
- Incomplete definition of fabrication techniques and production costing of the particles
- Fraction of effective photo-reactive area (photon capture area) on a given base nanoparticle
- Annual production quantity of the photoactive nanoparticles (This study assumed an annual production quantity sufficient for supplying a 500 tonne H_2 capacity each year, yielding a particle cost of $304/kg. Nanoparticle cost would increase to ~$3500/kg if annual production corresponded to that required to produce only 10 tonnes H_2 each year)

Key Unique Type 1 characteristics include:

1. Lowest predicted H_2 costs, given study efficiency assumptions
2. Product gas in this system is a stoichiometric mixture of H_2 and O_2 raising safety concern
3. December output is 31% of June output, so the system would need to be enlarged if December output were a driving requirement rather than just the yearly average.

Key Unique Type 2 characteristics include:

1. Low predicted H_2 costs, given study efficiency assumptions
2. Performance results hinge on minimal losses due to ion transport
3. Nanoparticles separately tailored for O_2 production and H_2 production
4. December output is 31% of June output, so the system would need to be enlarged if December output were a driving requirement rather than just the yearly average.

11.4.2 Photocell PEC

The Type 3 and 4 Photocell systems have benefited extensively from the current high development activity in the solar cell area, particularly in efforts to drive down the costs of thin film solar cells. Solar cells can be used to generate solar electricity to separately electrolyze water. However, with sufficient development, the PEC cell concept can be more efficient since it eliminates the materials and fabrication costs of the solar cell current carrier conductor grid. The PEC cell can also be used under pressure to eliminate the need for a separate compression stage.

Relative to the particle bed systems, variation in output between summer and winter for the photocell systems is significantly less.

Key unique Type 3 characteristics include:

1. Highest H_2 production costs, due to large areas of PEC component
2. Benefits from and relies on development of low cost thin film PV materials
3. For PEC cells, cell packaging costs are significantly higher than the PV material costs
4. Highest gas compression cost, because compressor is sized for peak hourly production
5. Tilt angle, nominally the latitude angle, can be optimized to achieve the most level H_2 gas output of all the options over the full year including environmental variations.

Key unique Type 4 characteristics include:

1. Moderately low H_2 costs, near the Type 2 estimate
2. In-cell compression of gas eliminates need for separate compressor
3. Increased efficiency possible with PEC development, and high temperature operation
4. Decreased H_2 cost with higher concentration ratio – to potentially below $3/kg
5. Offset reflector array for the concentrator reduces structural and piping costs.
6. Under clear conditions, December output is 53% of June output, so the system would need to be enlarged if December output were the driving requirement rather than the yearly average.

11.5 *PEC System Development Recommendations*

Type 1 System:

- Resolve H_2/O_2 mixture issues
- Develop/demonstrate high capture area nanoparticles with requisite photovoltage

Type 2 Dual Bed System:

- Develop/demonstrate ion-bridge between beds for minimal diffusion losses
- Develop/demonstrate ionic charge carriers (I, Br, Fe, etc.)
- Develop/demonstrate high capture area nanoparticles with requisite photovoltages for O_2 and H_2 generation
- Develop/demonstrate water circulation system

Type 3 Panel System:

- Develop PEC cell structures with greatly reduced cell packaging costs

Type 4 Concentrator System:

- Develop lower cost composite structures for concentrator
- Demonstrate high pressure PEC cell operation
- Increase concentrator ratio to ~ 20:1, with potential for additional 10% cost reduction
- Investigate high temperature operations, to increase efficiency or lower voltage requirement

In addition to development of the reactor components, further definition is needed on the actual seasonal hydrogen demand requirements. Also, further definition is needed on the control system and safety requirements to assure satisfactory plant operation.